CARIBOU MONITORING STUDY FOR THE BEAR TOOTH UNIT PROGRAM, ARCTIC COASTAL PLAIN, ALASKA, 2019

Alexander K. Prichard
Joseph H. Welch
Matthew J. Macander

Prepared for
ConocoPhillips Alaska, Inc.
Anchorage, Alaska

Prepared by
ABR, Inc.—Environmental Research & Services
Fairbanks, Alaska

CARIBOU MONITORING STUDY FOR THE BEAR TOOTH UNIT PROGRAM, ARCTIC COASTAL PLAIN, ALASKA, 2019

Prepared for

ConocoPhillips Alaska, Inc.
P.O. Box 100360
Anchorage, Alaska 99510-0360

Prepared by

Alexander K. Prichard
Joseph H. Welch
Matthew J. Macander

ABR, Inc.—Environmental Research & Services
P.O. Box 80410
Fairbanks, Alaska 99708-0410

August 2020

TABLE OF CONTENTS

List of Figures iv
List of Tables v
List of Appendices v
Acknowledgments vi
Introduction 1
Background 1
Study Objectives 3
Study Area 4
Methods 5
Caribou Distribution and Movements 5
Aerial Transect Surveys 5
Density Mapping 6
Radio Telemetry 6
Seasonal Occurrence in the Study Area 8
Aerial Photography 8
Remote Sensing 9
Snow Cover 9
Vegetative Biomass 10
Forage Modeling 10
Habitat Classification 11
Resource Selection Analysis 11
Results 13
Weather Conditions 13
Caribou Distribution and Movements 16
Aerial Transect Surveys 16
Radio Telemetry 18
Movements Near Proposed Willow Infrastructure 25
Aerial Photography 25
Remote Sensing 30
Snow Cover 30
Vegetative Biomass 35
Resource Selection Analysis 35
Discussion 41
Weather, Snow, and Insect Conditions 41
Caribou Distribution and Movements 41
Resource Selection 42
Aerial Photography 46
Conclusion 46

LIST OF FIGURES

Figure 1. Location of the caribou monitoring study area on the central North Slope of Alaska and detailed view showing locations of the Bear Tooth North and Bear Tooth South survey areas, 2001–2019 2

Figure 2. Population size of the Teshekpuk and Central Arctic caribou herds, 1975–2019, based on Alaska Department of Fish and Game census estimates 3

Figure 3. Habitat types used for caribou habitat-selection analysis in the Bear Tooth Unit study areas, National Petroleum Reserve-Alaska 12

Figure 4. Snow depth, long-term mean, and 95% confidence interval at the Kuparuk airstrip, May–June 2019 and daily average air temperature, long-term mean, and 95% confidence interval at Kuparuk, May–September 2019 14

Figure 5. Hourly air temperature, wind speed, mosquito probability index, and oestrid fly probability index at Nuiqsut, 15 June–7 September 2019 15

Figure 6. Distribution and size of caribou groups during each of seven seasons in the Bear Tooth North and Bear Tooth South survey areas, April–October 2019 17

Figure 7. Mean seasonal densities of caribou in the NPRA caribou survey areas based on inverse distance-weighting interpolation of aerial survey results, 2002–2019 19

Figure 8. Seasonal distribution of Central Arctic Herd female caribou based on fixed-kernel density estimation of telemetry locations, 2001–2019 20

Figure 9. Seasonal distribution of Teshekpuk Caribou Herd females based on fixed-kernel density estimation of telemetry locations, 1990–2019 21

Figure 10. Seasonal distribution of Teshekpuk Caribou Herd males based on fixed-kernel density estimation of telemetry locations, 1997–2019 22

Figure 11. Distribution of parturient females of the Teshekpuk Caribou Herd during calving based on fixed-kernel density estimation of telemetry locations, 1990–2019 23

Figure 12. Proportion of Central Arctic Herd and Teshekpuk Caribou Herd caribou within the Bear Tooth Unit-North and Bear Tooth Unit-South survey areas, based on fixed-kernel density estimation, 1990–2019 24

Figure 13. Movements of GPS-collared Teshekpuk Caribou Herd based on 95% isopleths of dynamic Brownian Bridge movement models 26

Figure 14. Movements of GPS-collared caribou from the Teshekpuk Caribou Herd and Central Arctic Herd in the vicinity of the proposed Willow development during each of 8 seasons 27

Figure 15. Proportion of Teshekpuk Caribou Herd caribou within 4 km of the proposed Willow development alignments, based on fixed-kernel density estimation, 1990–2019 29

Figure 16. Extent of snow cover between early May and mid-June on the central North Slope of Alaska in 2019, as estimated from MODIS satellite imagery 31

Figure 17. Median snowmelt data and vegetation index metrics, as estimated from MODIS satellite imagery time series, 2000–2019 32

Figure 18. Departure of 2019 values from median snowmelt data and vegetation index metrics, as estimated from MODIS satellite imagery time series 33

Figure 19. Metrics of relative vegetative biomass during the 2019 growing season on the central North Slope of Alaska, as estimated from NDVI-calculated from MODIS satellite imagery. 34
Figure 20. Predicted relative probability of use of the NPRA study area by caribou during each of eight seasons, 2002–2019, based on resource selection function analysis 39

LIST OF TABLES

Table 1. Number of Teshekpuk Caribou Herd and Central Arctic Herd radio-collar deployments and total number of collared animals that provided movement data for the ASDP and GMT caribou study 7
Table 2. Number and density of caribou in the Bear Tooth North and Bear Tooth South survey areas, April–September 2019 16
Table 3. Proportion of collared Teshekpuk Herd caribou that crossed the proposed Willow alignment at least once in each season, 2000–2019. 29
Table 4. Number of aerial surveys, radio collars, and locations for each sample type used in resource selection function analysis for the NPRA survey area, 2002–2019. 35
Table 5. Three top-performing seasonal resource selection function models, AICc scores, and the probability that each model was the best model in the candidate set for the GMT, BTN, and BTS survey areas, 2002–2019 36
Table 6. Mean Spearman's correlation coefficient of seasonal resource selection function model fit using k-fold cross-validation for the NPRA survey area, 2002–2019 37
Table 7. Independent variables and their probability of being in the best resource selection function model for the NPRA survey area during eight seasons, 2002–2019 38
Table 8. Model-weighted parameter estimates for resource selection function models for the NPRA survey area during eight seasons, 2002–2019 40

LIST OF APPENDICES

Appendix A. Cover-class descriptions of the NPRA earth-cover classification 56
Appendix B. Snow depth and cumulative thawing degree-days at the Kuparuk airstrip, 1983–2019 58
Appendix C. 2019 imaging season summary report. North Slope aerial caribou imaging to support automated counts. Survey report submitted by TerraSond, Inc. 61
Appendix D. Timing of annual snowmelt, compared with median date of snowmelt, on the central North Slope of Alaska during 2000–2019, as estimated from MODIS satellite imagery 95
Appendix E. Differences between annual relative vegetative biomass values and the 2000–2019 median during the caribou calving season on the central North Slope of Alaska, as estimated from NDVI calculated from MODIS satellite imagery. 96

Appendix F. Differences between annual relative vegetative biomass values and the 2000–2019 median at estimated peak lactation for caribou on the central North Slope of Alaska, as estimated from NDVI calculated from MODIS satellite imagery 97
Appendix G. Differences between annual relative vegetative biomass values and the 2000–2019 median at estimated peak biomass on the central North Slope of Alaska, as estimated from NDVI calculated from MODIS satellite imagery 98

ACKNOWLEDGMENTS

This study was funded by ConocoPhillips Alaska, Inc., (CPAI) and was administered by Robyn McGhee, CPAI Environmental Studies Coordinator, for whose support we are grateful. Valuable assistance with field logistics was provided by Justin Blank, Zac Hobbs, and Krista Kenny. Alaska Department of Fish and Game (ADFG) biologists played crucial collaborative roles in this study by capturing caribou, deploying radio collars, and providing telemetry data under a cooperative agreement among ADFG, CPAI, and ABR. We thank ADFG biologists Lincoln Parrett, Carmen Daggett, and Elizabeth Lenart for their professional cooperation and assistance. Brian Person of the North Slope Borough Department of Wildlife Management (NSB) provided GPS and satellite telemetry data, valuable information, and advice. Bob Gill and Ron Vogt of 70 North LLC provided safe and efficient piloting of survey airplanes under flying conditions that often were less than optimal. Assistance in the field was provided by ABR employees John Shook, Katie Hayden, Forrest Rosenbower, and Robert McNown. Support during data collection, analysis, and report production was provided by Christopher Swingley, Dorte Dissing, Will Lentz, Pamela Odom, and Tony LaCortiglia. Review by Adrian Gall, Robyn McGhee, and Jasmine Woodland improved this report.

INTRODUCTION

BACKGROUND

The caribou monitoring study for the Bear Tooth Unit (BTU) area is being conducted on the Arctic Coastal Plain of northern Alaska in the northeastern portion of the National Petroleum Reserve–Alaska (NPRA; Figure 1). This region is used primarily by one herd of barren-ground caribou (*Rangifer tarandus granti*)—the Teshekpuk Caribou Herd (TCH), although some animals from the Central Arctic Herd (CAH) may use the area in some years. The TCH generally ranges from the Colville River to the Chukchi Sea north of the Brooks Range (Person et al. 2007, Wilson et al. 2012, Parrett 2015a).

Most of the TCH remains on the coastal plain year-round. Most calving occurs around Teshekpuk Lake and the primary area of insect-relief habitat in midsummer is the swath of land between Teshekpuk Lake and the Beaufort Sea coast (Kelleyhouse 2001; Carroll et al. 2005; Parrett 2007, 2015a; Person et al. 2007; Yokel et al. 2009; Wilson et al. 2012). Since 2010, the calving distribution of the TCH appears to have expanded west, with some calving extending west of Atqasuk (Parrett 2015a; Prichard et al. 2019a).

Most TCH caribou winter on the coastal plain, generally west of the Colville River, although approximately one third of the herd, including a disproportionate amount of males, winter in the central Brooks Range (Parrett 2015a, Prichard et al. 2019d) and, in a highly unusual movement, a large proportion of the TCH wintered as far east in the Arctic National Wildlife Refuge (ANWR) in 2003–2004 following an October rain-on-snow event (Bieniek et al. 2019).

The TCH increased substantially in size from the mid-1970s, when it consisted of only a few thousand animals, to the early 1990s (Figure 2; Parrett 2015a). The TCH experienced a dip in numbers in the early 1990s, but increased steadily from 1995 to its peak estimated size of 68,932 animals in July 2008 (Parrett 2015a). The herd subsequently declined to 39,172 animals in 2013, but stabilized to 41,542 (SE = 3,486) by July 2015 and increased to a minimum of 56,255 by July 2017 (Klimstra 2018, Parrett 2015b). Although the new higher-resolution digital photography introduced in 2017 may have contributed to higher population counts since 2015, the increase in estimated herd size indicates that the TCH has remained stable or increased since 2015.

The summer range of the Central Arctic Herd (CAH) of caribou is generally between the Colville and Canning rivers. Individuals sometimes cross over to the west of the Colville River, particularly during late summer. CAH caribou typically calve in two groups; between the Colville and Kuparuk Rivers; and between the Sagavanirktok and Canning rivers (Wolfe 2000, Arthur and Del Vecchio 2009, Lenart 2015). They use the Beaufort Sea coast during periods of mosquito harassment (White et al. 1975, Dau 1986, Lawhead 1988), and generally winter in or near the Brooks Range, usually east of the Dalton Highway/Trans-Alaska Pipeline (TAPS) corridor (Arthur and Del Vecchio 2009, Lawhead et al. 2015, Lenart 2015, Nicholson et al. 2016), although some animals have remained north of the Brooks Range on the coastal plain in recent years (Prichard et al. 2019d).

Population trends of the CAH have largely mirrored those of the TCH (Figure 2; Lenart 2009, 2015, 2017, 2019). The herd grew rapidly from ~5,000 animals in the mid-1970s to a peak size of 68,442 caribou in 2010 (Lenart 2015a). The herd subsequently declined rapidly to 22,630 caribou by July 2016 (Lenart 2017). The herd then increased to 30,069 caribou by July 2019 (Lenart 2019), although, similar to the TCH, some of the recent apparent increase in herd size may have been a result of higher-resolution digital photography for conducting the photocensus. The magnitude of the decline from 2010 to 2016 may have been affected by emigration of some CAH animals to the Porcupine Caribou Herd and TCH, with which the CAH often intermixes on winter range.

This monitoring study builds on prior research funded by ConocoPhillips Alaska, Inc., (CPAI; and its heritage companies Phillips Alaska, Inc., and ARCO Alaska, Inc.) that was conducted on the Colville River delta and adjacent coastal plain east of the delta (Alpine transportation corridor) beginning in 1992 and in the northeastern portion of the NPRA beginning in 1999 (Johnson et al. 2015; Jorgenson et al. 1997, 2003, 2004). Since 1990, contemporaneous, collaborative telemetry studies of caribou distribution and movements have been conducted in the region west of the

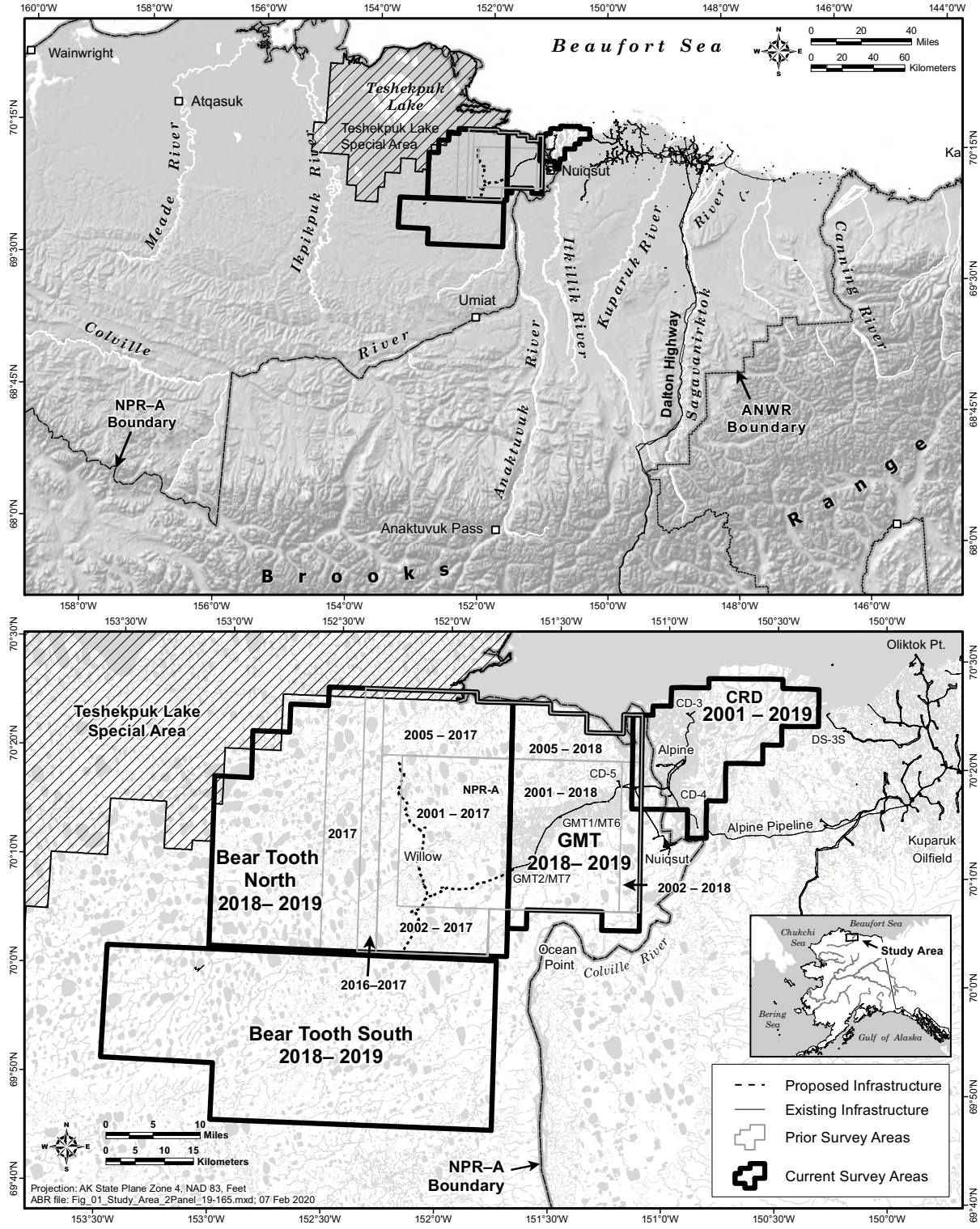

Figure 1. Location of the caribou monitoring study area on the central North Slope of Alaska and detailed view showing locations of the Bear Tooth North and Bear Tooth South survey areas, 2001–2019.

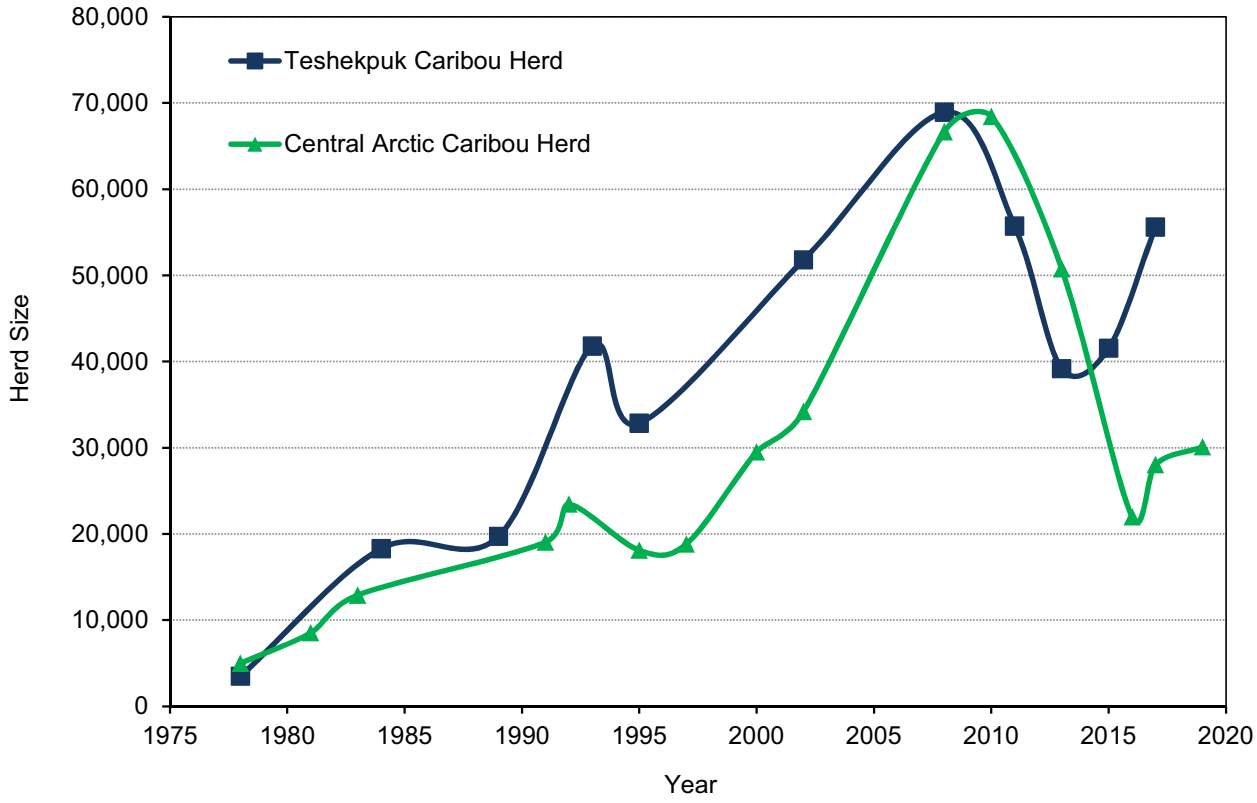

Figure 2. Population size of the Teshekpuk and Central Arctic caribou herds, 1975–2019, based on Alaska Department of Fish and Game census estimates.

Colville River by the Alaska Department of Fish and Game (ADFG), the North Slope Borough (NSB), and the Bureau of Land Management (BLM) (Philo et al. 1993, Carroll et al. 2005, Person et al. 2007, Wilson et al. 2012, Parrett 2015a, Prichard et al. 2017, 2018b, 2019c, 2019d). Consultants working for BP Exploration (Alaska), Inc., conducted aerial transect surveys over much of the TCH calving grounds during 1998–2001 (Noel 1999, 2000; Jensen and Noel 2002; Noel and George 2003) and the NSB conducted aerial survey areas of calving caribou between Wainwright and Atqasuk during 2013–2015 (Prichard et al. 2019a).

STUDY OBJECTIVES

Evaluation of the natural and anthropogenic factors affecting caribou in the study area fall into two broad categories: those affecting movements of individuals and those affecting distribution of herds. Clearly, these categories are linked and are not mutually exclusive, but the applicability of study methods differs between them. Information on the potential effects of development on caribou distribution can be collected using a variety of methods, including aerial transect surveys, radio telemetry, and other reported observations. Information about the potential effects on caribou movements, however, cannot be addressed adequately without employing methods such as radio telemetry that allow consistent tracking of individually identifiable animals.

Several broad tasks were identified for study:

1. Evaluate the seasonal distribution, abundance, and movements of caribou in the study area, using a combination of historical and current data sets from aerial transect surveys and radio telemetry data obtained for this study and from ADFG/NSB/BLM under a cooperative agreement.

2. Characterize important habitat conditions, such as snow cover, spatial pattern and timing of snowmelt, seasonal flooding (if possible), and estimated biomass of new vegetative growth in the study area by applying remote-sensing techniques.
3. Compare caribou distribution with habitat distribution, remote-sensing data, and other landscape features to better understand factors influencing the seasonal distribution of caribou.
4. Continue a pilot study to assess the feasibility of using high-resolution aerial photography to detect and enumerate caribou from survey altitudes higher than 150 m (500 feet).

STUDY AREA

CPAI began funding caribou surveys in the northeastern NPRA in 2001–2004 and continued these studies during 2005–2014 under the NSB Amended Development Permit 04-117 stipulation for the CD-4 drill site project. Based on the earlier permit stipulations, the study area was specified as the area within a 48-km (30-mi) radius around the CD-4 drill site (Lawhead et al. 2015). During 2004–2017, aerial transect surveys were conducted in 3 survey areas, which encompassed most of that 48-km radius (Lawhead et al. 2015): the NPRA survey area (expanded from 988 km² in 2001 to 1,310 km² in 2002; 1,720 km² in 2005); the Colville River Delta survey area that encompasses CD-1 through CD-4 (494 km²); and the Colville East survey area (1,432–1,938 km², depending on the survey and year). Although 2014 was the tenth year of study, the NSB requested that annual monitoring be continued. In 2016, the study area was redefined to focus on the NPRA and Colville River Delta (CRD) survey areas, and so survey results for the Colville East survey area were reported separately (Prichard and Welch 2020). In 2016 and 2017, the NPRA survey area was expanded westward by 1 and 2 transects, respectively (1,818 km² in 2016; 2,119 km² in 2017). In 2018, the NPRA survey area was again redefined to focus on the two recently constructed drill sites (CD-5 and GMT1/MT6, constructed in winter 2013–2014 and 2016–2017, respectively), and the GMT2/MT7 drill site, as well as their connecting access roads (constructed during the winter of 2018–2019) and pipelines (Figure 1, bottom). This newly defined Greater Mooses Tooth (GMT) survey area (776.6 km²) also includes the Nuiqsut Spur Road that was constructed by the Kuukpik Corporation in winter 2013–2014 to connect the village of Nuiqsut to the CD-5 access road. The results of research conducted in the CRD and GMT survey areas were reported separately (Prichard et al. 2020).

The portion of the previous NPRA survey area west of GMT2/MT7 was expanded west and south to focus on the Willow prospect and other potential future developments within the Bear Tooth Unit (BTU). Results of studies within this new expanded study area are reported on here. For surveys and analysis, the BTU study area was split up into 2 survey areas, BTU North (BTN) and BTU South (BTS; Figure 1). To provide a wider context for analytical results and avoid duplication, some of the analyses in this report were conducted for all NPRA survey areas (GMT, BTN, and BTS; Figure 1) and those results are included in both this report and the CRD and GMT report (Prichard et al. 2020*).* Results for the BTU area for 2018 were reported in Prichard et al. (2019d).

The study area is located on the central Arctic Coastal Plain of northern Alaska (Figure 1, top). The climate in the region is arctic maritime (Walker and Morgan 1964). Winter lasts about eight months and is generally cold and windy. The summer thaw period lasts about three months (June–August) and the mean summer air temperatures in Nuiqsut during 1990–2020 range from 6.2–9.9°C (43.2– 49.9°F; http://climate.gi.alaska.edu/Climate/Normals, accessed 27 January 2020) with a strong regional gradient of summer temperatures increasing with distance inland from the coast (Brown et al. 1975). Mean summer precipitation measured at Kuparuk and Colville Village is 9.7–12.5 cm (3.8–4.94 in), most of which falls as rain in July and August (http://climate.gi.alaska.edu/Climate/Normals, accessed 27 January 2020). The soils are underlain by permafrost and the temperature of the active layer of thawed soil above permafrost ranges from 0 to 10°C during the growing season.

Spring is brief, lasting about 3 weeks from late May to mid-June, and is characterized by the flooding and break-up of rivers and smaller tundra streams. In late May, water from melting snow flows both over and under the ice on the Colville River, resulting in flooding on the Colville River delta that typically peaks during late May or the first week of June (Walker 1983; annual hydrology reports to CPAI by Michael Baker Jr., Inc.). Break-up of the river ice usually occurs when floodwaters are at maximal levels. Water levels subsequently decrease throughout the summer, with the lowest levels occurring in late summer and fall, just before freeze-up (Walker 1983; annual hydrology reports to CPAI by Michael Baker Jr., Inc.). Summer weather is characterized by low precipitation, overcast skies, fog, and persistent northeasterly winds. The less common westerly winds often bring storms that are accompanied by high wind-driven tides and rain (Walker and Morgan 1964). Summer fog occurs more commonly at the coast and on the delta than it does farther inland.

METHODS

To evaluate the distribution and movements of TCH caribou in the study area, ABR biologists conducted aerial transect surveys in 2019 and analyzed existing telemetry data sets provided by ADFG, NSB, BLM, and the U.S. Geological Survey (USGS), and from GPS collars deployed specifically for this study in 2006–2010, 2013–2014, and 2016–2019. The majority of telemetry collars were scheduled to record one location every 2 hours during summer with less frequent locations during the winter; a typical collar deployment lasted 3 years.

Eight seasons per year were used for analysis of telemetry and aerial survey data, based on mean movement rates and observed timing of caribou life-history events (adapted from Russell et al. 1993 and Person et al. 2007): winter (1 December–30 April); spring migration (1–29 May); calving (30 May–15 June); postcalving (16–24 June); mosquito harassment (25 June–15 July); oestrid fly harassment (16 July–7 August, a period that also includes some mosquito harassment); late summer (8 August–15 September); and fall migration, a period that includes the breeding season, or rut (16 September–30 November).

Weather And Insect Conditions

Temperature and wind data can be used to predict the occurrence of harassment by mosquitoes (at least five *Aedes* species) and oestrid flies (warble fly *Hypoderma tarandi* and nose bot fly *Cephenemyia trompe*) (White et al. 1975, Fancy 1983, Dau 1986, Russell et al. 1993, Mörschel 1999, Yokel et al. 2009). To estimate spring and summer weather conditions in the area during 2019, we used meteorological data from National Weather Service reporting stations at Kuparuk and Nuiqsut. Thawing degree-day sums (TDD; total daily degrees Celsius above zero) were calculated using average daily temperatures at the Kuparuk airstrip. Average index values of mosquito activity were estimated based on hourly temperatures from Nuiqsut, using equations developed by Russell et al. (1993). The estimated probability of oestrid-fly activity was calculated from average hourly wind speeds and temperatures recorded at Nuiqsut, using equations developed by Mörschel (1999).

CARIBOU DISTRIBUTION AND MOVEMENTS

AERIAL TRANSECT SURVEYS

Transect surveys provided information on the seasonal distribution and density of caribou in the study area. Surveys of the BTN and BTS survey areas (Figure 1, bottom) were conducted periodically from April to September 2019 in a fixed-wing airplane (Cessna 207), following the same procedures used since 2001 in the NPRA survey area (Lawhead et al. 2015 and references therein).

In 2019, aerial transect surveys in the BTN and BTS survey areas were scheduled for mid-April (late winter), mid-May (spring migration), early June (calving), late June (postcalving), late July (oestrid fly), late August (late summer), and mid to late September (fall migration). Due to inclement weather, the BTN survey area in late winter and in the BTS survey area in late winter and fall migration were only partially completed.

During all aerial surveys, 2 observers looked out opposite sides of the airplane and recorded data independently. The pilot navigated the airplane

along transect lines using a GPS receiver and maintained an altitude of ~150 m (500 ft) above ground level (agl) or ~90 m (300 ft) agl. Surveys were flown at 90 m agl only during the calving survey and only on the seven westernmost transects in the BTN survey area. The lower flight altitude was chosen to increase the ability to detect calves due to the anticipated high levels of calving activity near Teshekpuk Lake.

Transect lines were spaced at intervals of 3.2 km (2 mi) in BTN and 4.8 km (3 mi) in BTU South, following section lines on USGS topographic maps (scale 1:63,360). Observers counted caribou within an 800-m-wide strip on each side of the airplane when flying at 150 m agl or a 400-m-wide strip when flying at 90 m agl. Therefore, we sampled ~50% of the BTN survey area when flying 150 m agl, 25% of the western portion of BTN when flying at 90 m agl during the calving survey, and 33% of the BTS survey area while flying 150 m agl. The number of caribou observed in the transect strips was therefore adjusted (e.g., multiplied by 2, 3, or 4) to estimate the total number of caribou in the survey area on each survey. The strip width was delimited visually for the observers by placing tape markers on the struts and windows of the aircraft, as recommended by Pennycuick and Western (1972), or by measuring distances to recognizable landscape features displayed on maps in GPS receivers.

When caribou were observed within the transect strip, a GPS location was recorded when the plane was perpendicular to the animal or herd, the numbers of "large" caribou (adults and yearlings) and calves were recorded, and the perpendicular distance from the transect center-line was assigned to one of four 100-m or 200-m intervals, depending on the strip width. For plotting on maps, the midpoint of the distance interval was used (e.g., 300 m for the 200–400-m interval). Thus, the maximal mapping error for distance was estimated to be ~100 m. Confidence intervals for estimates of total caribou and calves were calculated with a standard error formula modified from Gasaway et al. (1986), using 3.2-km segments of the transects as the sample units.

DENSITY MAPPING

To summarize aerial survey data in the BTN and BTS survey areas for the period 2002–2019, we used the inverse distance-weighted (IDW) interpolation technique of the *gstat* package (Pebesma 2004) in program *R* (R Core Team 2019) to map seasonal densities of caribou. Transect strips in the BTN and BTS survey areas were subdivided into 208 and 114 grid cells, respectively. Each grid cell was 1.6 km wide by 1.6 or 3.2 km long, depending on the transect length. We calculated density in each grid cell by dividing the total number of caribou observed in a grid cell on each survey by the land area in the grid cell. The best power (from 1 to 1.2) and the best number of adjacent centroids (from 10 to 24) to use in the calculations were selected based on the values that minimized the residual mean square error. This analysis produced color maps showing surface models of the estimated density of all caribou (large caribou plus calves) observed over the entire survey area for each season.

RADIO TELEMETRY

Satellite Collars

Satellite (Platform Transmitter Terminal; PTT) telemetry used the Argos system (operated by CLS America, Inc.; CLS 2016) and locations were transferred monthly to the NSB for data archiving. Locations were transmitted either at 6 h/day for a month after deployment and then 6 h every other day throughout the year, or once every 6 days in winter and every other day during summer (Lawhead et al. 2015). The CAH satellite collars were programmed to operate 6 h/day or 6 h every 2 days (Fancy et al. 1992, Lawhead et al. 2015).

Satellite-collar data were obtained from ADFG, NSB, and BLM for TCH animals during the period July 1990–November 2019 (Lawhead et al. 2006, 2007, 2008, 2009, 2010, 2011, 2012, 2013, 2014, 2015; Person et al. 2007; Prichard et al. 2017, 2018, 2019d, this study) and for CAH caribou during the periods October 1986–July 1990 (from USGS), July 2001–September 2004, and April 2012–September 2016 (Cameron et al. 1989, Fancy et al. 1992, Lawhead et al. 2006, Lenart 2015; Table 1). In the TCH sample (based on herd affiliation at capture), 185 collars deployed

Table 1. Number of TCH and CAH radio-collar deployments and total number of collared animals that provided movement data for the ASDP and GMT caribou study.

Herd [a] / Collar Type	Years	Female		Male		Total Deployments
		Deployments	Individuals	Deployments	Individuals	
Teshekpuk Herd						
VHF collars [b]	1980–2005	n/a		n/a		212
Satellite collars	1990–2019	97	86	88	79	185
GPS collars	2004–2019	289	207	15	14	304
Central Arctic Herd						
VHF collars [b]	1980–2005	n/a		n/a		412
Satellite collars	1986–1990	16		1		17
Satellite collars	2001–2004	10	10	2	2	12
Satellite collars	2012–2018	6	6	6	6	12
GPS collars	2003–2019	182	127	0	0	182

[a] Herd affiliation at time of capture.
[b] n/a = not available, but most collared animals were females.

on 165 different caribou (86 females, 79 males) transmitted signals for a mean duration of 563 days per collar. The CAH 1986–1990 sample included 17 caribou (16 females, 1 male). The CAH 2001–2004 and 2012–2019 deployment samples included 24 collars deployed on 24 caribou (16 females, 8 males), transmitting for a mean duration of 641 days per collar. Only collars that transmitted for >14 d were included in analysis. Satellite telemetry locations are considered accurate to within 0.5–1.0 km of the true locations (CLS 2016), but the data require screening to remove spurious locations (Lawhead et al. 2015).

GPS Collars

GPS collars purchased by BLM, NSB, ADFG, and CPAI (TGW-3680 GEN-III or TGW-4680 GEN-IV store-on-board configurations with Argos satellite uplink, manufactured by Telonics, Inc., Mesa, AZ) were deployed 304 times by ADFG biologists on 221 different TCH caribou (207 females, 14 males; Table 1) during 2004 and 2006–2019, with a mean deployment duration of 575 days. GPS collars (purchased by CPAI and ADFG) were deployed 182 times on 127 different female CAH caribou during 2003–2019, with a mean duration of 563 days. Only collars that transmitted for >14 d were included in analysis. Collars were programmed to record locations at 2-, 3-, 5-, or 8-h intervals, depending on the desired longevity of the collar (Arthur and Del Vecchio 2009, Lawhead et al. 2015).

GPS collars were deployed on female caribou, with the exception of six collars deployed on TCH males. Females are preferred for GPS collar deployment because the collar models used are subject to antenna problems when using the expandable collars that are required to allow for increased neck size of males during the rut (Dick et al. 2013; C. Reindel, Telonics, pers. comm.). Caribou were captured by ADFG personnel firing a handheld net-gun from a Robinson R-44 piston-engine helicopter. In keeping with ADFG

procedures for the region, no immobilizing drugs were used.

Data reports from Argos satellite uplinks were downloaded daily from CLS America, Inc., (Largo, MD) and the full dataset was downloaded after the collars were retrieved. Data were screened to remove spurious locations using methods described in Lawhead et al. (2015).

SEASONAL OCCURRENCE IN THE STUDY AREA

Seasonal use of the BTN and BTS survey areas was evaluated using several methods. We used Kernel Density Estimation (KDE) to calculate utilization distributions of caribou during different periods. We first calculated the mean location of each caribou for every 2-day period during the year. We then used fixed-kernel density estimation in the *ks* package for *R* (Duong 2017) to create utilization distribution contours of caribou distribution for every 2-day period throughout the year (all years combined) based on these mean locations. We then calculated an average utilization distribution for each combination of season, herd, and sex by calculating the average pixel values for each two-day utilization distribution. By calculating the average of utilization distributions based on the mean location for each animal we were able to account for movements within a season while not biasing the calculation due to autocorrelation among locations for a single caribou or due to unequal sample sizes among caribou. The plug-in method was used to calculate the bandwidth of the smoothing parameter. Because caribou are sexually segregated during some seasons, kernels were analyzed separately for females and males, although the sample size for male CAH caribou was insufficient to allow kernel density analysis. We also calculated a separate kernel for parturient TCH females during the calving season to delineate the calving range of the TCH.

We also calculated KDE by month (all years combined) for TCH males, TCH females, and CAH females. The proportion of each monthly utilization distribution from KDE within the survey areas was then calculated to determine the predicted monthly proportions of the herds expected to be using the study areas.

To visualize movements of caribou outfitted with GPS collars, we used dynamic Brownian Bridge Movement Models (dBBMM) to create utilization distribution maps of movements based on the locations of collared individuals (Kranstauber et al. 2014). These dBBMM models, a modification of earlier Brownian bridge models (Horne et al. 2007), use an animal's speed of movement and trajectory calculated from intermittent GPS locations to create a probability map describing relative use of the area traversed. We computed the 95% isopleth of movements for each individual TCH caribou outfitted with a GPS collar in the area and then overlaid the isopleth layers for each season to calculate the relative proportion of collared caribou using each 100-m pixel. This visualization displays the seasonal use of the area by TCH caribou as a function of both caribou distribution and movements. The dBBMM models were computed using the *move* package in *R* (Kranstauber et al. 2017).

We also examined GPS- and satellite-collar data to describe movements of individual caribou in the immediate vicinity of existing and proposed infrastructure. All GPS-collared TCH segments were mapped to visualize movements in the study area. We also calculated the proportion of collared TCH caribou that crossed the alignments at least once during a season for each year. We excluded animals that were present for less than half the season or with fewer than 30 locations per season. Locations within 30 days of collaring were removed. Additionally, we calculated the proportion of each monthly utilization distribution within 4 km of the proposed road and pad alignments (Proposed road alignment Alternative B, 1 October 2019).

AERIAL PHOTOGRAPHY

High-resolution digital photography is increasingly being used for aerial surveys of wildlife due to the potential for more accurate and auditable counts, increased observer safety, higher flight altitudes with lower levels of disturbance to animals and local residents, and the potential for automating counts. Recent improvements in digital camera technology may provide a promising method to accurately quantify caribou presence while flying at higher altitudes (e.g., ≥1,000 feet

agl) than currently used for visual surveys (300 or 500 feet agl). Therefore, we conducted a pilot study in 2018 and 2019 to test the feasibility of using cameras mounted on survey aircraft to identify caribou at different times of year and under a variety of environmental conditions. ABR contracted TerraSond, Inc., based in Palmer, AK, to provide the high-resolution cameras, photo processing, and digital photo interpretation. A report discussing the 2019 methodology and results was completed by TerraSond (Appendix C) and is summarized below. We used digital imagery from multiple sensors, including:

- high-resolution digital cameras (red-green-blue; RGB);
- high-resolution near infrared (NIR) sensors (2018 only); and
- thermal imagery sensors (2019 only).

We used aerial photography in conjunction with our regular aerial strip transect surveys (at 500 ft agl) as well as dedicated flights for photography to capture images at multiple angles and heights (300–2,000 feet agl) to develop and test methods. The imagery collected was assessed to determine whether caribou can be identified consistently in photographs and if the detection of caribou can be partially or fully automated. Images were screened for caribou and scripts were developed to identify the specific spectral signatures of caribou that could be applied to other images to automate the process of finding targets that had a high probability of being caribou.

REMOTE SENSING

We analyzed 2019 snow cover and 2000–2019 vegetation greenness using gridded, daily reflectance and snow-cover products from MODIS Terra and Aqua sensors. The snow-cover data were added to the data compiled for 2000–2018 (see Lawhead et al. 2015, Prichard et al. 2017, and Prichard et al. 2018 for detailed description of methods). The entire vegetation index record, based on atmospherically corrected surface reflectance data, was processed to ensure comparability of greenness metrics.

For data from 2000–2015, we applied a revised cloud mask that incorporated snow-cover history to reduce false cloud detection during the active snowmelt season. However, the automated revised cloud mask algorithm did not work on the 2016–2019 imagery due to changes in the data and data format from the aging MODIS sensors. For 2016–2019, we applied manual cloud masks for the snowmelt season and applied the standard cloud mask for images collected in June and later.

We analyzed and summarized the data using Google Earth Engine, a cloud computing service (Gorelick et al. 2017). For final analysis and visualization, we exported the results to the Alaska Albers coordinate system (WGS-84 horizontal datum) at 240-m resolution.

SNOW COVER

Snow cover was estimated using the fractional snow algorithm developed by Salomonson and Appel (2004). Only MODIS Terra data were used for snow mapping through 2016 because MODIS Band 6, which was used in the estimation of snow cover, was not functional on the MODIS Aqua sensor. However, a Quantitative Image Restoration algorithm has recently been applied to restore the missing Aqua Band 6 data to a scientifically usable state for snow mapping (Riggs and Hall 2015). The aging Terra sensor was no longer reliable for snow mapping in 2017, so we used MODIS Aqua data for snow mapping in 2017–2019. The 2019 analysis was based on MYD10A1.006 data (MODIS/Aqua Snow Cover Daily L3 Global 500 m Grid).

A time series of images covering the April–June period was analyzed for each year during 2000–2019. Pixels with >50% water (or ice) cover were excluded from the analysis. For each pixel in each year, we identified:

1. The first date with 50% or lower snow cover (i.e., “melted”);
2. The closest prior date with >50% snow cover (i.e., “snow”);
3. The midpoint between the last observed date with >50% snow cover and the first observed date with <50% snow cover, which is an unbiased estimate of the actual snowmelt date (the first date with <50% snow cover);
4. The duration between the dates of the two satellite images with the last

observed "snow" date and the first observed "melted" date, providing information on the uncertainty in the estimate of snowmelt date. When the time elapsed between those two dates exceeded a week because of extensive cloud cover or satellite sensor malfunction, the pixel was assigned to the "unknown" category.

VEGETATIVE BIOMASS

The Normalized Difference Vegetation Index (NDVI; Rouse et al. 1973) is used to estimate the biomass of green vegetation within a pixel of satellite imagery at the time of image acquisition. The rate of increase in NDVI between two images acquired on different days during green-up has been hypothesized to represent the amount of new growth occurring during that time interval (Wolfe 2000, Kelleyhouse 2001, Griffith et al. 2002). NDVI is calculated as follows (Rouse et al. 1973; http://modis-atmos.gsfc.nasa.gov/NDVI/index.html):

$$NDVI = (NIR - VIS) \div (NIR + VIS)$$

where:

NIR = near-infrared reflectance (wavelength 0.841–0.876 μm for MODIS), and

VIS = visible light reflectance (wavelength 0.62–0.67 μm for MODIS).

We derived constrained view-angle (sensor zenith angle ≤40°) maximum-value composites from daily surface reflectance composites acquired over targeted portions of the growing season in 2000–2019. The data products used were MOD09GA.006 (Terra Surface Reflectance Daily Global 1 km and 500 m) and MYD09GA.006 (MYD09GA.006 Aqua Surface Reflectance Daily L2G Global 1 km and 500 m). NDVI during the calving period (NDVI_Calving) was calculated from a 10-day composite period (1–10 June) for each year during 2000–2019 (adequate cloud-free data were not available to calculate NDVI_Calving over the entire study area in some years). NDVI values near peak lactation (NDVI_621) were interpolated based on the linear change from two composite periods (15–21 June and 22–28 June) in each year. NDVI_Rate was calculated as the linear change in NDVI from NDVI_Calving to NDVI_621 for each year. Finally, NDVI_Peak was calculated from all imagery obtained between 21 June and 31 August each year during 2000–2019. Due to the availability of new forage models, NDVI_Calving, NDVI_621, NDVI_Rate, and NDVI_Peak were not included in analyses of caribou distribution in 2019, but we included summaries of these metrics in this report for comparison with previous reports.

FORAGE MODELING

We applied forage models from Johnson et al. (2018) that incorporate daily NDVI values as well as habitat type, distance to coast, and days from peak NDVI to predict biomass, nitrogen, and digestible energy for a given location on a given day. These models may provide metrics that are more directly related to caribou forage needs than NDVI alone.

We used the MCD43A4.Version 6 daily product at 500-m resolution (Schaaf and Wang 2015). This is the Nadir Bidirectional Reflectance Distribution Function Adjusted Reflectance (NBAR) product, and it provides 500 meter reflectance data that are adjusted using a bidirectional reflectance distribution function (BRDF) to model the reflectance values as if they were collected from a nadir view (i.e., viewed from directly overhead). The NBAR data are produced daily within 16-day retrieval periods using data from both MODIS platforms (i.e., the Terra and Aqua satellites). The product is developed using a single observation from each 16-day period for each 500 m pixel, with priority given to the central day in each compositing period (i.e., the ninth day) to provide the most representative information possible for each period of the year. Other observations in the period are used to parameterize the BRDF model that is required to adjust the observation to nadir. Similar to other MODIS vegetation index products such as MOD13Q1, it has a 16-day composite period, but unlike other products it has a temporal frequency of one day, with the 16-day window shifting one day with each new image. Thus it avoids any artificial steps at the break between composite intervals, and is a good tool to assess daily phenology normals. It is more likely to provide an observation for a given day

than true daily products such as the MOD09GA.006/MYD09GA.006 products used for the NDVI composite metrics (above).

Johnson et al. (2018) calibrated the forage models for 4 broad vegetation classes (tussock tundra, dwarf shrub, herbaceous mesic, and herbaceous wet). Following their approach, we used the Alaska Center for Conservation Science (ACCS) land cover map for northern, western, and interior Alaska (Boggs et al. 2016), aggregated on the "Coarse_LC" attribute. This map is based on the North Slope Science Initiative mapping effort (NSSI 2013) with the addition of the aggregation field. We calculated the modal land cover class for each 500-m pixel.

For each date from the start of the calving season through the end of the late summer season (30 May–15 September) and for each year with telemetry locations (2002–2019) we mapped daily NDVI (dNDVI), annual NDVIMax, and days to NDVIMax. Then, we applied the equations from Johnson et al. (2018) to calculate daily forage nitrogen content, and forage biomass for the 4 broad vegetation classes. We set the forage metrics to zero for water, snow/ice, and barren classes and set it to undefined for other vegetation classes that were not included in the Johnson et al. (2018) models. The areas with undefined forage metrics within the study area were primarily low and tall shrub, which compose a small proportion of the surface area.

HABITAT CLASSIFICATION

We used the NPRA earth-cover classification created by BLM and Ducks Unlimited (2002) for habitat classification for analyses (Figure 3). The BTN and BTS survey areas contained 15 cover classes from the NPRA earth-cover classification (Appendix A), which we lumped into nine types to analyze caribou habitat use. The Barren Ground/Other, Dunes/Dry Sand, Low Shrub, and Sparsely Vegetated classes, which mostly occurred along Fish and Judy creeks, were combined into a single Riverine habitat type. The two flooded-tundra classes were combined as Flooded Tundra and the Clear-water, Turbid-water, and *Arctophila fulv*a classes were combined into a single Water type; these largely aquatic types are used very little by caribou, so the Water type was excluded from the analysis of habitat preference.

RESOURCE SELECTION ANALYSIS

Caribou group locations were analyzed with respect to multiple factors including habitat, snow-cover classes, longitude, distance to coast, estimated daily values of vegetative NDVI, estimated annual maximum values of vegetative NDVI, forage nitrogen content, and forage biomass. We evaluated the relationship of those factors to caribou distribution by using resource selection function (RSF) models (Boyce and McDonald 1999, Manly et al. 2002). RSF models allow simultaneous comparison of selection for multiple variables and incorporation of caribou locations from both aerial surveys and radio telemetry. RSF models compare actual locations with random locations (use vs. availability). They are a useful tool for quantifying important factors influencing habitat selection during different seasons and for assessing relative importance of different areas to caribou based on the spatial pattern of those factors.

We used group locations from aerial surveys and locations from GPS-collared individuals for the RSF analysis. Locations of satellite-collared animals were not used due to the lower accuracy of those locations. We used caribou locations from aerial transect surveys conducted during 2002–2018 in the BTN, BTS, and GMT combined survey areas, but the seasonal sample sizes for the Colville River Delta survey area were too small to support RSF analysis. The available telemetry data spanned the period 11 May 2003–31 December 2019 and were filtered to include only locations falling within the aerial survey area. To standardize the time between GPS-collar locations, maintain an adequate sample size, and reduce the effect of autocorrelation on results, we subsampled GPS locations at 48-h intervals in all seasons. We assumed that 48 h was enough time for a caribou to move across the entire study area, so autocorrelation would be minimal (Lair 1987, McNay et al. 1994). We excluded caribou locations in waterbodies on the habitat map and in areas that were excluded from the NDVI calculations because they were predominantly water-covered.

To estimate resource selection, we used logistic regression (Manly et al. 2002). For each actual caribou or caribou group location, we generated 25 random locations in non-water

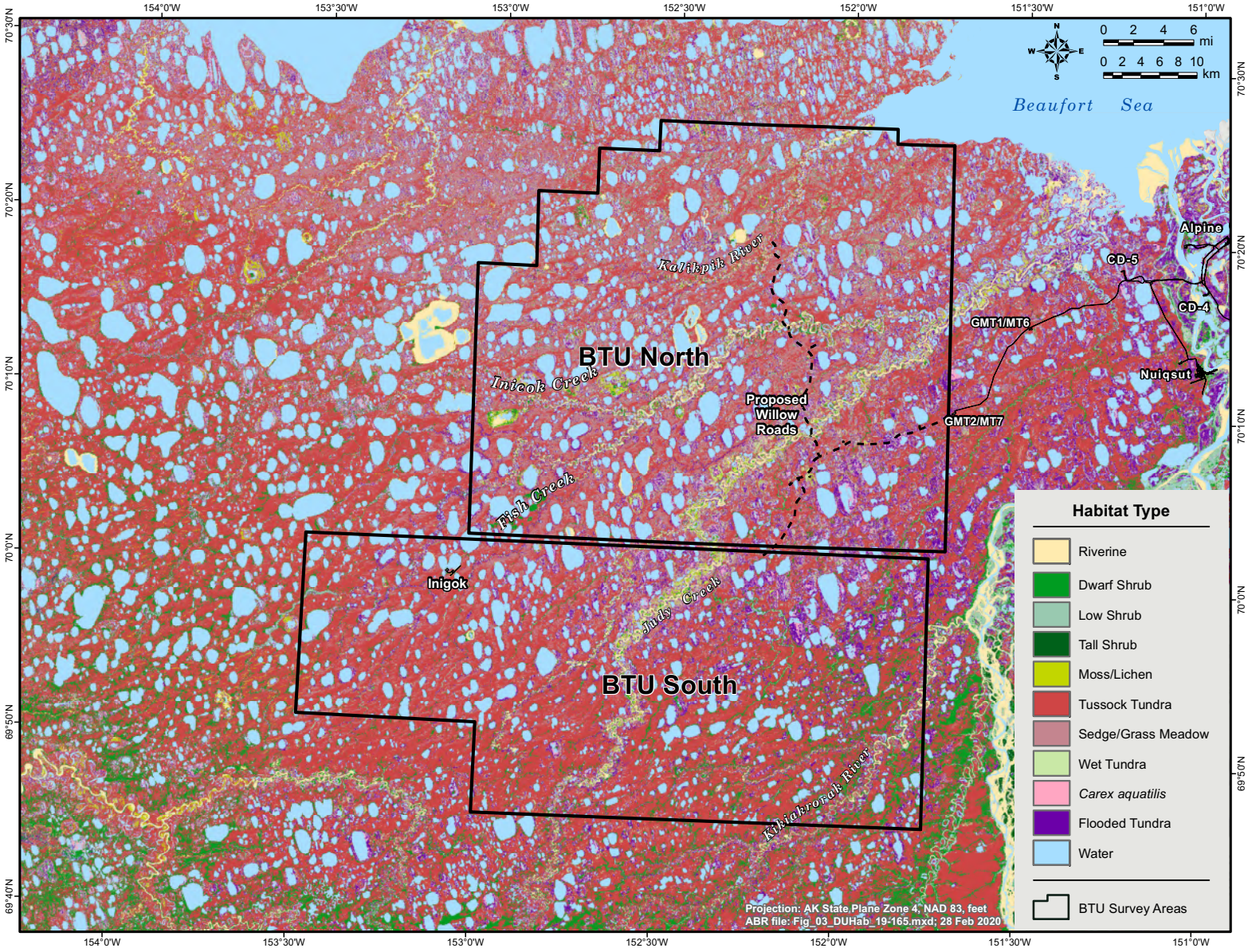

Figure 3. Habitat types used for caribou habitat-selection analysis in the Bear Tooth Unit study areas, National Petroleum Reserve-Alaska.

habitats within the same survey area as the actual location. We were therefore testing for selection at the level of specific areas or attributes for animals that were within the survey area. For this analysis we use the terms "selection" and "avoidance" to refer to attributes that are used more or less than expected by caribou, when compared with random points.

We ran logistic regression models to compare actual caribou locations to random locations using the nine explanatory variables: habitat type (merged into the eight non-water categories; Figure 3); daily NDVI, daily nitrogen, daily biomass, and maximum NDVI for each respective day and year the group location was recorded (calculated across 500 m pixels); landscape ruggedness (Sappington et al. 2007; calculated over a 150-m by 150-m box centered at each 30-m pixel); the median snow-free date (date at which the pixel is typically snow-free; Macander et al. 2015); distance to coast; and west-to-east distribution. We used the natural logarithm of the landscape ruggedness variable to account for a skewed distribution (most values close to one) in that variable. The median snow-free date was used only for the winter, spring migration, and calving seasons, and daily NDVI, nitrogen, and biomass variables were used only for the calving, postcalving, mosquito, oestrid fly, and late summer seasons.

All locations were tested for collinearity between explanatory variables by calculating variance inflation factors (VIF) using the *corvif* function from the package AED in *R* (Zuur et al. 2009). In addition, continuous variables were scaled (subtracted the mean and divided by the standard deviation) to aid in model convergence and parameter interpretation (Zuur et al. 2009). Because aerial survey data had low spatial precision (estimated error 100–200 m) compared to the habitat map (30-m pixels), we calculated the most common habitat in a 210-m by 210-m area (7 × 7 pixels) centered on the estimated group location.

For each season, we tested all combinations of the variables (no interactions were included) using the *glmulti* package in *R* (Calcagno and de Mazancourt 2010) using Akaike's Information Criterion adjusted for small sample sizes (AICc) to compare models. We calculated the unconditional (model-weighted) coefficients and standard error (SE) of each parameter by calculating a weighted average of different models that was weighted by the probability that each model was the best model in the candidate set (Akaike's weight; Burnham and Anderson 2002).

We tested the fit of the best models for each season using *k*-fold cross-validation (Boyce et al. 2002). At each step, we withheld one-fifth of the caribou locations (testing data) and calculated relative probabilities of use for locations used by those caribou based on the remaining data (training data). We repeated this process five times; i.e., for each one-fifth of the caribou locations. We used the mean Pearson's rank correlation coefficient for the five testing data sets as a measure of model fit.

For each season, we created a map of the relative probability of use of the survey area based on the multi-year model output from the RSF models. We used the model-weighted parameter estimates from all independent variables that had a 50% or greater probability of being in the best model (e.g., the sum of all Akaike weights for all models that included the variable was >0.5). We used daily NDVI, and calculated nitrogen and biomass for the midpoint of each season in 2019 and maximum NDVI in 2019 as inputs of these variables for mapping purposes.

RESULTS

WEATHER CONDITIONS

Spring 2019 was warmer than the 35-year average (1983-2018) and snow melted earlier than usual at the Kuparuk airport (Figure 4, Appendix B). May temperatures were near or above the 1983–2018 average with daily temperatures rising above freezing on 21–25 May. Snow depth at the Kuparuk airstrip remained below or near average until 20 May before completely melting by 23 May when temperatures warmed. Temperatures were near average during the calving and postcalving periods in early and mid-June. Other weather stations are located closer to the study area (CD5, Nuiqsut, Alpine, Colville Village), but those datasets cover a shorter period of time and they do not all measure snow depth. While specific temperature and snow depth values may differ by station, the seasonal trends are generally similar among stations. Survey crews flying 3–5 June

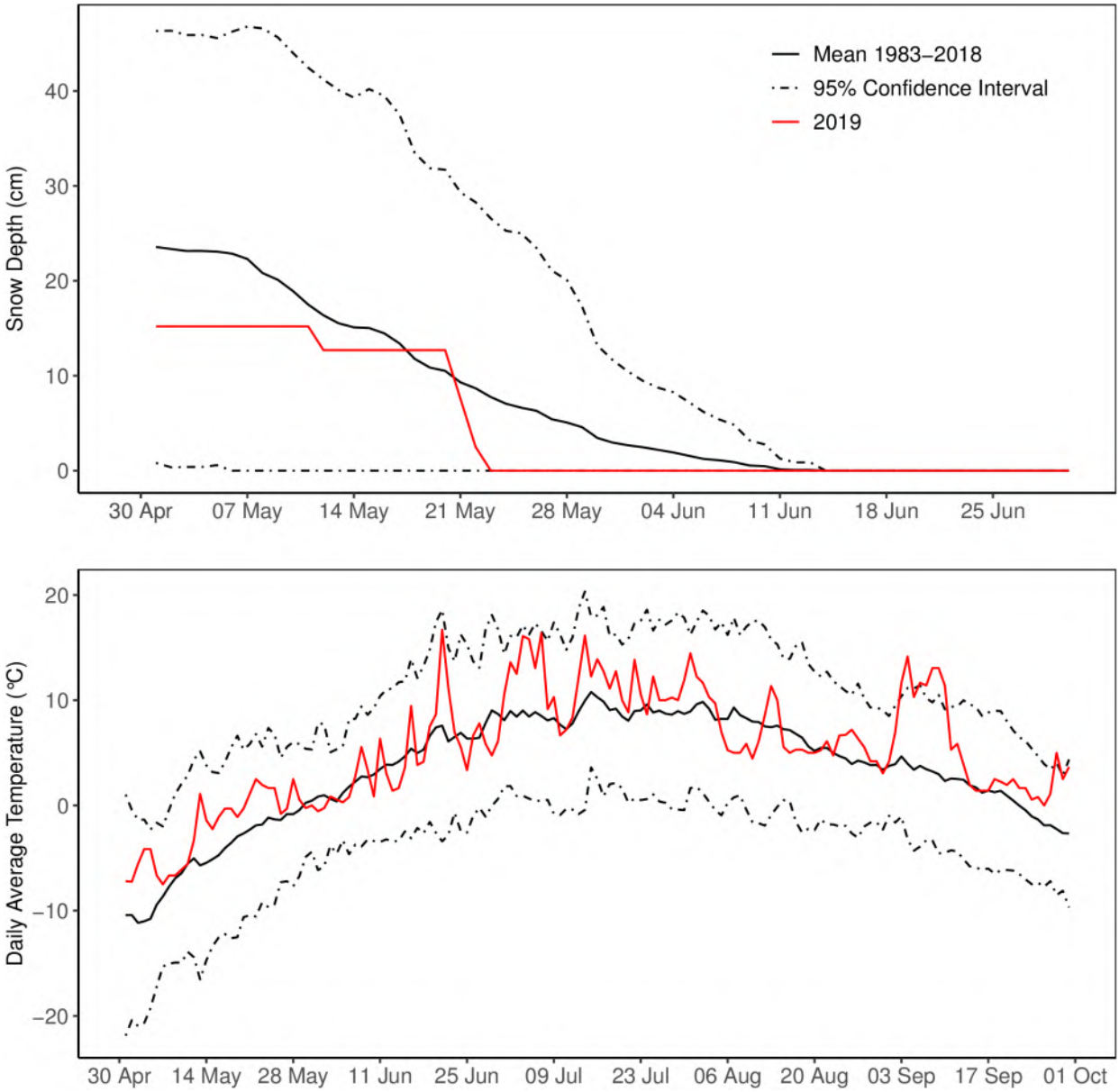

Figure 4. Snow depth, long-term mean (1983–2018), and 95% confidence interval at the Kuparuk airstrip, May–June 2019 (top) and daily average air temperature, long-term mean, and 95% confidence interval at Kuparuk, May–September 2019 (bottom).

confirmed that most inland areas were snow free and only the northern few miles of the BTN and GMT survey areas had substantial areas of patchy snow.

Mosquitos in the study area usually emerge from the middle of June through early July, whereas oestrid flies do not generally emerge until mid-July. Daily air temperatures in mid- and late June were near average, but a warm period with temperatures near the upper 95% confidence limit starting June 21 led to a high probability of insect activity for several days (Figure 5). ABR biologists conducting ground-based surveys for other projects near the Colville River delta reported noticeable mosquito activity starting around the 23 June, but cooler temperatures kept mosquito activity low until their departure on 27 June.

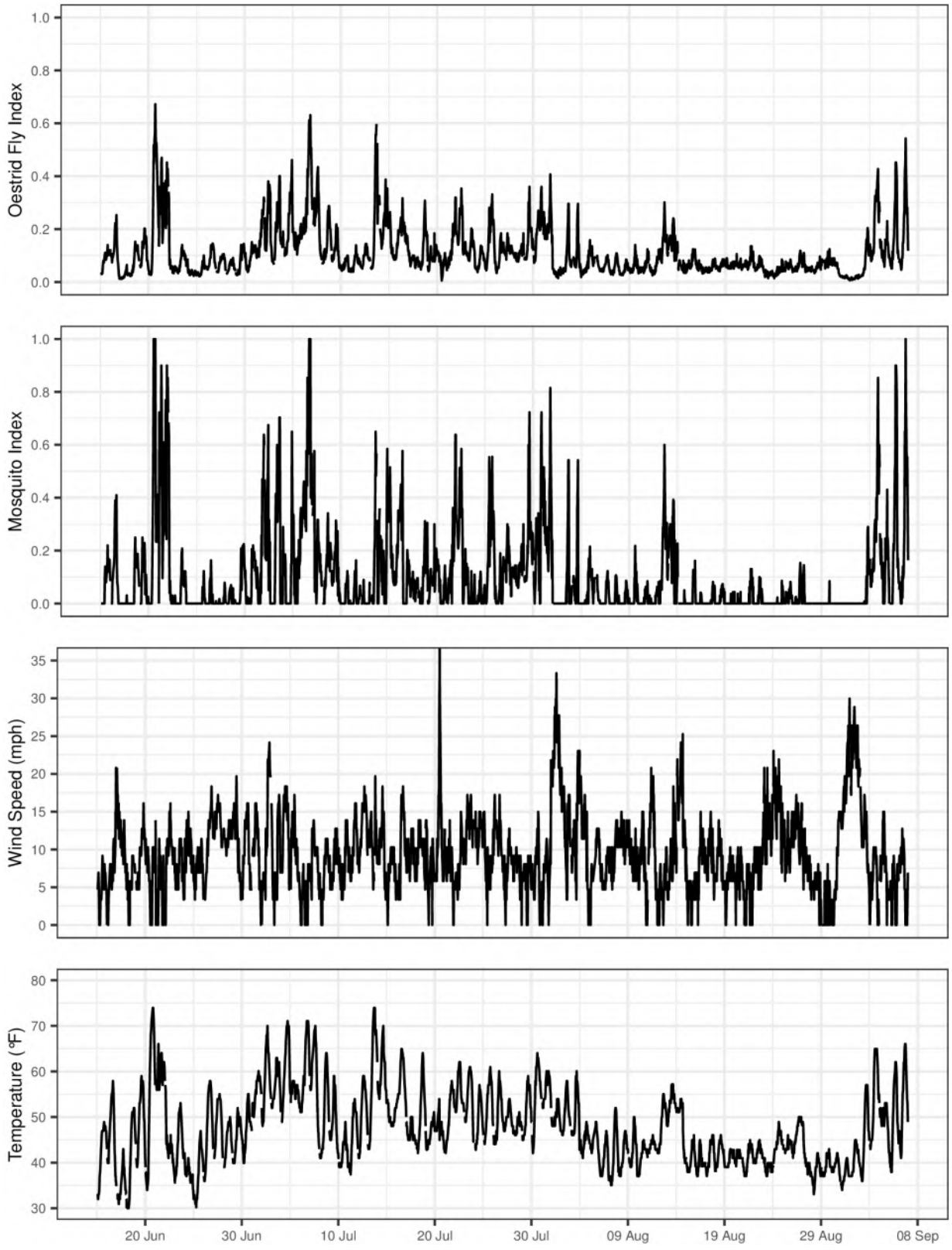

Figure 5. Hourly air temperature, wind speed, mosquito probability index, and oestrid fly probability index at Nuiqsut, 15 June–7 September 2019.

The remainder of the 2019 insect season generally had average temperatures in late June and well above average temperatures in July. August temperatures were near the long-term average (Figure 4, Appendix B). Similar to these temperature trends, the average estimated mosquito and fly activity started out near average in June, increased to above average in July, and were near average again for August. Although, insects are likely to be less prevalent by September, early September temperatures in 2019 were well above average. These patterns resulted in 16 days with a high probability of mosquito harassment and 4 days with a high probability oestrid fly activity (>50% probability; Figures 5), although only two days with expected high oestrid fly activity occurred during the period when oestrid flies are typically active (mid-July to mid-August).

CARIBOU DISTRIBUTION AND MOVEMENTS

AERIAL TRANSECT SURVEYS

BTN Survey Area

Seven aerial surveys of the BTN survey area were attempted between 14 April and 3 October 2019 (Figure 6). The late winter surveys in April were only partially completed due to inclement weather, and no mosquito season survey was planned, but all other surveys of the BTN survey area were completed as scheduled. The estimated density ranged from a high of 1.78 caribou/km² during the 30 September–3 October survey to a low of <0.06 caribou/km² during the 29–31 July survey (Table 2). Assuming a TCH population size of 56,255, ~6.7% of the herd was estimated to be in the BTN survey area during the fall migration

Table 2. Number and density of caribou in the Bear Tooth North and Bear Tooth South survey areas, April–September 2019.

Survey Area and Date	Total Area (km²)[a]	Observed Large Caribou[b]	Observed Calves[c]	Observed Total Caribou	Mean Group Size[d]	Estimated Total Caribou[e]	SE[f]	Density (caribou/km²)[g]
BTN								
April 14	1,483	542	nr	542	4.2	1,084	72.7	0.73
May 13–16	2,122	88	nr	88	4.0	176	44.9	0.08
June 3–5 (East)	999	55	4	59	2.4	118	20.9	0.12
June 3 (West)	561	123	8	131	3.4	524	84.3	0.93
June 18–19	2,122	1,133	2	1,135	6.1	2,270	148.1	1.07
July 29–31	2,122	67	nr	67	1.1	134	16.2	0.06
August 27	2,122	176	nr	176	2.1	352	44.8	0.17
Sept 30– Oct 3	2,122	1,884	nr	1,884	8.2	3,768	386.1	1.78
BTS								
April 14	414	102	nr	102	3.8	306	132.3	0.74
May 13–16	1,747	72	nr	72	8.0	216	54.7	0.12
June 3–5	1,747	221	3	224	3.7	672	110.1	0.38
June 18–19	1,747	189	1	190	4.9	570	308.3	0.33
July 29–31	1,747	18	nr	18	1.1	54	30.4	0.03
August 26	1,747	244	nr	244	2.8	732	132.6	0.42
October 3	641	301	nr	301	9.1	903	586.3	1.41

[a] Survey coverage was 50% of this area in BTN, 25% in BTN West on June 6–8, and 33% in BTS.
[b] Adults + yearlings.
[c] nr = not recorded; calves not differentiated reliably due to larger size.
[d] Mean Group Size = Observed Total Caribou ÷ number of caribou groups observed.
[e] Estimated Total Caribou = Observed Total Caribou adjusted for survey coverage.
[f] SE = Standard Error of Estimated Total Caribou, calculated following Gasaway et al. (1986), using transects as sample units.
[g] Density = Estimated Total Caribou ÷ Area.

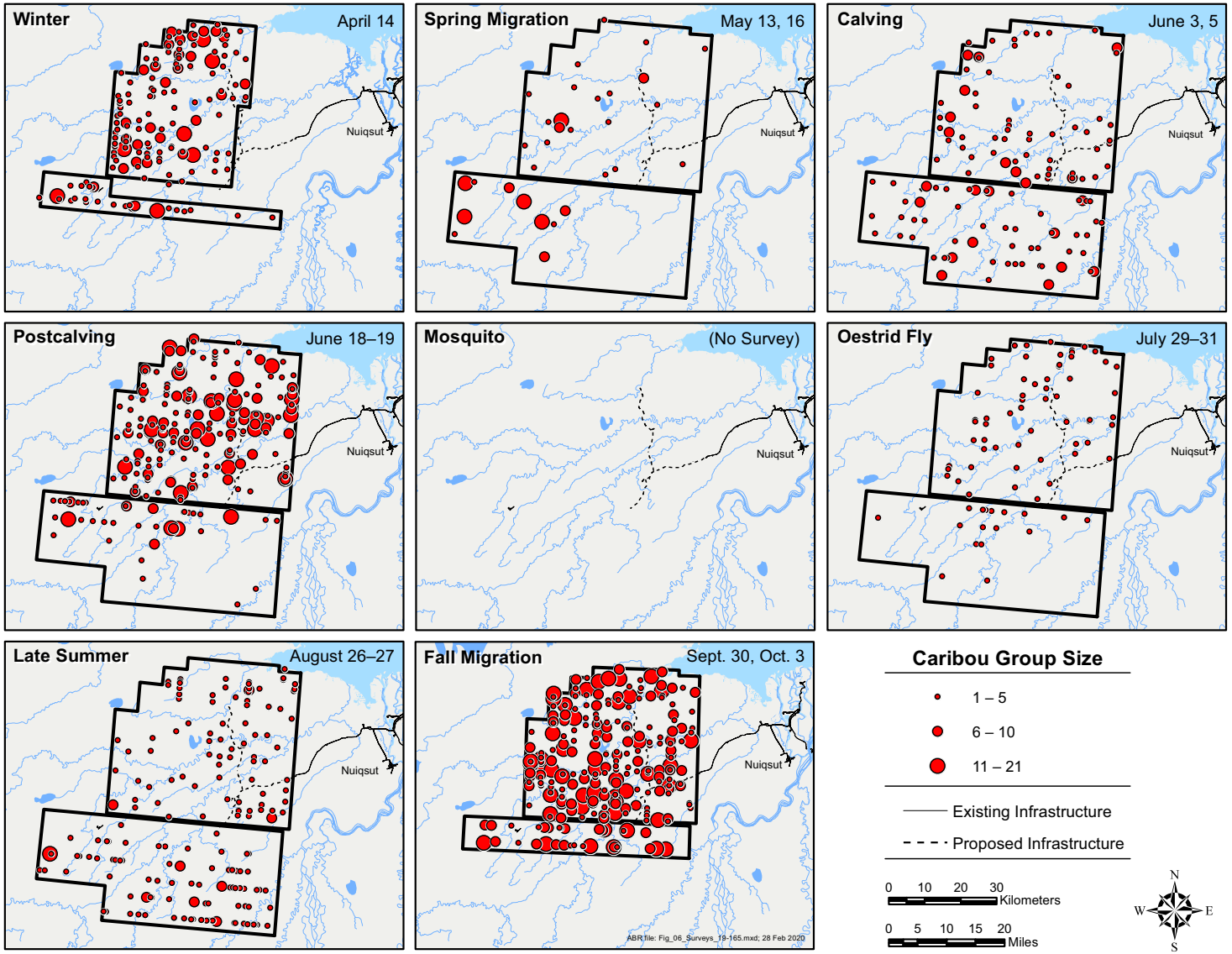

Figure 6. Distribution and size of caribou groups during each of seven seasons in the Bear Tooth North and Bear Tooth South survey areas, April–October 2019.

survey. Only 12 calves were observed in the BTN survey areas during the calving survey (Table 2).

BTS Survey Area

Seven aerial surveys of the BTS survey area were attempted between 14 April and 3 October 2019 (Figure 6). The late winter survey in April and the fall migration survey in October were only partially surveyed due to inclement weather, but all other surveys of the BTS survey area were completed as scheduled. We only observed 3 calves during the calving survey and one calf during the postcalving survey. The estimated density of caribou in BTS ranged from a high of 1.41caribou/km² in October to a low of 0.03 caribou/km² on 29–31 July (Table 2).

Seasonal trends in density were similar to those observed in 2018 in both survey areas with a few exceptions (Prichard et al 2019d). In the BTN survey area in 2018, densities during the late summer survey were three times higher than those observed in 2019, and although densities were highest during the fall survey in both years, densities were twice as high in 2019 as in 2018. The density during calving in 2019 (0.93 caribou/km²) was similar to the calving density in 2018 (0.74 caribou/km²; note—this density was incorrectly reported in Prichard et al. (2019d) due to an error in calculation of the area surveyed). In the BTS survey area, caribou densities increased dramatically from very low levels during the calving season (0.09 caribou/km²) to moderate densities a few weeks later in the postcalving survey during 2018 (0.80 caribou/km²; Prichard et al. 2019d). This result is in contrast to 2019 when densities remained relatively constant for both surveys (0.33–0.38 caribou/km²).

Results from the seasonal density mapping of caribou recorded on aerial surveys of the NPRA/BTN & BTS survey area during 2002–2019 also showed large differences among seasons (Figure 7). Densities of caribou have been highest in the western BTN and northern BTS survey areas. Caribou are most widely distributed across the area during fall migration. The highest mean density was observed during the oestrid fly season, but results from that season were highly influenced by several very large groups that were observed in 2005.

RADIO TELEMETRY

Radio collars provide detailed location and movement data throughout the year for a small number of individual caribou. The telemetry data also provide valuable insight into herd affiliation and distribution, which is not available from transect surveys. Mapping of the telemetry data from PTT and GPS collars clearly shows that the study area is located at the eastern edge of the annual range of the TCH and west of the annual range of the CAH (Figures 8–11).

Kernel Density Analysis

Seasonal concentration areas were analyzed using fixed-kernel density estimation, based on locations from satellite and GPS collars deployed on 273 TCH females and 89 TCH males during 1990–2019 and on 138 CAH females and 8 CAH males during 2001–2019. These numbers differ from the number of collar deployments listed earlier (Table 1) because some individuals switched herds after collaring. Kernels were used to produce 50%, 75%, and 95% utilization distribution contours (isopleths), which were assumed to correspond to density classes (high, medium, and low density) for female CAH caribou and for male and female TCH caribou (Figures 8–10); the sample size of CAH males was too small to conduct this analysis for males separately. Although these analyses use data covering 20–30 years, the results are more heavily weighted by the most recent years when more collars were deployed.

Female CAH caribou generally wintered between the Dalton Highway/TAPS corridor and Arctic Village, migrated north in the spring to calve in two areas on either side of the Sagavanirktok River, spent the mosquito season near the coast (mostly east of Deadhorse), and dispersed across the coastal plain on both sides of the Sagavanirktok River and Dalton Highway/TAPS corridor during the oestrid fly and late summer seasons (Figure 8).

TCH caribou generally wintered on the Arctic Coastal Plain between Nuiqsut and Wainwright or in the central Brooks Range near Anaktuvuk Pass, migrated to their calving grounds near Teshekpuk Lake, and spent the rest of the summer on the coastal plain, primarily between Nuiqsut and

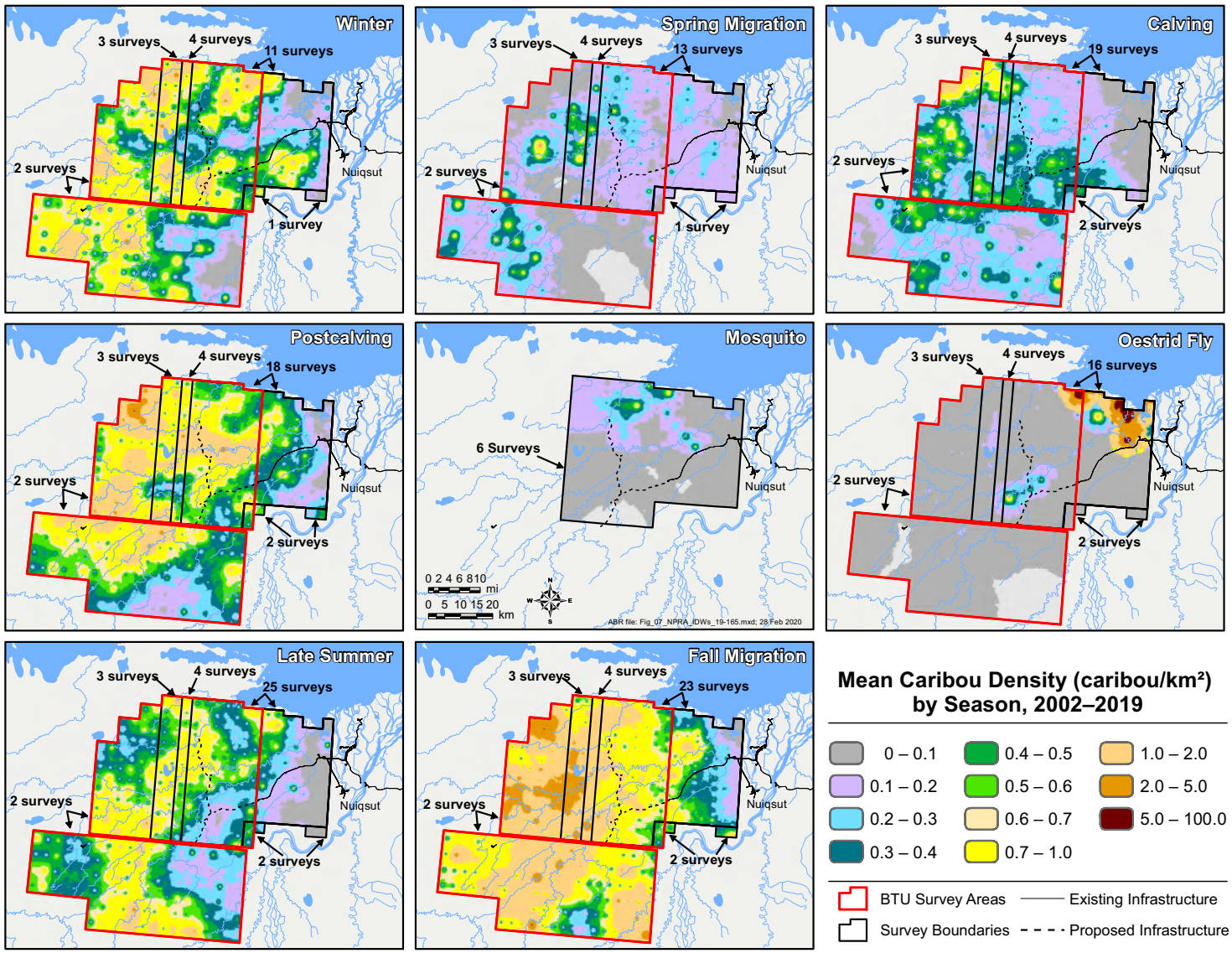

Figure 7. Mean seasonal densities of caribou in the NPRA caribou survey areas based on inverse distance-weighting interpolation of aerial survey results, 2002–2019.

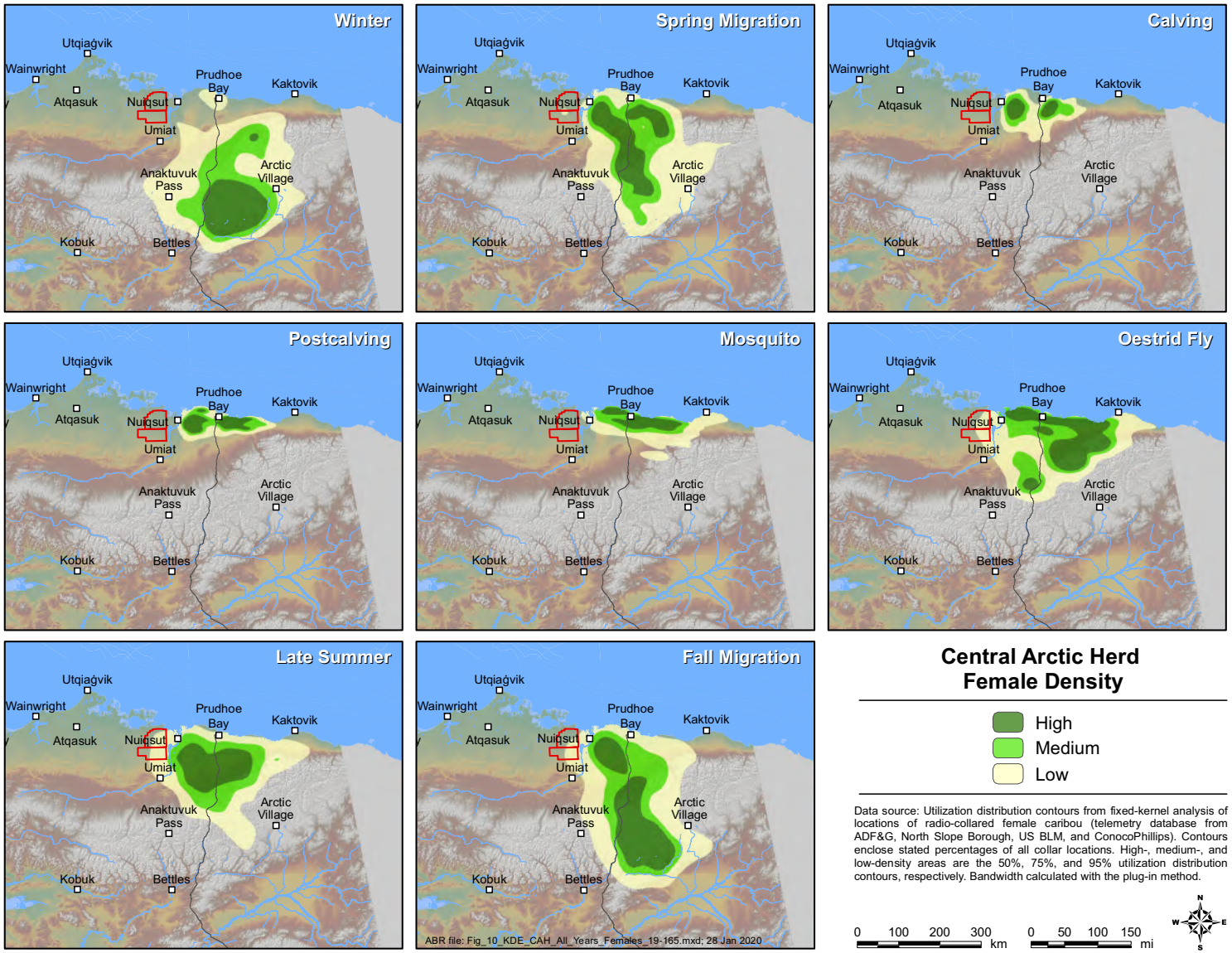

Figure 8. Seasonal distribution of Central Arctic Herd female caribou based on fixed-kernel density estimation of telemetry locations, 2001–2019.

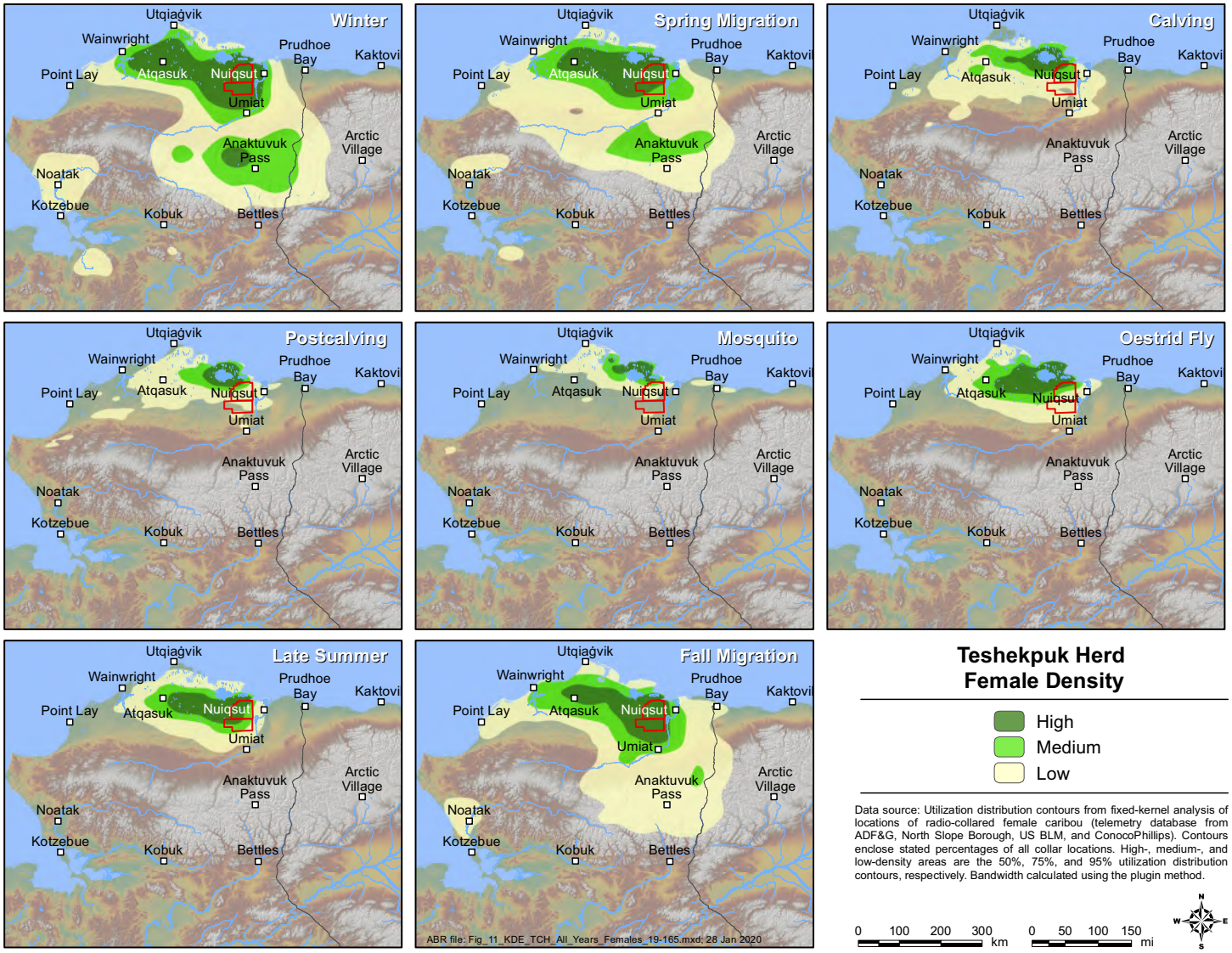

Figure 9. Seasonal distribution of Teshekpuk Caribou Herd females based on fixed-kernel density estimation of telemetry locations, 1990–2019.

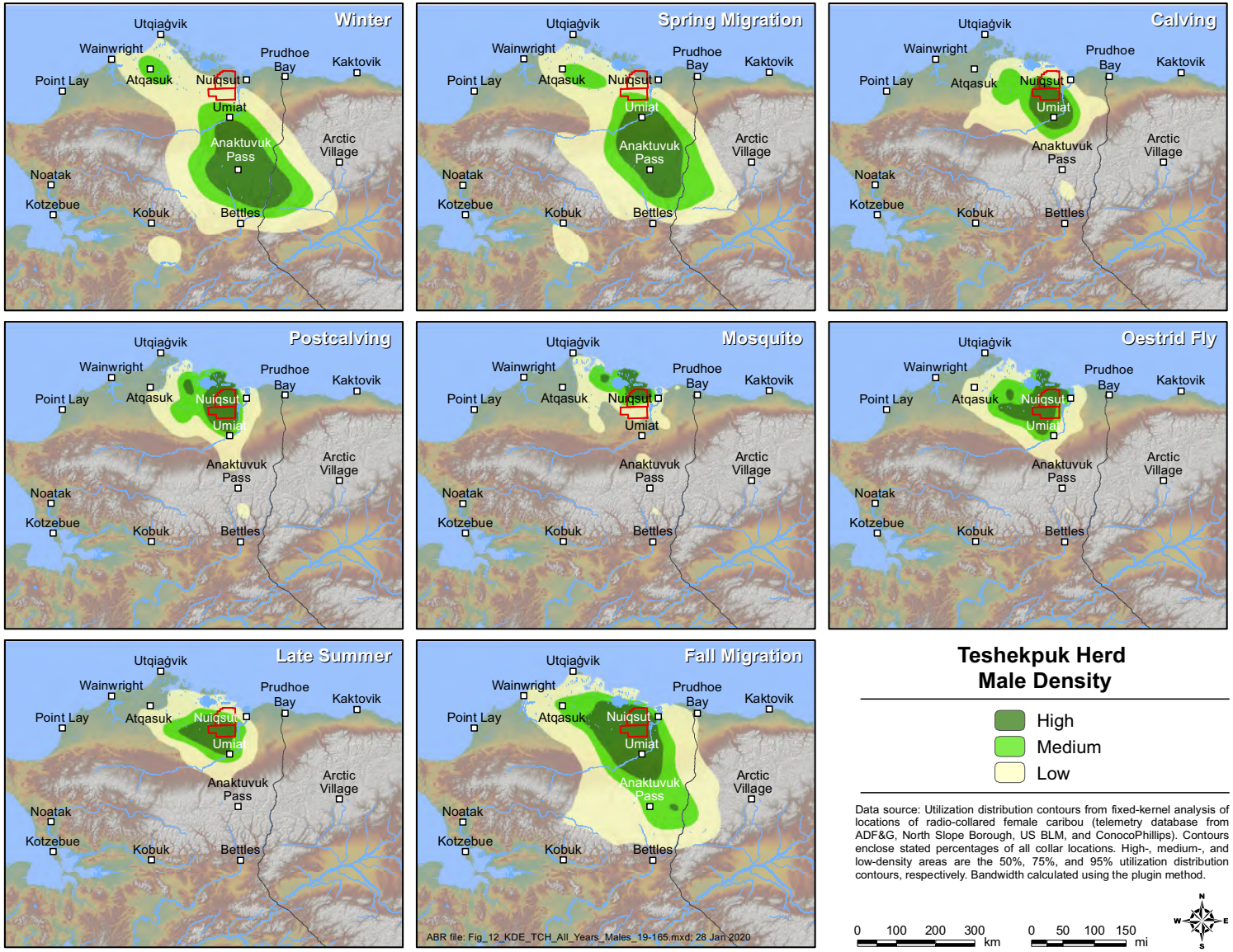

Figure 10. Seasonal distribution of Teshekpuk Caribou Herd males based on fixed-kernel density estimation of telemetry locations, 1997–2019.

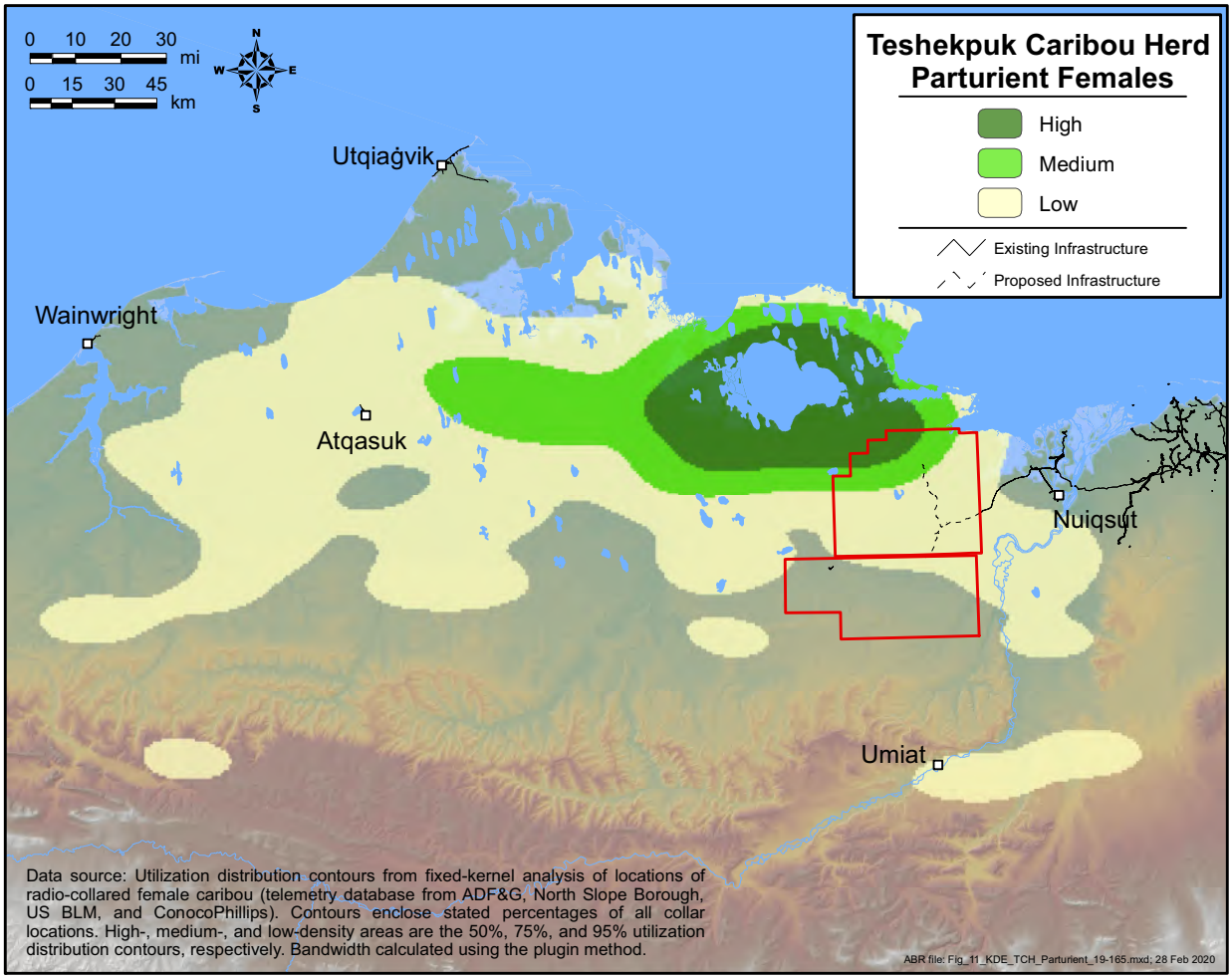

Figure 11. Distribution of parturient females of the Teshekpuk Caribou Herd during calving based on fixed-kernel density estimation of telemetry locations, 1990–2019.

Atqasuk (Figures 9–10). Compared with females, males were more likely to overwinter in the central Brooks Range instead of on the coastal plain. Males migrated to the summer range later in the year during the calving and postcalving seasons and were not distributed as far west during summer (Figures 10). The distribution of parturient TCH females during calving (Figure 11) was similar to the distribution of all TCH females during calving (Figure 9), but was more concentrated around Teshekpuk Lake.

The BTN survey area was squarely within the 95% utilization distribution of female TCH caribou from fall migration through spring migration and within at least the 50% utilization distribution in all other seasons (Figures 9). As a result, 4.1–13.8% of female TCH caribou (based on the proportion of the utilization distribution) are expected to be in the survey area at any time during the year, with the highest levels of use expected during September (Figure 12). Use of the BTN survey area by TCH males increased sharply from May to a peak in July (14.6% of the utilization distribution) during the oestrid fly season. Use by males dipped in August (5.0%) but then rose again in September (10.8%) during the onset of the fall migration before dropping below 1% by November as males migrated into the foothills and mountains of the Brooks Range or toward Atqasuk during the winter (Figure 12). In contrast, there was almost no use (0.0%–0.8%) of the BTN survey area by collared CAH females throughout the year (Figure 12).

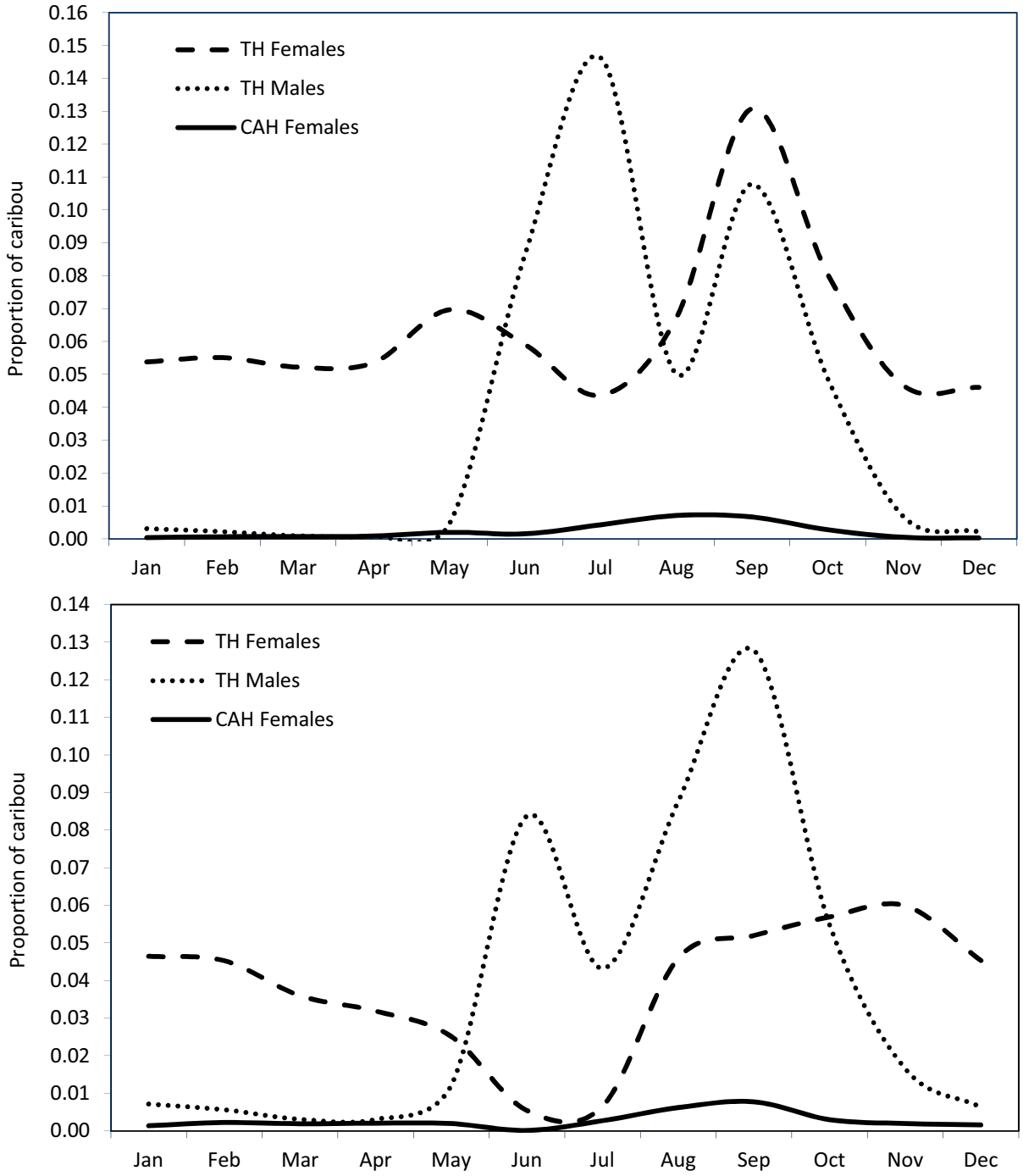

Figure 12. Proportion of Central Arctic Herd (CAH) and Teshekpuk Caribou Herd (TCH) caribou within the Bear Tooth Unit-North (top) and Bear Tooth Unit-South (bottom) survey areas, based on fixed-kernel density estimation, 1990–2019.

TCH females used the BTS survey area to a similar or lesser extent than the BTN survey area in all months (0.5–6.0% of the population based on the proportion of the utilization distribution; Figure 12). The main differences are apparent in May, June, and July when utilization of the BTS drops off dramatically. Caribou are located closer to Teshekpuk Lake from pre-calving through the mosquito season. The difference is also apparent in September when more caribou are located in the BTN survey area. Use of the survey area by males followed a similar pattern to use of the BTN survey area by females with little use from November through May (0.3%–1.7%) when males are in their winter ranges, and moderate use (4.3%–12.8%) from June through October. When compared to the BTN survey area, use of the BTS by males was similar in June as males are still migrating north from their winter range, lower in July when caribou are closer to the coast for mosquito relief, and higher in August and September when caribou disperse inland as insect harassment abates. There was almost no expected use (0.0%–0.8%) of the BTS survey area by collared CAH females throughout the year (Figures 8 and 12).

Movement mapping

Mapping of movements by TCH caribou in the study area derived from the dBBMMs corroborates the results from the KDE analysis, but provides more high-resolution details. The models show that TCH females use the BTU survey areas during all seasons, although their use of the area and movement rates vary widely among seasons (Figure 13). During winter, caribou are distributed widely but exhibit low rates of movement. During the spring migration and calving seasons, TCH females move across the study area from southeast to northwest as they migrate toward the core calving area bordering Teshekpuk Lake. During the postcalving and mosquito seasons, caribou largely remain west and north of the study area, often traversing the narrow corridors between Teshekpuk Lake and the Beaufort Sea (Yokel et al. 2009). During the oestrid fly season, TCH females move rapidly and often disperse inland away from Teshekpuk Lake, with occasional large movements through the survey areas. During late summer, caribou are usually found dispersed inland throughout much of both survey areas. TCH caribou disperse even more widely during fall migration. While many caribou move through the BTS area, movements are more rapid and fewer animals remain there compared to BTN, which is likely because animals to the south are more likely to be migrating towards the Brooks Range instead of remaining on the North Slope.

MOVEMENTS NEAR PROPOSED WILLOW INFRASTRUCTURE

Consistent with the location of existing infrastructure on the eastern edge of the TCH range, movements by collared TCH and CAH caribou near proposed Willow infrastructure have occurred more frequently than movements near existing infrastructure in the GMT and CRD survey areas to the east (Figure 14). Percentages of utilization distributions within 4 km of roads and pads ranged from 0.0%–2.8% with notable differences by sex (Figure 15). Males were most likely to be within 4 km of proposed roads and pads from July through October with almost no occurrence after the fall migration, whereas females maintained a similar presence for most of the winter months, decreased occurrence in June and July, and increased occurrence in September and October.

Analysis of GPS collars from 2002 through 2019 indicates that there were 651 crossings of the proposed Willow road alignment (Table 3; Figure 14). Up to 13% of collared caribou cross the proposed Willow road alignment in a given season (Table 3). The highest proportion of collared caribou crossings was during the fall migration season (mean = 13%; annual range = 5–46%), followed by winter (mean = 8%; annual range = 1–28%), and the oestrid fly season (mean = 6%; annual range = 0–36%). The lowest proportion of TCH crossings was during the postcalving (mean = 2%; annual range = 0–4%) and mosquito seasons (mean = 1%; annual range = 0–3%).

AERIAL PHOTOGRAPHY

Flights to test the feasibility of using imagery collected from aircraft mounted cameras to identify caribou continued in 2019. TerraSond provided a report detailing the results of those efforts (Appendix C). Building on lessons learned in 2018, TerraSond conducted one test flight prior to the May aerial survey to confirm that flying at 440 m

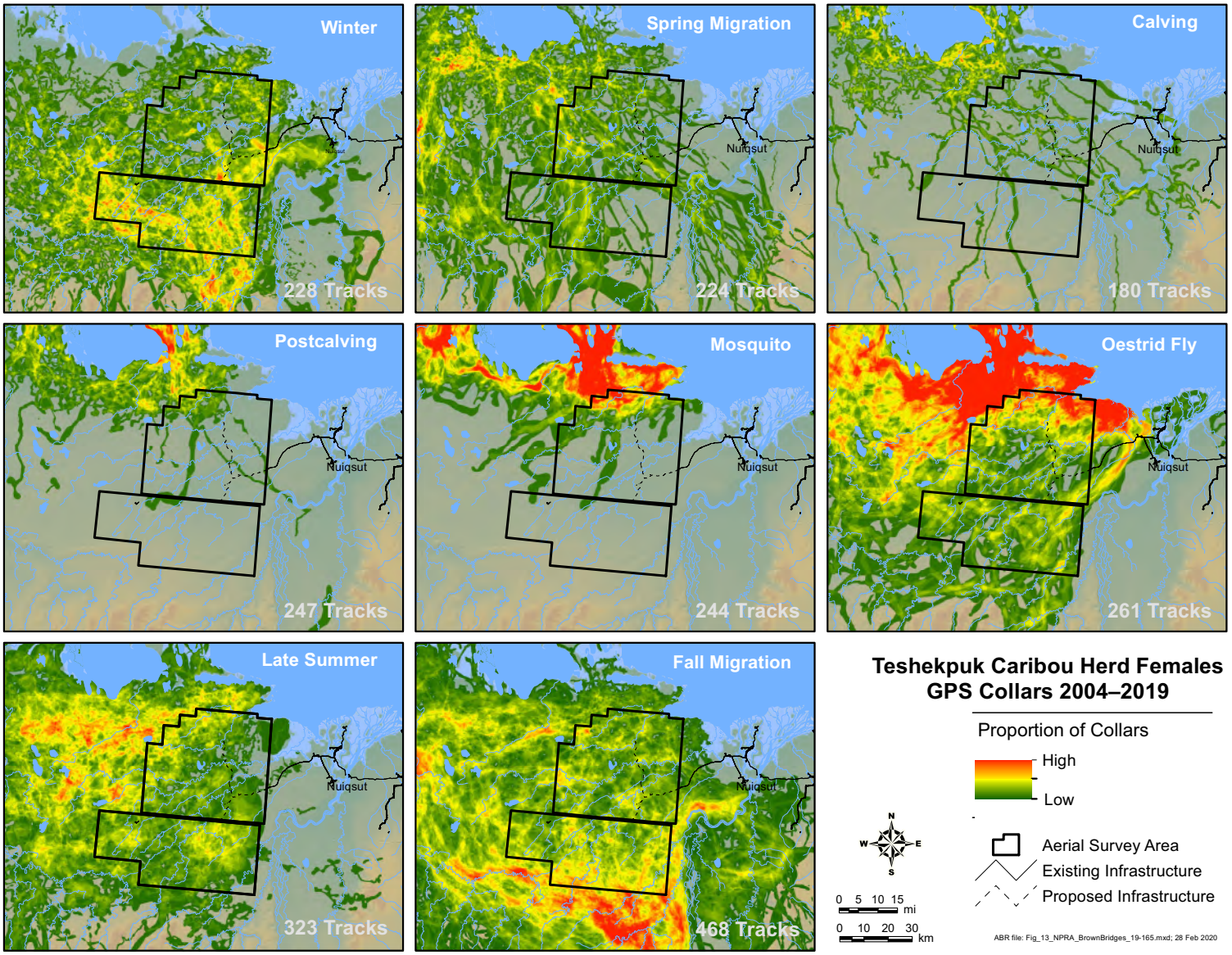

Figure 13. Movements of GPS-collared Teshekpuk Caribou Herd based on 95% isopleths of dynamic Brownian Bridge movement models.

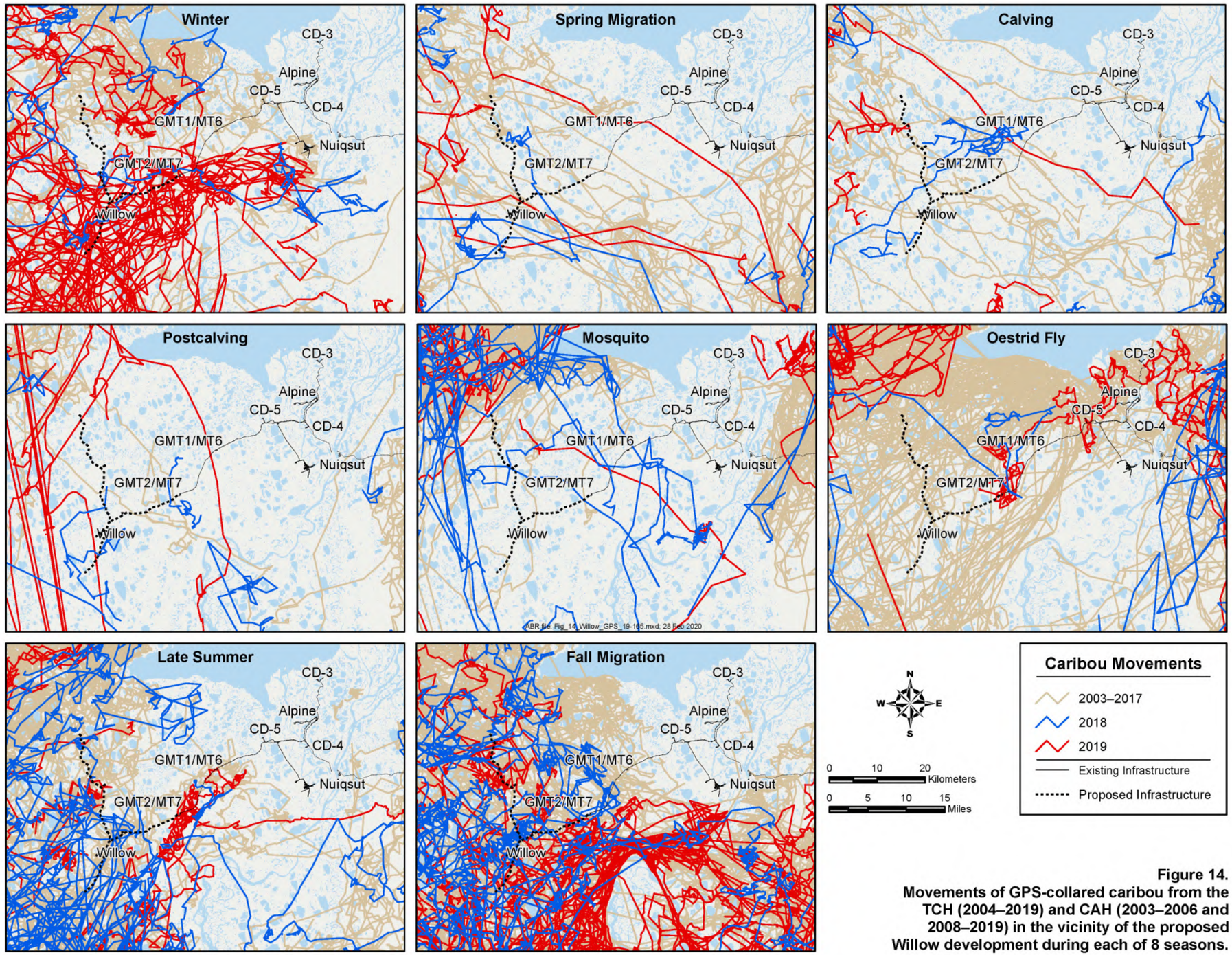

Figure 14.
Movements of GPS-collared caribou from the TCH (2004–2019) and CAH (2003–2006 and 2008–2019) in the vicinity of the proposed Willow development during each of 8 seasons.

Page intentionally left blank.

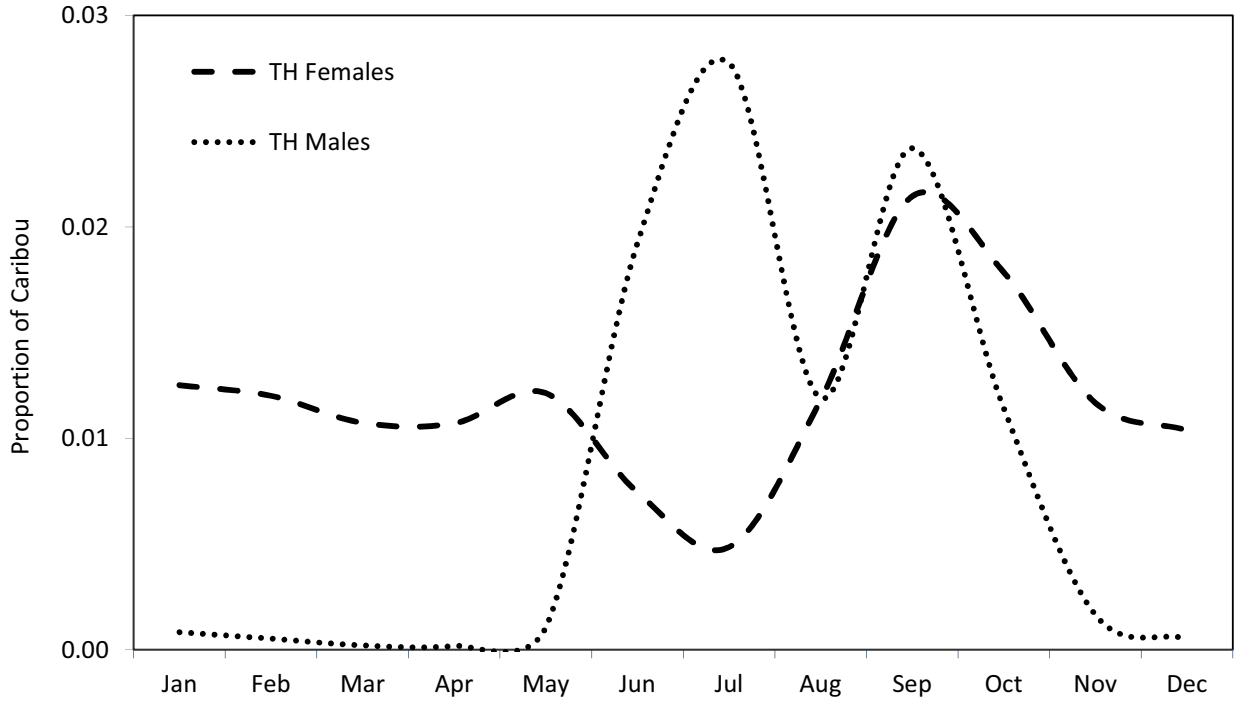

Figure 15. Proportion of Teshekpuk Caribou Herd caribou within 4 km of the proposed Willow development alignments, based on fixed-kernel density estimation, 1990–2019.

Table 3. Proportion of collared Teshekpuk Herd caribou that crossed the proposed Willow alignment at least once in each season, 2000–2019. Numbers in parenthesis indicate the number of collared caribou used in the analysis.

Year	Spring Migration	Calving	Postcalving	Mosquito	Oestrid Fly	Late Summer	Fall Migration	Winter
2000–2004						0.00 (10)	0.40 (10)	0.20 (10)
2005–2009	0.02 (49)	0.10 (49)	0.00 (49)	0.00 (39)	0.36 (45)	0.09 (76)	0.12 (75)	0.03 (70)
2010–2014	0.06 (90)	0.03 (86)	0.02 (83)	0.01 (86)	0.08 (111)	0.02 (125)	0.09 (119)	0.04 (104)
2015	0.10 (21)	0.05 (19)	0.00 (16)	0.00 (16)	0.04 (26)	0.08 (26)	0.46 (26)	0.04 (23)
2016	0.22 (23)	0.05 (22)	0.00 (22)	0.00 (21)	0.03 (40)	0.02 (51)	0.16 (50)	0.02 (47)
2017	0.02 (44)	0.02 (41)	0.00 (28)	0.00 (41)	0.00 (58)	0.01 (76)	0.05 (73)	0.01 (69)
2018	0.05 (64)	0.02 (58)	0.04 (28)	0.03 (63)	0.00 (66)	0.07 (86)	0.14 (83)	0.28 (80)
2019	0.03 (73)	0.01 (69)	0.03 (38)	0.00 (77)	0.00 (105)	0.02 (103)	0.10 (106)	
All Years	0.05 (364)	0.04 (344)	0.02 (264)	0.01 (343)	0.06 (451)	0.04 (553)	0.13 (542)	0.08 (403)

(1,450 feet) above ground level (agl) with a ground speed of 150–167 kph (80-90 knots) and a vertically facing camera would produce clear images. They then flew 7 missions from May through early October to collect imagery during different seasons: 13–14 May, 18–19 June, 22 July, 31 July, 16 August, 28 August, and 3 October. The 22 July and 16 August missions were exclusively for TerraSond image acquisition. During these photo flights, the pilot would fly to areas to collect imagery where high densities of caribou were known or expected to be. The remaining missions were conducted in conjunction with ABR aerial surveys. During surveys, the plane would either temporarily break off the survey to collect images of caribou at the desired altitudes and speeds or collect imagery after the aerial surveys were completed. The camera array included two high-resolution color imagery (RGB) cameras operated as a single array (10,200x3,456 pixels), and a low-resolution (640x512 pixel) forward looking infrared (FLIR) camera.

TerraSond created automated scripts that used color band thresholds to identify pixels with "caribou-like" signatures and identified clusters of caribou-like pixels that were the appropriate size for large or small caribou. These clusters could then be checked for the presence of caribou and counted.

REMOTE SENSING

Because MODIS imagery covers large areas at a relatively coarse resolution (250- to 500-m pixels), it was possible to evaluate snow cover and vegetation indices over a much larger region extending beyond the study area with no additional effort or cost. The region evaluated extends from the western edge of Teshekpuk Lake east to the Canada border and from the Beaufort Sea inland to the northern foothills of the Brooks Range. The ability to examine this large region allowed us to place the study area into a larger geographic context in terms of the chronology of snow melt and vegetation green-up, both of which are environmental variables that have been reported to be important factors affecting caribou distribution in northern Alaska.

SNOW COVER

Based on observations from survey crews and records from weather stations in the area (Figure 4; Appendix B), the timing of snow melt was approximately average for most of the region in 2019. Estimated snow cover from MODIS data indicated snowmelt was partially underway by 22 May, southern portions of the GMT survey area were snow free by 28–29 May, and the entire region was generally snow-free by 7 June with the exception of partially snow covered areas near the coast (Figure 16). Imagery collected during aerial surveys on 16 May indicates that areas of exposed tundra were not uncommon. This timing was similar or slightly earlier than the median date of snowmelt computed for the past 20 years (Figures 17–18, Appendix C).

The median dates of snow melt for each pixel computed using 2000–2019 data (where the date of melt was known within one week) indicate that nearly all of the snow on the coastal plain typically melts over a period of three weeks between 25 May and 11 June (Figure 17; Appendix C). Snow melt progressed northward from the foothills of the Brooks Range to the outer coastal plain, occurring earlier in the "dust shadows" of river bars and human infrastructure, and later in the uplands and numerous small drainage gullies southwest of the Kuparuk oilfield. The southern coastal plain, wind-scoured areas, and dust shadows typically melted during the last week of May (Figure 17). The central coastal plain and most of the Colville River delta usually melted in the first week of June, leaving snow on the northernmost coastal plain, in uplands, and in terrain features that trap snow, such as stream gullies. During the second week in June, most of the remaining snow melted, although some deep snow-drift remnants, lake ice, and *aufeis* persisted into early July (Figure 17). In the GMT survey area, snow melt occurs earliest near stream channels and a south-to-north gradient was apparent, with snow typically melting several days later near the coast.

Previous comparisons of the performance of the MODIS subpixel-scale snow-cover algorithm with aggregated Landsat imagery suggest that the overall performance of the subpixel algorithm is acceptable, but that accuracy degrades near the end of the period of snow melt (Lawhead et al. 2006).

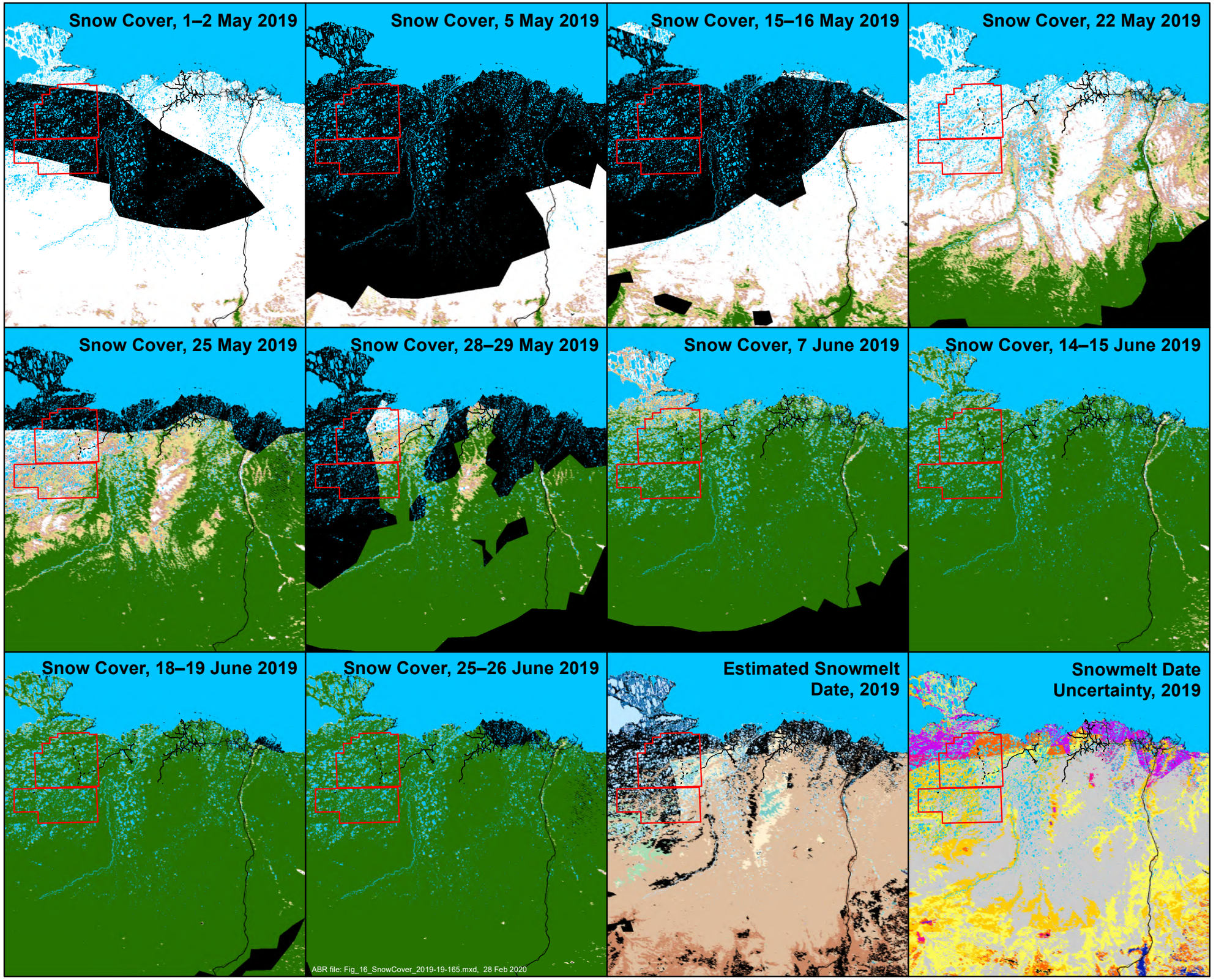

Figure 16. Extent of snow cover between early May and mid-June on the central North Slope of Alaska in 2019, as estimated from MODIS satellite imagery.

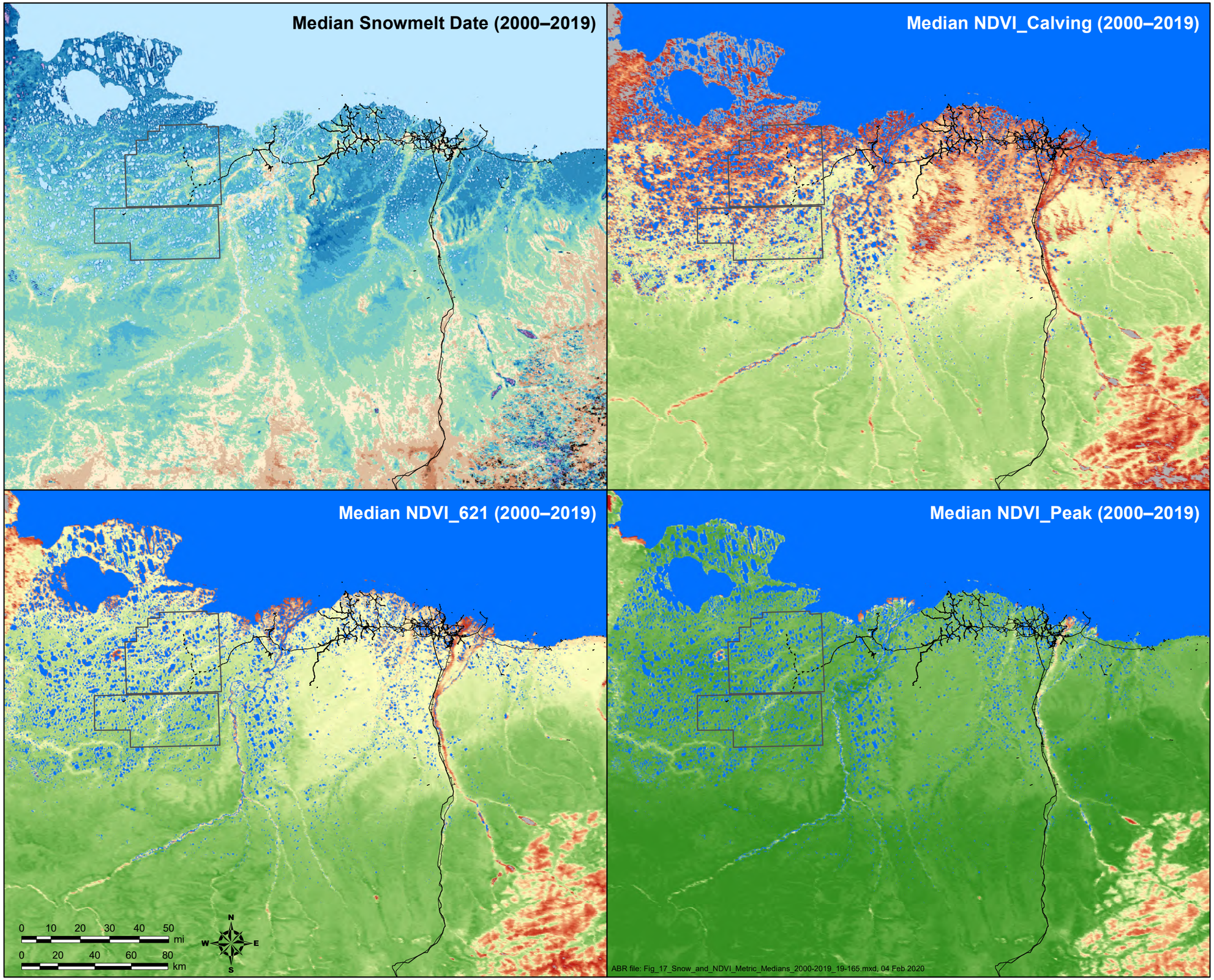

Figure 17.
Median snowmelt date and vegetation index metrics, as estimated from MODIS satellite imagery time series, 2000–2019.

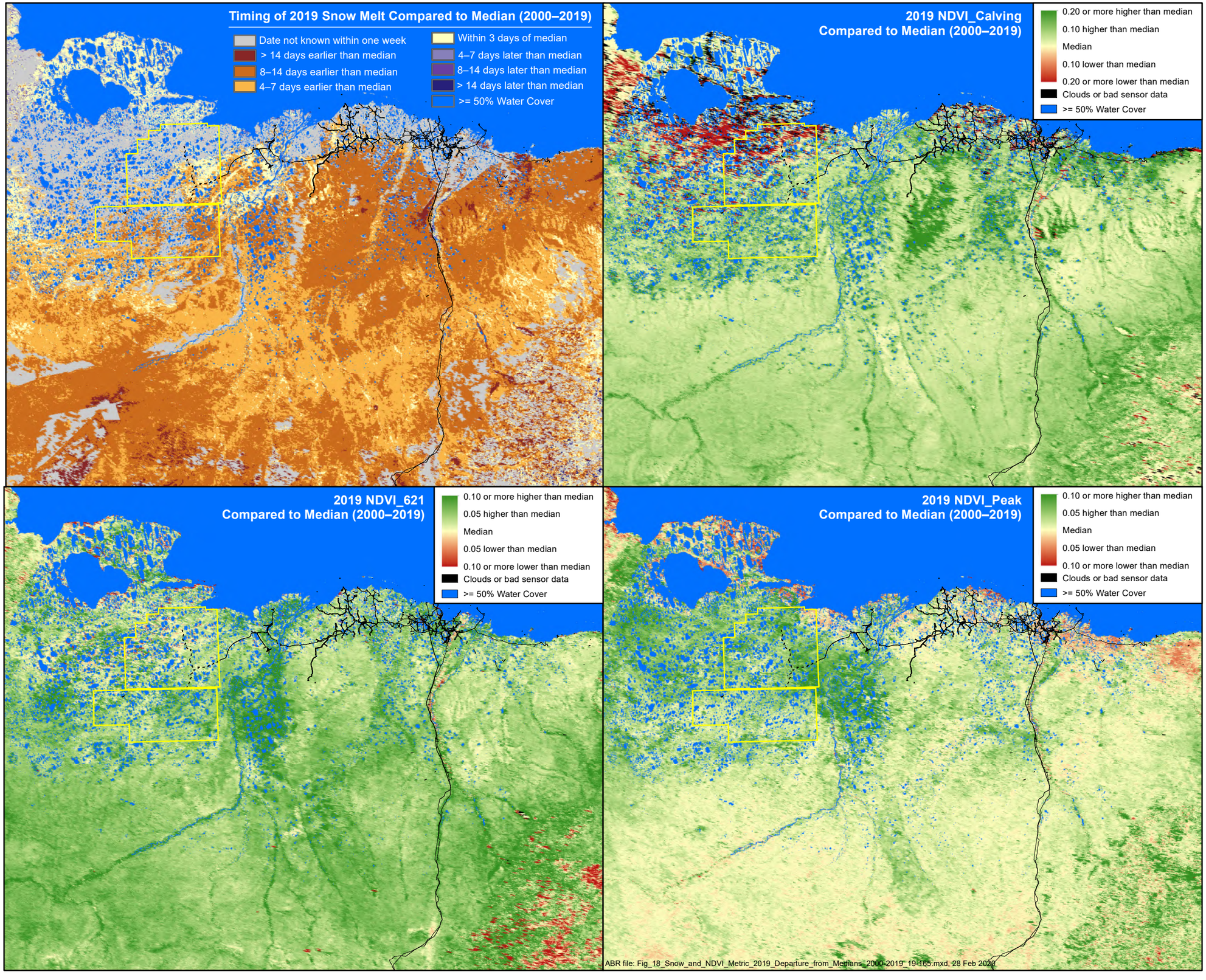

Figure 18. Departure of 2019 values from median snowmelt date and vegetation index metrics (2000–2019), as estimated from MODIS satellite imagery time series.

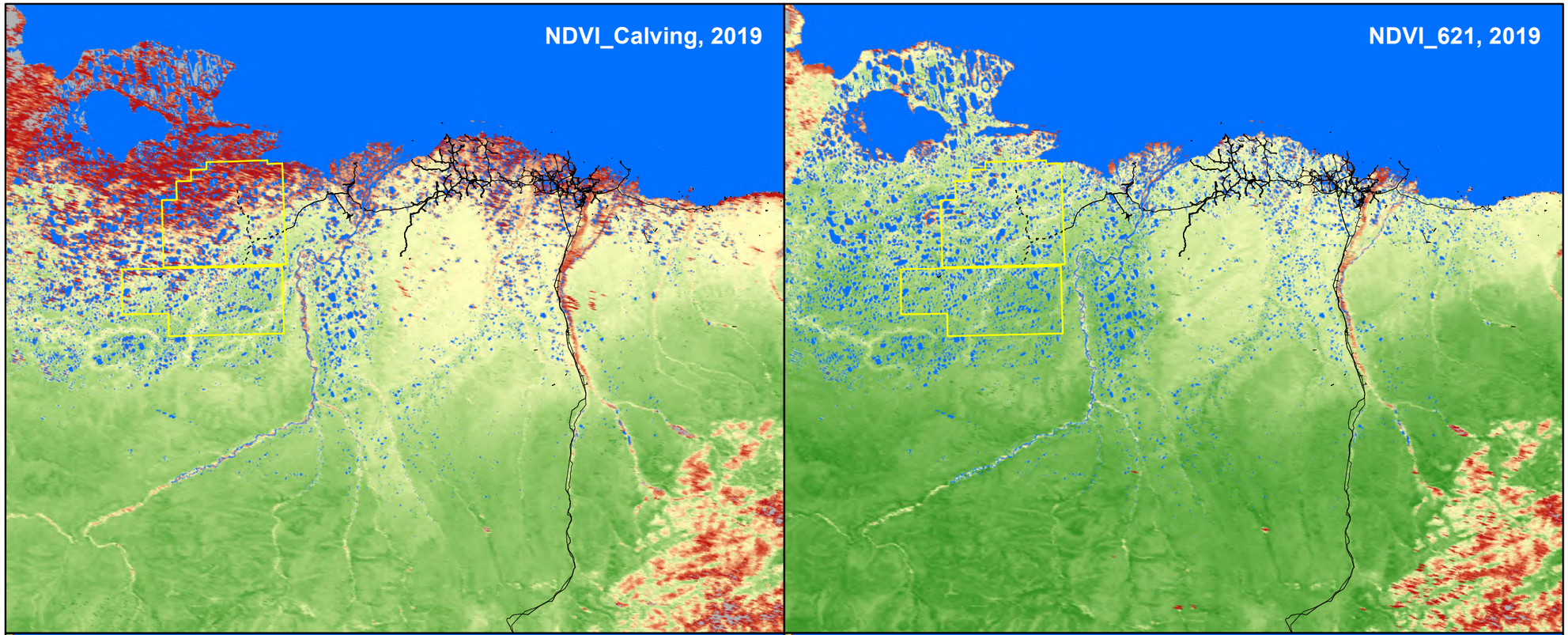

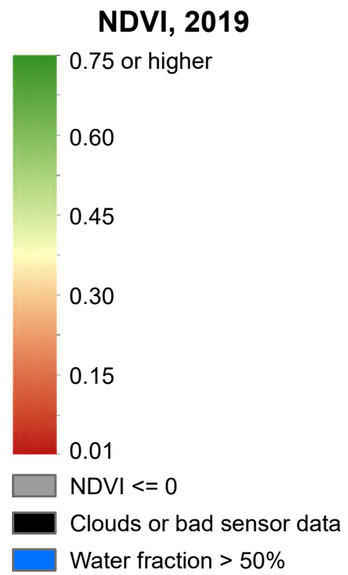

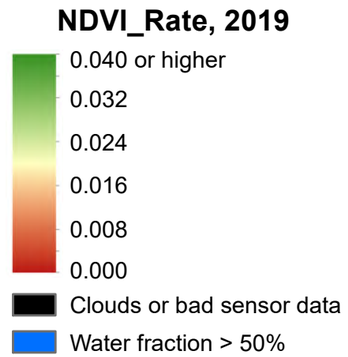

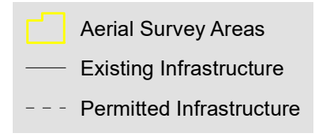

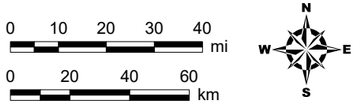

Figure 19.
Metrics of relative vegetative biomass during the 2019 growing season on the central North Slope of Alaska, as estimated from NDVI calculated from MODIS satellite imagery.

VEGETATIVE BIOMASS

Compared with median NDVI since 2000 (Figure 19), the estimated vegetative biomass during calving (NDVI_Calving) and during peak lactation (NDVI_621) in 2019 was above average through much of the study area (Figures 17–19; Appendices D–E). Those values are consistent with the average or slightly early snow melt in 2019. Peak NDVI was also higher than average in 2019 (Figure 18; Appendix F), indicating that 2019 was a good growing season. This is consistent with the above average temperatures recorded in much of July (Figure 4). In 2019, NDVI_Rate was low in inland areas with earlier snowmelt, but high in more coastal areas where snowmelt occurred later (Figure 19). This is consistent with a rapid increase in NDVI values coincident with snowmelt, as standing dead biomass is exposed.

RESOURCE SELECTION ANALYSIS

The RSF analysis of seasonal caribou density is restricted to the GMT and BTU survey areas. Seasonal sample sizes for the location data used in the RSF analysis ranged from 277 to 5,397 use locations for the years 2002–2019 (Table 4). Most of the top-ranking seasonal models for the survey areas contained habitat type, vegetative biomass (maximum NDVI or daily NDVI), a west-to-east distributional gradient, distance to coast, and landscape ruggedness (Table 5). Biomass, nitrogen, and median date of snow melt were included in some of the top seasonal models. Results of the *k*-fold cross-validation test indicated that the best models for the combined datasets for NPRA had reasonably good model fits (Spearman's r = 0.88–0.96; Table 6). The variables with the highest probability of being in the best RSF model (Table 7) varied by season but caribou resource selection in the area generally followed a gradient of increasing selection from east to west in all seasons and higher selection closer to the coast in most seasons (Figure 20). These results are consistent with the location of the survey area near the eastern edge of the TCH annual range.

The RSF model output produced several types of results. These results include the probability of each model being the best model in the set of candidate models (i.e., Akaike weight), which was used to rank the various models (Table 5) and to estimate the probability that each variable is included in the best model (i.e., the sum of Akaike weights for all models containing that variable; Table 7). We used all variables with a 50% or greater probability of being in the best model to produce seasonal RSF maps (Figure 20). In addition, by examining the unconditional parameter estimates we determined which individual parameters were significant (i.e., the 95% confidence interval did not contain zero), after accounting for model uncertainty (Table 8). These individual parameter estimate results were useful for examining the effect of each habitat type on caribou distribution.

For the winter season, all variables were included in the best model (Tables 5, 7), with the

Table 4. Number of aerial surveys, radio collars, and locations for each sample type used in resource selection function analysis for the NPRA survey area, 2002–2019.

	Aerial Surveys		Telemetry Data		Total
Season	Surveys	Locations	Collars	Locations	Locations
Winter	15	1,022	131	3,648	4,670
Spring Migration	14	433	64	423	856
Calving	25	1,205	41	158	1,363
Postcalving	22	1,596	33	72	1,668
Mosquito	5	82	79	195	277
Oestrid Fly	16	316	110	379	695
Late Summer	29	1,384	126	1,344	2,728
Fall Migration	27	2,106	208	3,291	5,397
Total	135	8,144	792	9,510	17,654

Table 5. Three top-performing seasonal resource selection function models, AICc scores, and the probability (Akaike weight) that each model was the best model in the candidate set for the GMT, BTN, and BTS survey areas, 2002–2019 (combined aerial survey and telemetry data).

Season	RSF Model	AICc	Akaike Weight
Winter	Habitat + MaxNDVI + EtoW + DistCoast + Ruggedness + Snow	38740	0.769
	Habitat + MaxNDVI + EtoW + Ruggedness + Snow	38743	0.219
	Habitat + MaxNDVI + EtoW + Ruggedness	38750	0.006
Spring Migration	Habitat + MaxNDVI + EtoW + DistCoast + Ruggedness + Snow	7020	0.483
	MaxNDVI + EtoW + DistCoast + Ruggedness + Snow	7021	0.315
	Habitat + MaxNDVI + EtoW + DistCoast + Ruggedness	7024	0.058
Calving	Habitat + dailyNDVI + Nitrogen + EtoW + Ruggedness	10551	0.082
	Habitat + dailyNDVI + EtoW + Ruggedness	10552	0.065
	Habitat + dailyNDVI + Nitrogen + EtoW + Ruggedness + Snow	10552	0.063
Postcalving	Habitat + dailyNDVI + Biomass + EtoW + DistCoast + Ruggedness	13609	0.246
	Habitat + dailyNDVI + EtoW + DistCoast + Ruggedness	13609	0.170
	Habitat + dailyNDVI + MaxNDVI + Biomass + EtoW + DistCoast + Ruggedness	13610	0.106
Mosquito	Habitat + dailyNDVI + EtoW + DistCoast + Ruggedness	2007	0.136
	Habitat + Nitrogen + EtoW + DistCoast + Ruggedness	2007	0.122
	Habitat + Biomass + EtoW + DistCoast + Ruggedness	2007	0.121
Oestrid Fly	Habitat + dailyNDVI + EtoW + DistCoast + Ruggedness	5655	0.186
	Habitat + Biomass + EtoW + DistCoast + Ruggedness	5655	0.142
	Habitat + Nitrogen + EtoW + DistCoast + Ruggedness	5655	0.124
Late Summer	Habitat + dailyNDVI + Biomass + EtoW + DistCoast + Ruggedness	21669	0.255
	Habitat + dailyNDVI + Biomass + EtoW + Ruggedness	21670	0.148
	Habitat + dailyNDVI + MaxNDVI + Biomass + EtoW + DistCoast + Ruggedness	21671	0.095
Fall Migration	Habitat + EtoW + DistCoast + Ruggedness	45458	0.347
	Habitat + EtoW + Ruggedness	45459	0.312
	Habitat + MaxNDVI + EtoW + Ruggedness	45460	0.151

Table 6. Mean Spearman's correlation coefficient of seasonal resource selection function model fit using k-fold cross-validation for the NPRA survey area, 2002–2019 (combined aerial survey and telemetry data).

Season	Correlation Coefficient
Winter	0.96
Spring Migration	0.89
Calving	0.92
Postcalving	0.90
Mosquito	0.89
Oestrid Fly	0.88
Late Summer	0.93
Fall Migration	0.88

snowmelt date being considered a surrogate for snow depth. This model performed very well with a 77% chance of being the best model in the candidate set (Table 5). Areas that were farther west, with higher values of landscape ruggedness, with later snowmelt dates and with higher MaxNDVI values were selected by caribou (Figure 20). Although distance to coast was included in the best model, the model-weighted variable was not significant. All habitat types (*Carex aquatilis*, Flooded Tundra, Moss/Lichen, Riverine, Tussock Tundra, and Wet Tundra) were avoided relative to the reference habitat (Sedge/Grass Meadow; Table 8).

All of the variables also were included in the best model for spring migration (Tables 5, 7). This model had a 48% chance of being the best model in the candidate set (Table 5). The model results were driven primarily by a west-to-east density gradient, with caribou selecting areas farther west reflecting the western distribution of high-density calving by the TCH (Figure 11). Areas with higher landscape ruggedness were selected, as well are areas closer to the coast. Although the habitat variable was included in the best model and improved model performance, none of the individual habitat classes were significantly different from the reference class (Sedge/Grass Meadow; Table 8). This selection for higher landscape ruggedness may reflect selection for areas having less snow and spring flooding, or higher proportions of preferred forage species (Nellemann and Thomsen 1994, Nellemann and Cameron 1996).

During the calving season, the variables habitat, daily NDVI, nitrogen, west-to-east, and landscape ruggedness were included in the best model (Tables 5, 7), although all of the top models had low Akaike weights (Table 7) indicating substantial model uncertainty. Caribou were more likely to be located in the western portion of the study area and in areas with higher daily NDVI and lower terrain ruggedness values (Table 8; Figure 20), reflecting the western distribution of high-density calving by the TCH. The lack of a strong performing top model likely indicates that aside from the above three variables, the remaining variables are not particularly influential in predicting habitat selection.

During the postcalving season, the variables habitat, daily NDVI, biomass, west-to-east, distance to coast, and landscape ruggedness were included in the best model (Tables 5, 7). This model had a 25% chance of being the best model in the candidate set (Table 5). Caribou tended to select areas farther west, closer to the coast, with higher NDVI, and with higher landscape ruggedness, although NDVI was not a significant variable in the model (Table 8; Figure 20). Selection of areas in the northwestern portion of the survey area likely reflects caribou movement toward the primary area of mosquito-relief habitat north of Teshekpuk Lake. Selection for higher landscape ruggedness may reflect higher densities of preferred forage species (Nellemann and Thomsen 1994, Nellemann and Cameron 1996).

During the mosquito season, habitat, daily NDVI, west-to-east gradient, distance to coast, and landscape ruggedness were included in the best model (Tables 5, 7). Models with biomass or nitrogen in place of NDVI performed almost as well as the top model with NDVI but none of the coefficients were significant or had a >50% chance of being in the top model (Tables 5, 7, 8), indicating their lack of importance in predicting caribou distribution. Caribou primarily selected areas farther west, closer to the coast, and with higher ruggedness (Table 8; Figure 20). These results suggest that mosquito harassment is the primary driver of caribou distribution during this season, and the need to access mosquito-relief

Table 7. Independent variables and their probability of being in the best resource selection function model (i.e., the sum of all Akaike weights for all models that included the variable) for the NPRA survey area during eight seasons, 2002–2019 (combined aerial survey and telemetry data). Variables with a probability ≥0.5 were used in RSF maps (Figure 22).

Variable	Winter	Spring Migration	Calving	Postcalving	Mosquito	Oestrid Fly	Late Summer	Fall Migration
West to East	1.00	1.00	1.00	1.00	1.00	1.00	1.00	1.00
Distance to Coast	0.77	1.00	0.40	1.00	1.00	1.00	0.63	0.51
Max NDVI	1.00	0.91	0.40	0.30	0.28	0.33	0.29	0.30
Daily NDVI	–	–	1.00	0.89	0.47	0.49	0.84	–
Nitrogen	–	–	0.58	0.34	0.43	0.42	0.31	–
Biomass	–	–	0.33	0.60	0.44	0.44	0.92	–
Snowmelt Date	0.99	0.88	0.40	–	–	–	–	–
Ruggedness	1.00	1.00	0.99	1.00	0.99	1.00	0.99	0.95
Habitat	1.00	0.67	0.70	0.84	0.28	1.00	1.00	1.00

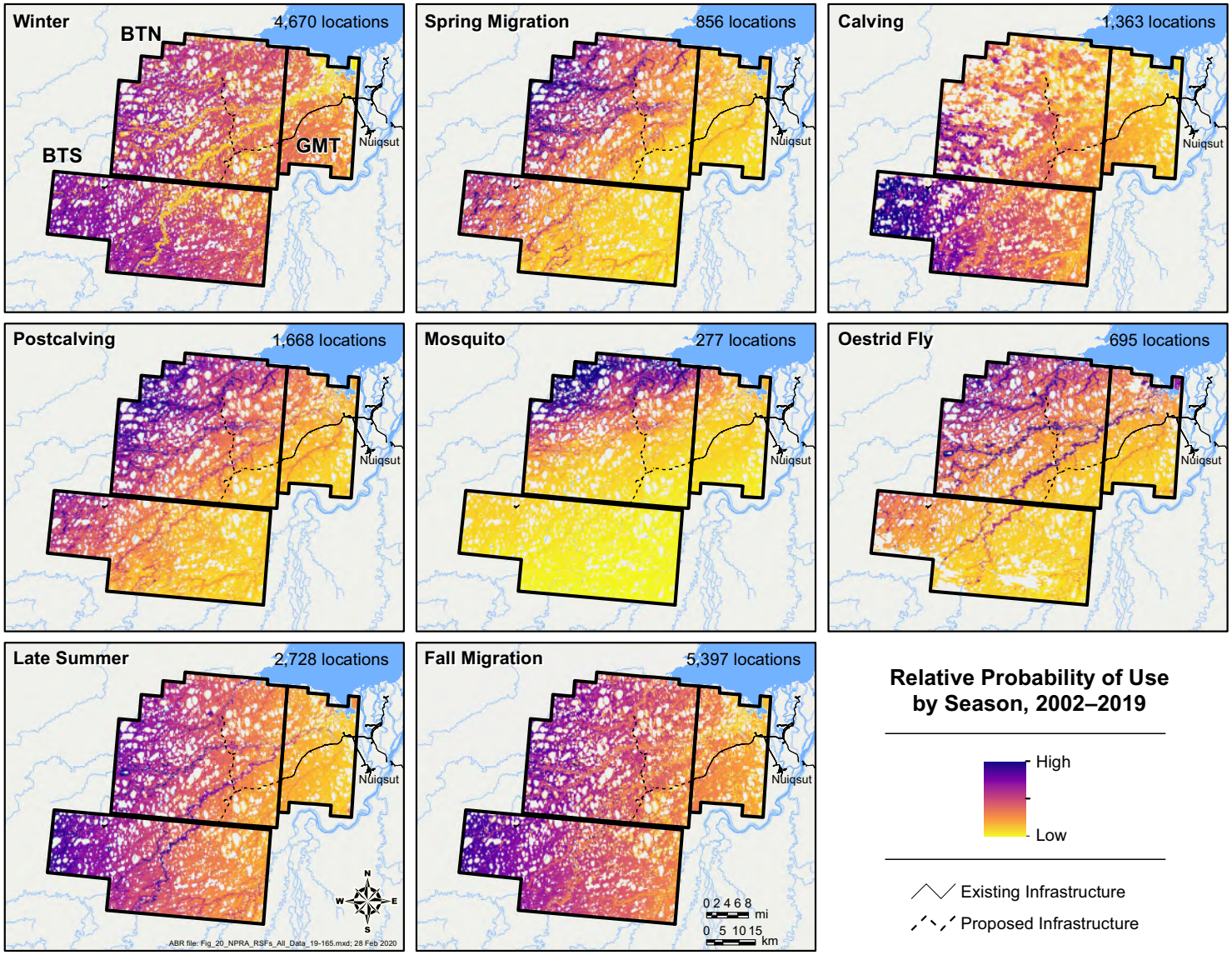

Figure 20. Predicted relative probability of use of the NPRA study area by caribou during each of eight seasons, 2002–2019, based on resource selection function analysis.

Table 8. Model-weighted parameter estimates for resource selection function models for the NPRA survey area during eight seasons, 2002–2019 (combined aerial survey and telemetry data). Coefficients in bold type indicate that the 95% confidence interval did not contain zero.

Variable	Winter	Spring Migration	Calving	Postcalving	Mosquito	Oestrid Fly	Late Summer	Fall Migration
West to East	**-0.11**	**-0.60**	**-0.38**	**-0.48**	**-1.03**	**-0.50**	**-0.27**	**-0.21**
Distance to Coast	0.03	**-0.49**	-0.02	**-0.48**	**-1.61**	**-0.61**	-0.03	-0.01
Max NDVI [a]	**0.04**	-0.09	0.02	0.00	0.01	-0.01	0.00	0.00
Daily NDVI [a]	–	–	**0.42**	0.16	0.03	-0.05	0.11	–
Biomass [a]	–	–	-0.02	0.08	-0.01	-0.01	-0.10	–
Nitrogen [a]	–	–	-0.07	0.01	0.01	-0.01	0.00	–
Snowmelt Date	**0.06**	-0.08	0.01	–	–	–	–	–
Ruggedness	**0.10**	**0.30**	**-0.11**	**0.19**	**0.25**	**0.19**	**0.07**	**-0.04**
Carex aquatilis [b]	**-1.30**	-0.35	-0.30	-0.34	-0.47	0.23	**-0.48**	**-0.91**
Dwarf Shrub [b]	**-0.52**	-0.04	-0.49	0.03	0.14	**1.06**	0.14	**-0.23**
Flooded Tundra [b]	**-0.99**	-0.12	**-0.44**	-0.19	-0.70	**0.49**	**-0.32**	**-0.61**
Moss/Lichen [b]	**-1.41**	-0.33	-0.82	0.23	-0.25	**1.18**	0.38	0.18
Riverine [b]	**-1.50**	-0.29	-0.35	**0.32**	-0.09	**1.22**	**0.38**	**-0.36**
Tussock Tundra [b]	**-0.13**	-0.12	-0.16	0.02	-0.12	**0.35**	-0.02	**-0.14**
Wet Tundra [b]	**-0.94**	0.04	-0.26	0.09	-0.43	**0.44**	0.00	**-0.44**

[a] Max NDVI values were used all year, while the daily NDVI, Biomass, and Nitrogen values which are derived daily during the growing season were used for the Calving, Postcalving, Mosquito, Oestrid Fly, and Late Summer seasons.

[b] Habitat classes were compared to the reference class "Sedge/Grass Meadow."

habitat near the coast is more important than factors such as habitat quality.

During the oestrid fly season, the variables habitat, daily NDVI, west-to-east, distance to coast, and landscape ruggedness were included in the best model, although there was a fair amount of model uncertainty (Tables 5, 7). As with the mosquito season, nitrogen and biomass appear to be almost interchangeable with daily NDVI with regards to model performance, though none were significant or had a >50% chance of being in the top model (Tables 5, 7, 8). Caribou selected areas farther west, closer to the coast, and with greater ruggedness (Table 8; Figure 20). Relative to Sedge/Grass Meadow habitat, caribou selected for all other habitats.

During late summer, habitat type, daily NDVI, biomass, west-to-east gradient, distance to coast, and landscape ruggedness were included in the best model (Tables 5, 7). This model had a 26% chance of being the best model in the candidate set (Table 5). Caribou selected areas farther west, and with higher ruggedness. Although the analysis indicated that caribou tended to select areas closer to the coast and with lower biomass, neither variable was significant in the model (Table 8). Relative to Sedge/Grass Meadow habitat, caribou also selected Riverine habitat types and avoided *Carex aquatilis* and Flooded Tundra habitat types (Table 8, Figure 20).

During fall migration, habitat type, west-to-east, distance to coast, and landscape ruggedness were included in the best RSF model (Tables 5, 7). This model performed moderately well with a 35% chance of being the best model in the candidate set (Table 5). Caribou selected areas farther west, closer to the coast, and with low landscape ruggedness. Relative to Sedge/Grass Meadow habitat, caribou also avoided *Carex aquatilis*, Flooded Tundra, Tussock Tundra, and Wet Tundra habitats (Table 8; Figure 20).

DISCUSSION

WEATHER, SNOW, AND INSECT CONDITIONS

Weather conditions exert strong effects on caribou populations throughout the year in arctic Alaska. Deep winter snow and icing events increase the difficulty of travel, decrease forage availability, and increase susceptibility to predation (Fancy and White 1985, Griffith et al. 2002). Severe cold and wind events can cause direct mortality of caribou (Dau 2005). Late snow melt can delay spring migration, cause lower calf survival, and decrease future reproductive success (Finstad and Prichard 2000, Griffith et al. 2002, Carroll et al. 2005). In contrast, hot summer weather can depress weight gain and subsequent reproductive success by increasing insect harassment at an energetically stressful time of year, especially for lactating females (Fancy 1986, Cameron et al. 1993, Russell et al. 1993, Weladji et al. 2003).

Weather condition variability results in large fluctuations in caribou density during the insect season as caribou aggregate and move rapidly through the study area in response to fluctuating insect activity. On the central Arctic Coastal Plain (including the study area), caribou typically move upwind and toward the coast in response to mosquito harassment and then disperse inland when mosquito activity abates in response to cooler temperatures and increased winds (Murphy and Lawhead 2000, Yokel et al. 2009, Wilson et al. 2012).

The absence of mosquitoes during mid-to late June likely led to improved caribou body condition after calving, but the warm temperatures during July likely resulted in increased movement rates and decreased foraging, which can cause a decline in body condition. Cool conditions in late summer and delayed onset of seasonal snow cover due to high temperatures in September (typical of recent years on the coastal plain; Cox et al. 2017) may have allowed caribou to increase their forage rate and improve their body condition prior to the onset of winter, although forage quality is greatly diminished in the fall compared to the summer (Gustine et al. 2017, Johnson et al. 2018).

CARIBOU DISTRIBUTION AND MOVEMENTS

Analysis of GPS, satellite, and VHF telemetry data sets spanning nearly three decades clearly demonstrates that the study area is in the eastern portion of the annual range of the TCH, and west of the annual range of the CAH. Use of the BTN

and BTS survey areas by CAH caribou is usually very low, although several notable incursions have been recorded sporadically over the years. A few collared CAH females have switched to the TCH or calved west of the Colville River in isolated years (notably 2001), but it is a rare occurrence (Arthur and Del Vecchio 2009; Lenart 2009, 2015; Prichard 2016).

The TCH consistently uses the BTN and BTS survey areas to some extent during all seasons of the year. Females overwinter primarily on the coastal plain whereas most males tend to migrate south into the foothills and mountains of the Brooks Range to winter. Most TCH females calve around Teshekpuk Lake, northwest of the BTN and BTS survey areas (Kelleyhouse 2001, Carroll et al. 2005, Person et al. 2007, Wilson et al. 2012, Parrett 2015a, Prichard et al. 2019a). Males that wintered in the Brooks Range usually arrive on the coastal plain in June. When mosquito harassment begins in late June or early July, caribou move toward the coast where lower temperatures and higher wind speeds prevail (Murphy and Lawhead 2000, Parrett 2007, Yokel et al. 2009, Wilson et al. 2012). The TCH typically moves to the area between Teshekpuk Lake and the Beaufort Sea. After oestrid fly harassment begins in mid-July, the large groups that formed in response to mosquito harassment begin to break up and caribou disperse inland, seeking elevated or barren habitats such as sand dunes, mudflats, and river bars, with some using shaded locations in the oilfields under elevated pipelines and buildings (Lawhead 1988, Murphy and Lawhead 2000, Wilson et al. 2012, Prichard et al. 2019b).

In 2019, caribou density was moderate during the late winter season when most of the TCH is widely distributed on the Coastal Plain between Nuiqsut and Wainwright. Density was low during the spring migration survey but increased to moderate densities into the calving and postcalving seasons. During the spring migration survey, most females likely moved out of the survey area towards the calving grounds and males likely had not yet arrived from the south. Transect surveys during the mosquito season are inefficient for describing caribou habitat use because of the rapid speed of caribou movements during that period (Prichard et al. 2014). Caribou density was close to zero during the oestrid fly surveys on 29–31 July, as the majority of the herd moved to the west after the mosquito season. Densities did increase into the late summer season as caribou dispersed more easterly after insect harassment was predicted to have abated. Densities increased again to their highest levels during the fall migration season when large numbers of caribou migrated into or through the study area on their way to the south. High densities also have been recorded sporadically in the area in late winter (2.4 caribou/km² in April 2003) and the postcalving season (1.5 caribou/km² in late June 2001) (Burgess et al. 2002, Johnson et al. 2004, Lawhead et al. 2010).

The area near proposed Willow infrastructure is used more often than the area near existing and proposed ASDP and GMT infrastructure. Few crossings of the new GMT1/MT6 or GMT2/MT7 road alignments have occurred by collared caribou since 2004 (Prichard et al. 2018, 2019c, 2020). Approximately 13% of collared caribou crossed the proposed Willow alignment at least once during fall migration in a typical year (Table 3).

The harvest of caribou by Nuiqsut hunters tends to peak during the months of July and August, with lower numbers of caribou usually being taken in June and September–October and the smallest amount of harvest occurring in other months (Pedersen 1995, Brower and Opie 1997, Fuller and George 1997, Braem et al. 2011, SRB&A 2017). Using harvest data (Braem et al. 2011) and telemetry data from 2003–2007, Parrett (2013) estimated that TCH caribou comprised 86% of the total annual harvest by Nuiqsut hunters during those years. The construction of the Nuiqsut Spur Road and CD-5 access road resulted in increased use of those roads for subsistence harvest of caribou (SRB&A 2017) and the new GMT1/MT6 and GMT2/MT7 roads and the proposed Willow roads are likely to increase subsistence hunter access to seasonal ranges used consistently year-round by TCH caribou.

RESOURCE SELECTION

The two data sets (aerial transect surveys and radio telemetry) that we combined for the RSF analysis provided complementary information for investigating broad patterns of resource selection.

Telemetry data have higher spatial accuracy than do aerial survey data and are collected at high frequency throughout the year, albeit for a small sample of individual caribou. Because of the high variability in the amount of time spent in the study area by collared animals, we did not attempt to adjust for individual differences, other than limiting the frequency of locations in the analytical data set to one every 48 h. In contrast, aerial transect survey data provide information on all caribou groups detected in the area (subject to sightability constraints) at the time of each survey, but the locations have lower spatial accuracy and surveys are only conducted periodically throughout the year. That lower accuracy necessitated consolidating habitats into 210-m by 210-m quadrats of the most common classes, rather than using the habitat types in individual 30-m pixels that could have been used for the telemetry data alone. This need to aggregateadjacent habitat pixels may have reduced the accuracy of habitat selection analysis for uncommon habitats in the survey area.

The two different data types also had different timing, especially during the winter season; only one aerial survey was conducted in that season (mid to late April) in any given year, whereas telemetry locations were collected throughout the entire season. Despite these potential limitations, the combination of the two survey methods produced larger samples than were available for either data set alone and the resulting RSF models are broadly interpretable within the context of general patterns of caribou movements on the central Arctic Coastal Plain.

Use of the BTU and GMT survey areas by caribou varies widely among seasons. These differences are related to snow cover, vegetative biomass, distribution of habitat types, distance to the coast and west-to-east gradients, and landscape ruggedness. In general, broad geographic patterns in distribution (west to east, distance to coast) were the strongest predictors of caribou distribution, but other factors such as vegetative biomass and habitat types were important in some seasons, after taking into account the broad geographic patterns exhibited during key life cycle stages and reflected in the seasonal distribution patterns (Figures 8–10).

These geographic patterns in TCH distribution are most pronounced from spring migration through the mosquito season. Because the survey areas are on the eastern edge of the TCH range with the core of the calving range centered on Teshekpuk Lake, a natural west-to-east and north-to-south gradient of decreasing density occurs throughout the year. Caribou density typically is lowest in the eastern and southeastern sections of the survey areas where the GMT2/MT7 road alignment is located, and higher to the north and west. During calving, the highest densities of TCH females typically calve near Teshekpuk Lake (Figure 11; Person et al. 2007, Wilson et al. 2012, Parrett 2015a), so caribou density decreases with increasing distance to the east, away from the lake. Hence, more caribou are likely to occur in the western portion of the BTN survey area than in the eastern portion in these seasons. It is important to recognize that this pattern of distribution existed before construction of any BTU pipelines, roads, or any other infrastructure.

Because caribou aggregate into large groups when mosquitoes are present and move quickly when harassed by insects, density during the mosquito season and early part of the oestrid fly season fluctuates widely. Aerial-transect surveys in other regions of the oilfields during the mosquito and oestrid fly seasons have been sparse due to the difficulty of adequately sampling the highly variable occurrence of caribou at that time of year with that survey method, and therefore surveys are no longer conducted during mosquito harassment. However, caribou occurrence is generally low in the area of the proposed Willow infrastructure during the mosquito season as caribou are more likely to be further to the west and closer to the coast. For the remainder of the year, caribou density is more consistent with higher densities of caribou throughout the study area as caribou disperse more broadly after insect harassment abates.

During most seasons, caribou selected for higher landscape ruggedness, which tends to occur in riparian areas in the study area. Terrain ruggedness could be related to the quality or quantity of forage, the presence of dry ground and flooding, and the depth of snow and timing of snowmelt in certain areas. Different studies have reported conflicting conclusions regarding the importance of ruggedness, which may be related in part to the ways in which it has been calculated.

Nellemann and Thomsen (1994) and Nellemann and Cameron (1996) reported that CAH caribou selected areas of greater terrain ruggedness (as calculated by hand from topographic maps) in the Milne Point calving concentration area, but Wolfe (2000) and Lawhead et al. (2004), using a digital method of calculating terrain ruggedness, found no consistent relationship with terrain ruggedness in a larger calving area used by CAH females during calving. Those calculations of terrain ruggedness differed from the landscape ruggedness method we used in this study (developed by Sappington et al. 2007), which provides a finer-scale analysis based on digital elevation models and is much less correlated with slope than are the previous methods. Prichard et al. (2019b) found that caribou of the CAH selected for areas with higher terrain ruggedness during most seasons, but did not select terrain ruggedness during calving.

The avoidance of *Carex aquatilis*, Wet Tundra, and Flooded Tundra during fall and winter has been documented in previous years using different analyses (Lawhead et al. 2015, Prichard et al. 2019b). Caribou selected Riverine habitat along Fish and Judy creeks during the postcalving, oestrid fly, and late summer seasons and the avoidance of Riverine habitat during winter (Table 8). The riparian habitats along Fish and Judy creeks provide a complex interspersion of barren ground, dunes, and sparse vegetation (Figure 4) that provide good fly-relief habitat near foraging areas.

In all seasons except the oestrid fly season, most habitats are avoided when compared to Sedge/Grass Meadows, although the use of Tussock Tundra was similar to Sedge/Grass Meadows. Sedge/grass Meadows and Tussock Tundra are characterized as dry (<10% water) vegetated (>30% vegetated) habitats with <40% shrubs. The main difference between the two habitats is that Tussock Tundra is dominated by >40% tussock cotton grass (*Eriophorum vaginatum*) while Sedge/Grass Meadows are >50% other graminoid species, primarily sedges. These two habitat classes may not always be easily distinguished. Pixels mapped as Tussock Tundra were often mistaken for Sedge/Grass Meadow and were only correctly mapped 43% of the time. Pixels mapped as Sedge/Grass Meadow were more accurately mapped (83% accuracy; BLM and Ducks Unlimited 2002).

In winter, all habitats were avoided in comparison with the reference habitat, Sedge/Grass Meadow. Sedge/Grass Meadows was the most species-rich habitat and had the third highest abundance of lichen (3.58% lichen cover) behind Dwarf Shrub (4.81%) and Moss/lichen (12.87%). Tussock Tundra had similar levels of lichens to Sedge/Grass Meadow (3.40% lichens; BLM and Ducks Unlimited 2002). Lichens are a preferred winter diet item and sedges are preferred by TCH caribou in the summer (Joly et al. 2007, Parrett 2007). During calving, the only significant habitat association was an avoidance of the Flooded Tundra class.

Comparison of caribou habitat use across studies is complicated by the fact that different investigators have used different habitat classifications and each classification system has different accuracy concerns. Kelleyhouse (2001) and Parrett (2007) reported that TCH caribou selected wet graminoid vegetation during calving and Wolfe (2000) reported that CAH caribou selected wet graminoid or moist graminoid classes; those studies used the vegetation classification by Muller et al. (1998, 1999). Wilson et al. (2012) used TCH telemetry data and the habitat classification of BLM and Ducks Unlimited (2002), as in this study, to investigate summer habitat selection at two different spatial scales, and concluded that TCH caribou consistently selected Sedge/Grass Meadow and avoided flooded vegetation. Prichard et al. (2019b) reported that CAH caribou avoided *Carex aquatilis* and Wet Sedge habitats. In general, caribou appear to avoid habitats with standing water? during most seasons.

We used NDVI (NDVI at time of calving [NDVI_Calving], NDVI on 21 June [NDVI_621], and NDVI rate of change [NDVI_Rate]) to estimate vegetative biomass in this study because other researchers have reported significant relationships between caribou distribution and biomass variables during the calving period. The first flush of new vegetative growth that occurs in spring among melting patches of snow is valuable to foraging caribou (Kuropat 1984, Klein 1990, Johnstone et al. 2002), but the spectral signal of snow, ice, and standing water complicates NDVI-based inferences in patchy snow. Recently

melted areas such as snow, water, and lake ice all depress NDVI values (Macander 2005). Therefore, estimates of NDVI change rapidly as snow melts and exposes standing dead biomass, which has positive NDVI values (Sellers 1985 [cited in Hope et al. 1993], Stow et al. 2004), and the initial flush of new growth begins to appear. NDVI, therefore, has the potential to provide landscape-level information on plant phenology, biomass and forage quality, but has to be interpreting in with respect to water, ice, snow, and habitat type.

Griffith et al. (2002) reported that the annual calving grounds used by the Porcupine Caribou Herd during 1985–2001 generally were characterized by a higher daily rate of change in biomass than was available over the entire calving grounds. In addition, the area of concentrated calving contained higher biomass values (NDVI_Calving and NDVI_621) than was available in the annual calving grounds. They concluded that caribou used calving areas with high forage quality (inferred from an estimated high daily rate of change) and that, within those areas, caribou selected areas of high biomass. The relationship between annual NDVI_621 and June calf survival for the Porcupine Caribou Herd was strongly positive, as was the relationship between NDVI_Calving and the percentage of marked females calving on the coastal plain of ANWR (Griffith et al. 2002). We found that there was selection for areas that typically have high NDVI values during calving in our RSF analysis area for all years combined.

Because of the high correlation between NDVI values and habitat, it is difficult to distinguish whether caribou select specific habitats and areas with greater NDVI or simply avoid wet areas (that have low NDVI values due to the presence of water) and barrens during the calving season. Vegetation sampling in the NPRA survey area in 2005 indicated that moist tussock tundra had higher biomass than did moist sedge–shrub tundra (similar to Tussock Tundra and Sedge/Grass Meadow types in our classification), but that difference disappeared when evergreen shrubs, which are unpalatable caribou forage, were excluded (Lawhead et al. 2006). The species composition of the forage also varied somewhat, the Tussock Tundra areas had a higher biomass of tussock cottongrass (*Eriophorum vaginatum*), forbs, and lichens, and Moist Sedge-Shrub Tundra areas had a higher biomass of other graminoids.

Johnson et al. (2018) used daily NDVI values as well as habitat type, distance to coast, and days from peak NDVI to develop models to predict biomass, nitrogen, and digestible energy for a given location on a given day. These models should, if successful, provide metrics that are more directly related to caribou forage needs than NDVI alone. In our RSF models, inclusion of these variables was not consistent in seasons where it was a possible variable (calving through late summer), although biomass was included in at least one of the three top-performing RSF models during all seasons except calving (Table 5) and nitrogen was included in at least one of the three top-performing RSF models during all seasons except the postcalving and late summer seasons. Biomass and nitrogen were not, however, significant variables in any season. These results suggest that these derived values are not good predictors of caribou distribution in this area and at this scale of selection.

It is possible that these models do not predict biomass and nitrogen well in this area. Johnson et al. (2018) used a land cover map (Boggs et al. 2016) that was based on a land cover map created by Ducks Unlimited for the North Slope Science Initiative (NSSI 2013) that has discontinuities in classification methodology and imagery in our RSF analysis area. These discontinuities could translate into inaccurate forage metrics in our analysis area. Alternatively, caribou may not be selecting for forage nitrogen or forage biomass at this scale. Caribou distribution may be better predicted by high NDVI values which tend to be correlated with locations that have both large amounts of vegetation and less surface water in the pixel. Caribou movements are influenced by many factors other than forage and only a portion of GPS locations represent caribou that are actively feeding.

Date of snowmelt was not a significant predictor of caribou distribution. Previous studies have not produced consistent results concerning the calving distribution of northern Alaska caribou herds in relation to snow cover. Kelleyhouse (2001) concluded that TCH females selected areas of low snow cover during calving and Carroll et al. (2005) reported that TCH caribou calved farther

north in years of early snow melt. Wolfe (2000) did not find any consistent selection for snow-cover classes during calving by the CAH, whereas Eastland et al. (1989) and Griffith et al. (2002) reported that calving Porcupine Herd caribou preferentially used areas with 25–75% snow cover. The presence of patchy snow in calving areas is associated with the emergence of highly nutritious new growth of forage species, such as tussock cottongrass (Kuropat 1984, Griffith et al. 2002, Johnstone et al. 2002), and it also may increase dispersion of caribou and create a complex visual pattern that reduces predation (Bergerud and Page 1987, Eastland et al. 1989). Interpretation is complicated by high annual variability in the extent of snow cover and the timing of snowmelt among years, as well as by variability in detection of snowmelt dates on satellite imagery because of cloud cover. Habitat selection during the calving season may vary annually, depending on the timing of snow melt and plant phenology which may complicate our analysis conducted over multiple years.

AERIAL PHOTOGRAPHY

Collecting aerial imagery for automated counts showed promise in 2019. The in-flight laptop-to-camera integration system used in 2019 was much more streamlined and reliable compared to the system in 2018, which led to few hardware issues and missed opportunities to collect images. TerraSond's imagery analysis also showed that light-colored caribou rumps are at the bright end of the color distributions compared to the background tundra. By setting thresholds just below values identified as caribou rumps, simple image analyses can be applied to extract clusters of pixels that meet certain size and brightness criteria. These can then be reviewed, identified and counted which could provide a method to partially automate the counts if it could be applied across a large range of conditions.

Many limitations were encountered in 2019, however. TerraSond identified issues with image blur, underexposure, and a lack of adaptability of their script across varying lighting and landscape conditions. We believe that issues with image quality in overcast and other low-light conditions may be addressed by optimizing the shutter speed, ISO (sensor sensitivity), f/stop (aperture), and exposure of the camera in flight, prior to surveying. It may also help to use cameras with higher quality sensors optimized for rapid exposures in low light. Image blur was caused by airspeed issues that are more severe under adverse weather conditions (e.g. tailwind) and may be potentially addressed by limiting the flight speeds and providing additional training to pilots on the speeds necessary.

TerraSond's scripts appear to have been tested on only a relatively small number of photos, most of which were already identified as having caribou present. It is unclear how difficult it is to identify all caribou as targets from a much larger dataset of photos taken over a larger and more variable landscape. The existing method appears to be fairly ineffective when the landscape has patchy snow, such as in the spring or fall, therefore automated photography surveys are only likely to be feasible during snow-free periods.

One potential method to improve the automation of identifying caribou in varying landscape and lighting conditions is to use machine learning. The premise behind machine learning is that a large dataset of photos is fed through multiple algorithms which identify patterns. The computer then learns what patterns represent features common to caribou, and can learn to identify caribou under many different conditions. Future work by ABR may be able to test the use of machine-learning to assess if it can be effectively implemented to address this problem.

CONCLUSION

The current emphasis of this study is to monitor caribou distribution and movements in relation to the proposed infrastructure in the BTN and BTS survey areas and to compile predevelopment baseline data on caribou density and movements. Detailed analyses of the existing patterns of seasonal distribution, density, and movements are providing important insights about the ways in which caribou currently use the study area and why. Although both the TCH and CAH recently underwent declines in population, possibly due to decreased survival of adults particularly after the prolonged winter of 2012–2013, both herds increased in size in the most recent counts. The TCH calving distribution

has recently expanded to the west and the winter distribution has varied widely among years (Parrett 2013). The CAH has shown some changes in seasonal distribution, with more caribou remaining farther north during fall and early winter and more intermixing with adjacent herds (Prichard 2016, ADFG 2017).

For this report, we incorporated multiple types of data and several different analyses to better understand the seasonal distributions, movements, and habitat associations of caribou in the area. By conducting aerial surveys during different seasons over the course of 19 years in northeastern NPRA, we have compiled an extensive dataset that allows us to understand the seasonal patterns as well as the variability in caribou distribution over this specific area. The use of telemetry data provided high-resolution locations for a subset of caribou throughout the year. This large and growing database allows us to understand caribou movements through the area for the two different herds which use the area. It also allows us to put local caribou movements in the study area into the broader context of the annual herd ranges and seasonal herd distributions. Lastly, we incorporated aerial survey results and telemetry data with remote sensing information on land cover, vegetative biomass, forage nitrogen, and snow cover to better understand the factors determining caribou seasonal distribution. This understanding of the underlying factors that are important to caribou will be useful when evaluating potential future changes in caribou distribution that may be attributable to development or a changing climate.

The use of aerial imagery for counts of caribou during high altitude aerial surveys shows promise, but there are still limitations to overcome before considering this method as a replacement for traditional aerial surveys. Aerial imaging and analytical technologies can potentially make aerial quantification of caribou distribution safer and more accurate while greatly lowering the probability of disturbing local residents, as technology advances the use of aerial photography and automation will likely become increasingly effective.

LITERATURE CITED

ADFG (Alaska Department of Fish and Game). 2017. Central Arctic caribou herd news. Winter 2016–17 edition. Alaska Department of Fish and Game, Division of Wildlife Conservation, Fairbanks, Alaska. 6 pp.

Arthur, S. M., and P. A. Del Vecchio. 2009. Effects of oil field development on calf production and survival in the Central Arctic Herd. Final research technical report, June 2001–March 2006. Federal Aid in Wildlife Restoration Project 3.46, Alaska Department of Fish and Game, Juneau, Alaska. 40 pp.

Bergerud, A. T., and R. E. Page. 1987. Displacement and dispersion of parturient caribou as antipredator tactics. Canadian Journal of Zoology 65: 1597–1606.

Bieniek, P.A., U.S. Bhatt, J.E. Walsh, R. Lader, B. Griffith, J. K. Roach, and R.L. Thoman. 2018. Assessment of Alaska rain-on-snow events using dynamical downscaling. Journal of Applied Meteorology and Climatology 57: 1847–1863.

BLM (Bureau of Land Management) and Ducks Unlimited. 2002. National Petroleum Reserve–Alaska earth-cover classification. U.S. Department of the Interior, BLM Alaska Technical Report 40, Anchorage, Alaska. 81 pp.

Boggs, K., L. Flagstad, T. Boucher, T. Kuo, D. Fehringer, S. Guyer, and M. Aisu. 2016. Vegetation Map and Classification: Northern, Western, and Interior Alaska. Second edition. Alaska Center for Conservation Science, University of Alaska Anchorage, Anchorage, Alaska. 110 pp.

Boyce, M. S., and L. L. McDonald. 1999. Relating populations to habitats using resource selection functions. Trends in Ecology and Evolution 14: 268–272.

Boyce, M. S., P. R. Vernier, S. E. Nielsen, and F. K. A. Schmiegelow. 2002. Evaluating resource selection functions. Ecological Modelling 157: 281–300.

Braem, N. M., S. Pedersen, J. Simon, D. Koster, T. Kaleak, P. Leavitt, J. Patkotak, and P. Neakok. 2011. Monitoring of annual caribou harvests in the National Petroleum Reserve in Alaska: Atqasuk, Barrow, and Nuiqsut, 2003–2007. Technical Paper No. 361, Alaska Department of Fish and Game, Division of Subsistence, Fairbanks, Alaska. 201 pp.

Brower, H. K., and R. T. Opie. 1997. North Slope Borough subsistence harvest documentation project: data for Nuiqsut, Alaska, for the period July 1, 1994 to June 30, 1995. North Slope Borough Department of Wildlife Management, Barrow, Alaska.

Brown, J., R. K. Haugen, and S. Parrish. 1975. Selected climatic and soil thermal characteristics of the Prudhoe Bay region. Pages 3–11 *in* J. Brown, editor. Ecological investigations of the tundra biome in the Prudhoe Bay region, Alaska. Biological Papers of the University of Alaska, Special Report No. 2, Fairbanks, Alaska.

Burgess, R. M., C. B. Johnson, P. E. Seiser, A. A. Stickney, A. M. Wildman, and B. E. Lawhead. 2002. Wildlife studies in the Northeast Planning Area of the National Petroleum Reserve–Alaska, 2001. Report for Phillips Alaska, Inc., Anchorage, by ABR, Inc., Fairbanks, Alaska. 71 pp.

Burnham, K. P., and D. R. Anderson. 2002. Model Selection and Multimodel Inference: A Practical Information–Theoretic Approach. 2nd edition. Springer–Verlag, New York City, New York. 488 pp.

Calcagno, V., and C. de Mazancourt. 2010. *glmulti*: an *R* package for easy automated model selection with (Generalized) Linear Models. Journal of Statistical Software 34: 1–29.

Cameron, R. D., W. T. Smith, and S. G. Fancy. 1989. Distribution and productivity of the Central Arctic Caribou Herd in relationship to petroleum development. Research progress report, Federal Aid in Wildlife Restoration Project 3.35, Alaska Department of Fish and Game, Juneau, Alaska. 52 pp.

Cameron, R. D., W. T. Smith, S. G. Fancy, K. L. Gerhart, and R. G. White. 1993. Calving success of female caribou in relation to body weight. Canadian Journal of Zoology 71: 480–486.

Carroll, G. M., L. S. Parrett, J. C. George, and D. A. Yokel. 2005. Calving distribution of the Teshekpuk caribou herd, 1994–2003. Rangifer, Special Issue 16: 27–35.

CLS. 2016. Argos user's manual. CLS, Toulouse, France. Available online: http://www.argos-system.org/manual/ (accessed 16 February 2018).

Cox, C. J., R. S. Stone, D. C. Douglas, D. M. Stanitski, G. J. Divoky, G. S. Dutton, C. Sweeney, J. C. George, and D. U. Longenecker. 2017. Drivers and environmental responses to the changing annual snow cycle of northern Alaska. Bulletin of the American Meteorological Society 98: 2559–2577.

Dau, J. R. 1986. Distribution and behavior of barren-ground caribou in relation to weather and parasitic insects. M.S. thesis, University of Alaska, Fairbanks, Alaska. 149 pp.

Dau, J. 2005. Two caribou mortality events in northwestern Alaska: possible causes and management implications. Rangifer, Special Issue 16: 37–50.

Dick, B. L., S. L. Findholt, and B. K. Johnson. 2013. A self-adjusting expandable GPS collar for male elk. Journal of Wildlife Management 37: 887–892.

Duong, T. 2017. *ks*: Kernel Smoothing. *R* package version 1.10.7. Available online: https://CRAN.R-project.org/package=ks (accessed 16 February 2018).

Eastland, W. G., R. T. Bowyer, and S. G. Fancy. 1989. Caribou calving sites relative to snow cover. Journal of Mammalogy 70: 824–828.

Fancy, S. G. 1983. Movements and activity budgets of caribou near oil drilling sites in the Sagavanirktok River floodplain, Alaska. Arctic 36: 193–197.

Fancy, S. G. 1986. Daily energy budgets of caribou: a simulation approach. Ph.D. dissertation, University of Alaska, Fairbanks, Alaska. 226 pp.

Fancy, S. G., and R. G. White. 1985. Energy expenditure by caribou while cratering in snow. Journal of Wildlife Management 49: 987–993.

Fancy, S. G., K. R. Whitten, N. E. Walsh, and R. D. Cameron. 1992. Population dynamics and demographics of caribou in developed and undeveloped areas of the Arctic Coastal Plain. Pages 1–21 *in* T. R. McCabe, D. B. Griffith, N. E. Walsh, and D. D. Young, editors. Terrestrial research: 1002 Area, Arctic National Wildlife Refuge. Interim report, 1988–1990. U.S. Fish and Wildlife Service, Anchorage, Alaska.

Finstad, G. L., and A. K. Prichard. 2000. Climatic influence on forage quality, growth, and reproduction of reindeer on the Seward Peninsula, II: Reindeer growth and reproduction. Rangifer, Special Issue 12: 144.

Fuller, A. S., and J. C. George. 1997. Evaluation of subsistence harvest data from the North Slope Borough 1993 census for eight North Slope villages for calendar year 1992. North Slope Borough Department of Wildlife Management, Barrow, Alaska.

Gasaway, W. C., S. D. DuBois, D. J. Reed, and S. J. Harbo. 1986. Estimating moose population parameters from aerial surveys. Biological Papers of the University of Alaska, No. 22, Fairbanks, Alaska. 108 pp.

Gorelick, N., M. Hancher, M. Dixon, S. Ilyushchenko, D. Thau, and R. Moore. 2017. Google Earth Engine: planetary-scale geospatial analysis for everyone. Remote Sensing of Environment 202: 18–27.

Gustine, D., P. Barboza, L. Adams, B. Griffith, R. Cameron, and K. Whitten. 2017. Advancing the match-mismatch framework for large herbivores in the Arctic: Evaluating the evidence for a trophic mismatch in caribou. PLoS ONE 12(2): e0171807. doi:10.1371/journal.pone.0171807

Griffith, D. B., D. C. Douglas, N. E. Walsh, D. D. Young, T. R. McCabe, D. E. Russell, R. G. White, R. D. Cameron, and K. R. Whitten. 2002. Section 3: The Porcupine caribou herd. Pages 8–37 *in* D. C. Douglas, P. E. Reynolds, and E. B. Rhode, editors. Arctic Refuge coastal plain terrestrial wildlife research summaries. U.S. Geological Survey, Biological Resources Division, Biological Science Report USGS/BRD/BSR-2002-0001.

Hope, A. S., J. S. Kimball, and D. A. Stow. 1993. The relationship between tussock tundra spectral properties and biomass and vegetation composition. International Journal of Remote Sensing 14: 1861–1874.

Horne, J. S., E. O. Garton, S. M. Krone, and J. S. Lewis. 2007. Analyzing animal movements using Brownian bridges. Ecology 88: 2354–2363.

Jensen, P. G., and L. E. Noel. 2002. Caribou distribution in the northeast National Petroleum Reserve–Alaska, summer 2001. Chapter 3 *in* M. A. Cronin, editor. Arctic Coastal Plain caribou distribution, summer 2001. Report for BP Exploration (Alaska) Inc., Anchorage, by LGL Alaska Research Associates, Inc., Anchorage, Alaska.

Johnson, C. B., R. M. Burgess, A. M. Wildman, A. A. Stickney, P. E. Seiser, B. E. Lawhead, T. J. Mabee, J. R. Rose, and J. E. Shook. 2004. Wildlife studies for the Alpine Satellite Development Project, 2003. Annual report for ConocoPhillips Alaska, Inc., and Anadarko Petroleum Corp., Anchorage, by ABR, Inc., Fairbanks, Alaska. 155 pp.

Johnson, C. B., J. P. Parrett, T. Obritschkewitsch, J. R. Rose, K. B. Rozell, and P. E. Seiser. 2015. Avian studies for the Alpine Satellite Development Project, 2014. 12th annual report for ConocoPhillips Alaska, Inc., and Anadarko Petroleum Corp., Anchorage, by ABR, Inc., Fairbanks, Alaska. 124 pp.

Johnson, H. E., D. D. Gustine, T. S. Golden, L. G. Adams, L. S. Parrett, E. A. Lenart, P. S. Barboza. 2018. NDVI exhibits mixed success in predicting spatiotemporal variation in caribou summer forage quality and quantity. Ecosphere 9: 10.

Johnstone, J., D. E. Russell, and D. B. Griffith. 2002. Variations in plant forage quality in the range of the Porcupine caribou herd. Rangifer 22: 83–91.

Joly, K., M.J. Cole, and R.R. Jandt. 2007. Diets of overwintering caribou, Rangifer tarandus, track decadal changes in arctic tundra vegetation. Canadian Field Naturalist 121: 379-383.

Jorgenson, M. T., J. E. Roth, E. R. Pullman, R. M. Burgess, M. Raynolds, A. A. Stickney, M. D. Smith, and T. Zimmer. 1997. An ecological land survey for the Colville River delta, Alaska, 1996. Report for ARCO Alaska, Inc., Anchorage, by ABR, Inc., Fairbanks, Alaska. 160 pp.

Jorgenson, M. T., J. E. Roth, M. Emers, S. Schlentner, D. K. Swanson, E. R. Pullman, J. Mitchell, and A. A. Stickney. 2003. An ecological land survey for the Northeast Planning Area of the National Petroleum Reserve–Alaska, 2002. Report for ConocoPhillips Alaska, Inc., Anchorage, by ABR, Inc., Fairbanks, Alaska. 84 pp.

Jorgenson, M. T., J. E. Roth, M. Emers, W. Davis, E. R. Pullman, and G. V. Frost. 2004. An ecological land survey for the Northeast Planning Area of the National Petroleum Reserve–Alaska, 2003. Addendum to 2002 report for ConocoPhillips Alaska, Inc., and Anadarko Petroleum Corporation, Anchorage, by ABR, Inc., Fairbanks, Alaska. 40 pp.

Kelleyhouse, R. A. 2001. Calving-ground selection and fidelity: Teshekpuk Lake and Western Arctic herds. M.S. thesis, University of Alaska, Fairbanks, Alaska. 124 pp.

Klein, D. R. 1990. Variation in quality of caribou and reindeer forage plants associated with season, plant part, and phenology. Rangifer, Special Issue 3: 123–130.

Klimstra, R. 2018. Summary of Teshekpuk caribou herd photocensus conducted July 14, 2017. State of Alaska memorandum, Department of Fish and Game, Division of Wildlife Conservation (Northwest), Fairbanks, Alaska. 6 pp.

Kranstauber, B., K. Safi, and F. Bartumeus. 2014. Bivariate Gaussian bridges: directional factorization of diffusion in Brownian bridge models. Movement Ecology 2: 5. doi.org/10.1186/2051-3933-2-5.

Kranstauber, B., M. Smolla, and A.K. Scharf. 2017. *Move*: visualizing and analyzing animal track data. *R* package version 3.0.1. Available online: https://CRAN.R-project.org/package=move (accessed 16 February 2018).

Kuropat, P. J. 1984. Foraging behavior of caribou on a calving ground in northwestern Alaska. M.S. thesis, University of Alaska, Fairbanks, Alaska. 95 pp.

Lair, H. 1987. Estimating the location of the focal center in red squirrel home ranges. Ecology 68: 1092–1101.

Lawhead, B. E. 1988. Distribution and movements of Central Arctic Herd caribou during the calving and insect seasons. Pages 8–13 *in* R. Cameron and J. Davis, editors. Reproduction and calf survival. Proceedings of the 3rd North American Caribou Workshop. Wildlife Technical Bulletin No. 8, Alaska Department of Fish and Game, Juneau, Alaska.

Lawhead, B. E., A. K. Prichard, and M. J. Macander. 2006. Caribou monitoring study for the Alpine Satellite Development Program, 2005. First annual report for ConocoPhillips Alaska, Inc., Anchorage, by ABR, Inc., Fairbanks, Alaska. 102 pp.

Lawhead, B. E., A. K. Prichard, and M. J. Macander. 2007. Caribou monitoring study for the Alpine Satellite Development Program, 2006. Second annual report for ConocoPhillips Alaska, Inc., Anchorage, by ABR, Inc., Fairbanks, Alaska. 75 pp.

Lawhead, B. E., A. K. Prichard, and M. J. Macander. 2008. Caribou monitoring study for the Alpine Satellite Development Program, 2007. Third annual report for ConocoPhillips Alaska, Inc., Anchorage, by ABR, Inc., Fairbanks, Alaska. 89 pp.

Lawhead, B. E., A. K. Prichard, and M. J. Macander. 2009. Caribou monitoring study for the Alpine Satellite Development Program, 2008. Fourth annual report for ConocoPhillips Alaska, Inc., Anchorage, by ABR, Inc., Fairbanks, Alaska. 91 pp.

Lawhead, B. E., A. K. Prichard, and M. J. Macander. 2010. Caribou monitoring study for the Alpine Satellite Development Program, 2009. Fifth annual report for ConocoPhillips Alaska, Inc., Anchorage, by ABR, Inc., Fairbanks, Alaska. 101 pp.

Lawhead, B. E., A. K. Prichard, and M. J. Macander. 2011. Caribou monitoring study for the Alpine Satellite Development Program, 2010. Sixth annual report for ConocoPhillips Alaska, Inc., Anchorage, by ABR, Inc., Fairbanks, Alaska. 101 pp.

Lawhead, B. E., A. K. Prichard, and M. J. Macander. 2012. Caribou monitoring study for the Alpine Satellite Development Program, 2011. Seventh annual report for ConocoPhillips Alaska, Inc., Anchorage, by ABR, Inc., Fairbanks, Alaska. 90 pp.

Lawhead, B. E., A. K. Prichard, M. J. Macander, and J. H. Welch. 2013. Caribou monitoring study for the Alpine Satellite Development Program, 2012. Eighth annual report for ConocoPhillips Alaska, Inc., Anchorage, by ABR, Inc., Fairbanks, Alaska. 88 pp.

Lawhead, B. E., A. K. Prichard, M. J. Macander, and J. H. Welch. 2014. Caribou monitoring study for the Alpine Satellite Development Program, 2013. Ninth annual report for ConocoPhillips Alaska, Inc., Anchorage, by ABR, Inc., Fairbanks, Alaska. 94 pp.

Lawhead, B. E., A. K. Prichard, M. J. Macander, and J. H. Welch. 2015. Caribou monitoring study for the Alpine Satellite Development Program, 2014. Tenth annual report for ConocoPhillips Alaska, Inc., Anchorage, by ABR, Inc., Fairbanks, Alaska. 100 pp.

Lenart, E. A. 2009. GMU 26B and 26C, Central Arctic Herd. Pages 299–325 *in* P. Harper, editor. Caribou management report of survey and inventory activities, 1 July 2006–30 June 2008. Federal Aid in Wildlife Restoration Project 3.0, Alaska Department of Fish and Game, Juneau, Alaska.

Lenart, E. A. 2015. Units 26B and 26C, Central Arctic. Chapter 18 *in* P. Harper and L. A. McCarthy, editors. Caribou management report of survey and inventory activities, 1 July 2012–30 June 2014. Alaska Department of Fish and Game, Species Management Report ADF&G/DWC/SMR-2015-4, Juneau, Alaska.

Lenart, E. A. 2017. 2016 Central Arctic caribou photocensus results. State of Alaska memorandum, Department of Fish and Game, Division of Wildlife Conservation, Fairbanks, Alaska. 5 p.

Lenart, E. A. 2019. 2019 Central Arctic caribou photocensus results. State of Alaska Memorandum. Alaska Department Of Fish and Game, Division of Wildlife Conservation. Fairbanks, Alaska. 8 pp.

Macander, M. J. 2005. MODIS satellite vegetation indices over partially vegetated pixels on the Arctic Coastal Plain of Alaska. M.S. thesis, University of Alaska, Fairbanks. 113 pp.

Macander, M. J., C. S. Swingley, K. Joly, and M. K. Raynolds. 2015. Landsat-based snow persistence map for northwest Alaska. Remote Sensing of Environment 163: 23–31.

Manly, B. F. J., L. L. McDonald, D. L. Thomas, T. L. McDonald, and W. P. Erickson. 2002. Resource selection by animals: statistical design and analysis for field studies. Second edition. Kluwer Academic Publishers, Dordrecht, The Netherlands. 209 pp.

McNay, R. S., J. A. Morgan, and F. L. Bunnell. 1994. Characterizing independence of observations in movements of Columbian black-tailed deer. Journal of Wildlife Management 58: 422–429.

Mörschel, F. M. 1999. Use of climatic data to model the presence of oestrid flies in caribou herds. Journal of Wildlife Management 63: 588–593.

Muller, S. V., D. A. Walker, F. E. Nelson, N. A. Auerbach, J. G. Bockheim, S. Guyer, and D. Sherba. 1998. Accuracy assessment of a land-cover map of the Kuparuk River basin, Alaska: considerations for remote regions. Photogrammetric Engineering and Remote Sensing 64: 619–628.

Muller, S. V., A. E. Racoviteanu, and D. A. Walker. 1999. Landsat-MSS-derived land-cover map of northern Alaska: extrapolation methods and a comparison with photo-interpreted and AVHRR-derived maps. International Journal of Remote Sensing 20: 2921–2946.

Murphy, S. M., and B. E. Lawhead. 2000. Caribou. Chapter 4, pages 59–84 *in* J. Truett and S. R. Johnson, editors. The Natural History of an Arctic Oil Field: Development and the Biota. Academic Press, San Diego, California.

Nellemann, C., and R. D. Cameron. 1996. Effects of petroleum development on terrain preferences of calving caribou. Arctic 49: 23–28.

Nellemann, C., and M. G. Thomsen. 1994. Terrain ruggedness and caribou forage availability during snowmelt on the Arctic Coastal Plain, Alaska. Arctic 47: 361–367.

Nicholson, K. L., S. M. Arthur, J. S. Horne, E. O. Garton, and P. A. Del Vecchio. 2016. Modeling caribou movements: seasonal ranges and migration routes of the Central Arctic Herd. PLoS One 11(4): e0150333. doi:10.1371/journal.pone.0150333.

Noel, L. E. 1999. Calving caribou distribution in the Teshekpuk Lake area, June 1998. Data report for BP Exploration (Alaska) Inc., Anchorag, by LGL Alaska Research Associates, Inc., Anchorage, Alaska. 31 pp.

Noel, L. E. 2000. Calving caribou distribution in the Teshekpuk Lake area, June 1999. Report for BP Exploration (Alaska) Inc., Anchorage, by LGL Alaska Research Associates, Inc., Anchorage, Alaska. 29 pp.

Noel, L. E., and J. C. George. 2003. Caribou distribution during calving in the northeast National Petroleum Reserve–Alaska, June 1998 to 2000. Rangifer, Special Issue 14: 283–292.

North Slope Science Initiative (NSSI). 2013. North Slope Science Initiative land-cover mapping summary report. Report for NSSI by Ducks Unlimited, Inc., Rancho Cordova, California. 51 pp. + maps.

Parrett, L. S. 2007. Summer ecology of the Teshekpuk caribou herd. M.S. thesis, University of Alaska, Fairbanks, Alaska. 149 pp.

Parrett, L. S. 2013. Unit 26A, Teshekpuk Caribou Herd. Pages 314–355 *in* P. Harper, editor. Caribou management report of survey and inventory activities, 1 July 2010–30 June 2012. Alaska Department of Fish and Game, Species Management Report ADF&G/DWC/SMR-2013-3, Juneau, Alaska.

Parrett, L. S. 2015a. Unit 26A, Teshekpuk caribou herd. Chapter 17 *in* P. Harper and L. A. McCarthy, editors. Caribou management report of survey and inventory activities, 1 July 2012–30 June 2014. Alaska Department of Fish and Game, Species Management Report ADF&G/DWC/SMR-2015-4, Juneau, Alaska.

Parrett, L. S. 2015b. Summary of Teshekpuk caribou herd photocensus conducted July 6, 2015. State of Alaska memorandum, Department of Fish and Game, Division of Wildlife Conservation (Northwest), Fairbanks, Alaska. 6 pp.

Pebesma, E. J. 2004. Multivariate geostatistics in S: the *gstat* package. Computers & Geosciences 30: 683–691.

Pedersen, S. 1995. Nuiqsut. Chapter 22 *in* J. A. Fall and C. J. Utermohle, editors. An investigation of the sociocultural consequences of Outer Continental Shelf development in Alaska, Vol. V: Alaska Peninsula and Arctic. Technical Report No. 160, OCS Study MMS 95-014, Minerals Management Service, Anchorage, Alaska.

Pennycuick, C. J., and D. Western. 1972. An investigation of some sources of bias in aerial transect sampling of large mammal populations. East African Wildlife Journal 10: 175–191.

Person, B. T., A. K. Prichard, G. M. Carroll, D. A. Yokel, R. S. Suydam, and J. C. George. 2007. Distribution and movements of the Teshekpuk caribou herd, 1990–2005: prior to oil and gas development. Arctic 60: 238–250.

Philo, L. M., G. M. Carroll, and D. A. Yokel. 1993. Movements of caribou in the Teshekpuk Lake herd as determined by satellite tracking, 1990–1993. North Slope Borough Department of Wildlife Management, Barrow; Alaska Department of Fish and Game, Barrow; and U.S. Department of Interior, Bureau of Land Management, Fairbanks, Alaska. 60 p.

Prichard, A.K. 2016. Section 9. caribou distribution, habitat use, and herd fidelity. [In] Macander, M.J., G.V. Frost, and S.M. Murphy. Shell onshore/nearshore environmental studies, 2015. Draft report prepared for Shell Onshore/Nearshore Environmental Studies Program by ABR Inc., Fairbanks, Alaska.

Prichard, A.K., R.L. Klimstra, B.T. Person, and L.S. Parrett. 2019a. Aerial survey and telemetry data analysis of a peripheral caribou calving areain northwestern Alaska. Rangifer 43–58.

Prichard, A.K., B.E. Lawhead, and J.H. Welch. 2019b. Caribou Distribution and Movements near the Kuparuk Oilfield, 2008–2018. Report for ConocoPhillips Alaska, Inc., Anchorage, by ABR, Inc., Fairbanks, Alaska. 28 pp.

Prichard, A. K., M. J. Macander, J. H. Welch, and B. E. Lawhead. 2017. Caribou monitoring study for the Alpine Satellite Development Program, 2015 and 2016. Twelfth annual report for ConocoPhillips Alaska, Inc., Anchorage, by ABR, Inc., Fairbanks, Alaska. 62 pp.

Prichard, A. K., J. H. Welch, M. J. Macander, and B. E. Lawhead. 2018. Caribou monitoring study for the Alpine Satellite Development Program, 2017. Thirteenth annual report for ConocoPhillips Alaska, Inc., Anchorage, by ABR, Inc., Fairbanks, Alaska. 63 pp.

Prichard, A. K., J. H. Welch, M. J. Macander, and B. E. Lawhead. 2019c. Caribou monitoring study for the Alpine Satellite Development Program, 2018. Fourteenth annual report for ConocoPhillips Alaska, Inc., Anchorage, by ABR, Inc., Fairbanks, Alaska. 88 pp.

Prichard, A. K., J. H. Welch, M. J. Macander, and B. E. Lawhead. 2019d. Caribou monitoring study for the Bear Tooth Unit Program, Arctic Coastal Plain, Alaska, 2018. Annual report for ConocoPhillips Alaska, Inc., Anchorage, by ABR, Inc., Fairbanks, Alaska. 96 pp.

Prichard, A. K., and J. H. Welch. 2020. Mammal surveys in the Greater Kuparuk Area, northern Alaska, 2018–2019. Report for ConocoPhillips Alaska, Inc., and Greater Kuparuk Area, Anchorage, by ABR, Inc., Fairbanks, Alaska.

Prichard, A. K., J. H. Welch, and M. J. Macander. 2020. Caribou monitoring study for the Bear Tooth Unit Program, Arctic Coastal Plain, Alaska, 2019. Annual report for ConocoPhillips Alaska, Inc., Anchorage, by ABR, Inc., Fairbanks, Alaska.

Prichard, A. K., D. A. Yokel, C. L. Rea, B. T. Person, and L. S. Parrett. 2014. The effect of frequency of telemetry locations on movement-rate calculations in arctic caribou. Wildlife Society Bulletin 38: 78–88.

R Core Team. 2019. R: A language and environment for statistical computing. *R* Foundation for Statistical Computing, Vienna, Austria. URL: http://www.R-project.org.

Riggs, G. A., and D. K. Hall. 2015. MODIS snow products Collection 6 user guide. National Snow and Ice Data Center. Available online: https://nsidc.org/sites/nsidc.org/files/files/MODIS-snow-user-guide-C6.pdf (accessed 16 February 2018).

Rouse, J. W., R. H. Haas, J. A. Schell, and D. W. Deering. 1973. Monitoring vegetation systems in the Great Plains with ERTS. Third Earth Resources Technology Satellite Symposium, Greenbelt, MD, NASA (SP-351) 1: 309–317.

Russell, D. E., A. M. Martell, and W. A. C. Nixon. 1993. Range ecology of the Porcupine caribou herd in Canada. Rangifer, Special Issue 8. 167 pp.

Salomonson, V. V., and I. Appel. 2004. Estimating fractional snow cover from MODIS using the normalized difference snow index. Remote Sensing of Environment 89: 351–360.

Sappington, J., K. M. Longshore, and D. B. Thompson. 2007. Quantifying landscape ruggedness for animal habitat analysis: a case study using bighorn sheep in the Mojave Desert. Journal of Wildlife Management 71: 1419–1426.

Schaaf, C., and Z. Wang. 2015. MCD43A4 MODIS/Terra+Aqua BRDF/Albedo Nadir BRDF Adjusted Ref Daily L3 Global - 500m V006. Distributed by NASA EOSDIS Land Processes DAAC, https://doi.org/10.5067/MODIS/MCD43A4.006

Sellers, P. J. 1985. Canopy reflectance, photosynthesis, and transpiration. International Journal of Remote Sensing 21: 143–183. [original not reviewed; cited in Hope et al. 1993]

SRB&A. 2017. Nuiqsut caribou subsistence monitoring project: results of year 8 hunter interviews and household harvest surveys. Report for ConocoPhillips Alaska, Inc., Anchorage, by Stephen R. Braund & Associates, Anchorage, Alaska. 47 pp. + appendices.

Stow, D. A., A. Hope, D. McGuire, D. Verbyla, J. Gamon, F. Huemmrich, S. Houston, C. Racine, M. Sturm, K. Tape, L. Hinzman, K. Yoshikawa, C. Tweedie, B. Noyle, C. Silapaswan, D. Douglas, B. Griffith, G. Jia, H. Epstein, D. Walker, S. Daeschner, A. Pertersen, L. Zhou, and R. Myneni. 2004. Remote sensing of vegetation and land-cover change in arctic tundra ecosystems. Remote Sensing of Environment 89: 281–308.

Walker, H. J. 1983. Guidebook to permafrost and related features of the Colville River delta, Alaska. Guidebook 2. Alaska Division of Geological and Geophysical Surveys, Anchorage. 34 pp.

Walker, H. J., and H. H. Morgan. 1964. Unusual weather and riverbank erosion in the delta of the Colville River, Alaska. Arctic 17: 41–47.

Weladji, R. B., G. Steinheim, Ø. Holand, S. R. Moe, T. Almøy, and T. Ådnøy. 2003. Use of climatic data to assess the effect of insect harassment on the autumn weight of reindeer (*Rangifer tarandus*) calves. Journal of Zoology 260: 79–85.

White, R. G., B. R. Thomson, T. Skogland, S. J. Person, D. E. Russell, D. F. Holleman, and J. R. Luick. 1975. Ecology of caribou at Prudhoe Bay, Alaska. Pages 151–201 *in* J. Brown, editor. Ecological investigations of the tundra biome in the Prudhoe Bay region, Alaska. Biological Papers of the University of Alaska, Special Report No. 2, Fairbanks, Alaska.

Wilson, R. R., A. K. Prichard, L. S. Parrett, B. T. Person, G. M. Carroll, M. A. Smith, C. L. Rea, and D. A. Yokel. 2012. Summer resource selection and identification of important habitat prior to industrial development for the Teshekpuk caribou herd in northern Alaska. PLoS One 7(11): e48697. doi:10.1371/journal.pone.0048697.

Wolfe, S. A. 2000. Habitat selection by calving caribou of the central arctic herd, 1980–95. M.S. thesis, University of Alaska, Fairbanks. 83 pp.

Yokel, D. A., A. K. Prichard, G. Carroll, L. Parrett, B. Person, and C. Rea. 2009. Teshekpuk caribou herd movement through narrow corridors around Teshekpuk Lake, Alaska. Alaska Park Science 8(2): 64–67.

Zuur, A. F., E. N. Ieno, N. J. Walker, A. A. Saveliev, and G. M. Smith. 2009. Mixed-effects models and extensions in ecology with *R*. Springer, New York City, New York. 574 pp.

Appendix A. Cover-class descriptions of the NPRA earth-cover classification (BLM and Ducks Unlimited 2002).

Cover Class	Description
Clear Water	Fresh or saline waters with little or no particulate matter. Clear waters typically are deep (>1 m). This class may contain small amounts of *Arctophila fulva* or *Carex aquatilis*, but generally has <15 surface coverage by these species.
Turbid Water	Waters that contain particulate matter or shallow (<1 m), clear waterbodies that differ spectrally from Clear Water class. This class typically occurs in shallow lake shelves, deltaic plumes, and rivers and lakes with high sediment loads. Turbid waters may contain small amounts of *Arctophila fulva* or *Carex aquatilis*, but generally have <15 surface coverage by these species.
Carex aquatilis	Associated with lake or pond shorelines and composed of 50–80 % clear or turbid water >10 cm deep. The dominant species is *Carex aquatilis*. Small percentages of *Arctophila fulva, Hippuris vulgaris, Potentilla palustris,* and *Caltha palustris* may be present.
Arctophila fulva	Associated with lake or pond shorelines and composed of 50–80% clear or turbid water >10 cm deep. The dominant species is *Arctophila fulva*. Small percentages of *Carex aquatilis, Hippuris vulgaris, Potentilla palustris,* and *Caltha palustris* may be present.
Flooded Tundra–Low-centered Polygons	Polygon features that retain water throughout the summer. This class is composed of 25–50% water; *Carex aquatilis* is the dominant species in permanently flooded areas. The drier ridges of polygons are composed mostly of *Eriophorum russeolum, E. vaginatum, Sphagnum* spp., *Salix* spp., *Betula nana, Arctostaphylos* spp., and *Ledum palustre*.
Flooded Tundra–Non-patterned	Continuously flooded areas composed of 25–50% water. *Carex aquatilis* is the dominant species. Other species may include *Hippuris vulgaris, Potentilla palustris,* and *Caltha palustris*. Non-patterned class is distinguished from low-centered polygons by the lack of polygon features and associated shrub species that grow on dry ridges of low-centered polygons.
Wet Tundra	Associated with areas of super-saturated soils and standing water. Wet tundra often floods in early summer and generally drains of excess water during dry periods, but remains saturated throughout the summer. It is composed of 10–25% water; *Carex aquatilis* is the dominant species. Other species may include *Eriophorum angustifolium*, other sedges, grasses, and forbs.
Sedge/Grass Meadow	Dominated by the sedge family, this class commonly consists of a continuous mat of sedges and grasses with a moss and lichen understory. The dominant species are *Carex aquatilis, Eriophorum angustifolium, E. russeolum, Arctagrostis latifolia,* and *Poa arctica*. Associated genera include *Cassiope* spp., *Ledum* spp., and *Vaccinium* spp.
Tussock Tundra	Dominated by the tussock-forming sedge *Eriophorum vaginatum*. Tussock tundra is common throughout the arctic foothills north of the Brooks Range and may be found on well-drained sites in all areas of the NPRA. Cottongrass tussocks are the dominant landscape elements and moss is the common understory. Lichen, forbs, and shrubs are also present in varying densities. Associated genera include *Salix* spp., *Betula nana*, *Ledum palustre*, and *Carex* spp.
Moss/Lichen	Associated with low-lying lakeshores and dry sandy ridges dominated by moss and lichen species. As this type grades into a sedge type, graminoids such as *Carex aquatilis* may increase in cover, forming an intermediate zone.
Dwarf Shrub	Associated with ridges and well-drained soils and dominated by shrubs <30 cm in height. Because of the relative dryness of the sites on which this cover type occurs, it is the most species-diverse class. Major species include *Salix* spp., *Betula nana*, *Ledum palustre, Dryas* spp*., Vaccinium* spp*., Arctostaphylos* spp*., Eriophorum vaginatum,* and *Carex aquatilis.* This class frequently occurs over a substrate of tussocks.

Appendix A. Continued.

Cover Class	Description
Low Shrub	Associated with small streams and rivers, but also occurs on hillsides in the southern portion of the NPRA. This class is dominated by shrubs 0.3–1.5 m in height. Major species include *Salix* spp., *Betula nana*, *Alnus crispa*, and *Ledum palustre.*
Dunes/Dry Sand	Associated with streams, rivers, lakes and coastal beaches. Dominated by dry sand with <10% vegetative cover. Plant species may include *Poa* spp., *Salix* spp., *Astragalus* spp., *Carex* spp., *Stellaria* spp., *Arctostaphylos* spp., and *Puccinellia phryganodes*.
Sparsely Vegetated	Occurs primarily along the coast in areas affected by high tides or storm tides, in recently drained lake or pond basins, and in areas where bare mineral soil is being recolonized by vegetation. Dominated by non-vegetated material with 10–30% vegetative cover. The vegetation may include rare plants, but the most common species include *Stellaria* spp., *Poa* spp., *Salix* spp., *Astragalus* spp., *Carex* spp., *Arctostaphylos* spp., and *Puccinellia phryganodes*.
Barren Ground/ Other	Associated with river and stream gravel bars, mountainous areas, and human development. Includes <10% vegetative cover. May incorporate dead vegetation associated with salt burn from ocean water.

Appendix B. Snow depth (cm) and cumulative thawing degree-days (°C above freezing) at the Kuparuk airstrip, 1983–2019.

	Snow Depth (cm)			Cumulative Thawing Degree-days (ºC)						
Year	1 April	15 May	31 May	1–15 May	16–31 May	1–15 June	16–30 June	1–15 July	16–31 July	1–15 August
1983	10	5	0	0	3.6	53.8	66.2	74.7	103.8	100.3
1984	18	15	0	0	0	55.6	75.3	122.8	146.4	99.5
1985	10	8	0	0	10.3	18.6	92.8	84.7	99.4	100.0
1986	33	20	10	0	0	5.0	100.8	112.2	124.7	109.4
1987	15	8	3	0	0.6	6.7	61.4	112.2	127.8	93.1
1988	10	5	5	0	0	16.7	78.1	108.3	143.1	137.5
1989	33	–	10[a]	0	5.6	20.6	109.4	214.7	168.1	215.8
1990	8	3	0	0	16.1	39.7	132.2	145.0	150.0	82.5
1991	23	8	3	0	7.8	14.4	127.6	73.3	115.0	70.6
1992	13	8	0	0.3	20.3	55.0	85.3	113.9	166.1	104.2
1993	13	5	0	0	8.6	33.6	94.4	175.8	149.7	96.1
1994	20	18	8	0	4.4	49.2	51.7	149.7	175.8	222.2
1995	18	5	0	0	1.1	59.4	87.5	162.8	106.9	83.3
1996	23	5	0	8.1	41.7	86.1	121.1	138.9	168.1	95.8
1997	28	18	8	0	20.8	36.1	109.7	101.7	177.8	194.2
1998	25	8	0	3.6	45.8	74.2	135.0	158.9	184.4	174.4
1999	28	15	10	0	1.4	30.3	67.8	173.3	81.1	177.5
2000	30	23	13	0	0	36.7	169.7	113.3	127.5	118.6
2001	23	30	5	0	0.8	51.9	72.2	80.0	183.9	131.7
2002	30	trace	0	4.2	30.3	57.8	70.3	92.2	134.4	106.1
2003	28	13	trace	0	10.8	23.6	77.5	140.0	144.7	91.9
2004	36	10	5	0	8.9	26.4	185.6	148.1	151.4	153.3
2005	23	13	0	0	2.5	14.2	78.1	67.5	79.4	176.7
2006	23	5	0	0	23.3	93.3	153.1	82.2	186.1	109.7
2007	25	46	5	0	0	46.4	81.7	115.0	138.9	134.4
2008	20	18	0	0	32.8	71.7	138.9	172.2	132.5	86.1
2009	36	13	0	0	16.7	71.7	44.4	142.8	126.4	133.6
2010	41	43	13	0	1.4	53.3	51.1	126.7	168.9	149.2
2011[a]	25	18	0	0	27.8	12.5	101.2	122.4	171.6	143.2
2012[a]	48	53	2	0	1.7	26.8	137.3	140.2	195.2	143.5
2013	33	18	2	0	4.2	79.2	131.7	112.8	188.0	185.4

Appendix B. Continued.

	Snow Depth (cm)			Cumulative Thawing Degree-days (ºC)						
Year	1 April	15 May	31 May	1–15 May	16–31 May	1–15 June	16–30 June	1–15 July	16–31 July	1–15 August
2014	33	0[b]	0[b]	11.1	4.2	28.6	82.0	127.2	102.3	67.9
2015	38	14	3	1.4	46.4	78.9	197.2	117.9	95.7	106.9
2016	25	0	0	15.6	12.4	63.7	131.2	174.7	130.8	98.1
2017	36	14	0	0	12.1	5.2	121.3	173.4	174.5	150.5
2018	41	20	15	1.35	0	6.6	47.7	137.0	195.9	55.25
2019	23	13	0	1.1	11.9	31.1	108.5	180.3	181.3	118.0
Mean	**25**	**14**	**3**	**1.3**	**11.8**	**41.5**	**102.1**	**129.5**	**145.8**	**125.0**

[a] Kuparuk weather data were not available for 17 June–9 December 2011, 4–14 August 2012, and 30–31 August 2012, so cumulative TDD for those periods were estimated by averaging Deadhorse and Nuiqsut temperatures (Lawhead and Prichard 2012).

[b] Kuparuk airport station reported no snow after 8 May 2014, whereas other weather stations nearby reported snow until 31 May and patchy snow was present in the GKA survey areas into early June. Therefore, if accurate, the airport information was not representative of the study area.

Page intentionally left blank.

Appendix C. 2019 imaging season summary report. North Slope aerial caribou imaging to support automated counts. Survey report submitted by TerraSond, Inc.

Page intentionally left blank.

TERRASOND®

PRECISION GEOSPATIAL SOLUTIONS®

North Slope
Aerial Caribou Imaging to Support Automated Counts

2019 IMAGING SEASON SUMMARY REPORT

Report Date:
10/15/2019

Submitted to:

ABR inc.

Submitted by:

TerraSond Limited

Part of the ACTEON group

1617 S Industrial Way Ste 3,
Palmer, AK 99645
907.745.7215

TABLE OF CONTENTS

1 2019 OBJECTIVES 1

2 AERIAL IMAGING ACQUISITION 1

2.1 **SPRING 2019** 1

2.1.1 May 13 – 14, 2019 Spring Aerial Mission 01 1

2.1.2 June 18 - 19, 2019 Summer Aerial Mission 02 4

2.2 **SUMMER 2019** 4

2.2.1 July 22, 2019 Survey Summer Aerial Mission 01 4

2.2.2 July 31, 2019 Survey Summer Aerial Mission 02 5

2.2.3 August 16, 2019 Survey Summer Aerial Mission 03 6

2.2.4 August 28, 2019 Survey Summer Aerial Mission 04 7

2.3 **FALL 2019** 8

2.3.1 October 3, 2019 Survey Fall Aerial Mission 8

3 ANALYSIS 9

3.1 Threshold Analysis (*ImageJ*) 9

3.2 Script Overview 11

3.3 Ecosystem Change / Biological Change 13

3.3.1 Spring 13

3.3.2 Summer 15

3.3.3 Fall 17

4 LIMITATIONS / INSIGHT 17

4.1 Motion Blur 18

4.2 Sun Angle 18

4.3 Adobe Lightroom, Aperture Adjustments, Shutter Speed, and Dim Photos 20

4.4 Forward Looking Infrared (FLIR) 22

4.5 Overlap 24

5 CONCLUSION 25

LIST OF FIGURES

Figure 1. A photo taken of the conditions present during the May 13th, 2019 flight. 2
Figure 2. An image showing a close-up of two running caribou during Spring aerial mission one 3
Figure 3. RGB imagery acquired by the integrated camera system on June 18th, 2019 of 22 caribou. 4
Figure 4. An image that was acquired on July 22, 2019 that was adjusted in Adobe Lightroom which consisted of a slight amount of motion blur. 5
Figure 5. An image captured on July 31, 2019 of a moose or caribou in the riparian area. 6
Figure 6. An image that was taken on August 16, 2019 and adjusted in Adobe Lightroom of one caribou south of Teshekpuk Lake. 7
Figure 7. A zoomed in photo of two caribou in the black circles taken on August 28th, 2019. 8
Figure 8. An image acquired on October 3, 2019 during the fall aerial survey of four caribou showing a high color discrepancy. 9
Figure 9. An example of threshold evaluation on an individual band with ImageJ. 10
Figure 10. RGB imagery acquired by the integrated camera system on June 24th, 2019 of 2 caribou. The contours were used for sizing analysis. 11
Figure 11. A workflow diagram of the CINS processing methodology. 12
Figure 12. The CINS automated caribou script accurately identifying and tagging caribou in an image taken on June 19th, 2019. 13
Figure 13. A photo showing caribou during the spring period and how well they blend in during this time of the year on May 14th, 2019. 14
Figure 14. An image taken on May 14th, 2019 that was turned into a 16-bit black and white image with threshold analysis from ImageJ. 15
Figure 15. An example of the typical conditions in early summer with a herd of caribou. 16
Figure 16. An example of a fall image that is analogous to the early spring image after plant senescence. 17
Figure 17. An example of motion blur that was captured on July 22nd, 2019. 18
Figure 18. The solar elevation on the North Slope of Alaska throughout the season. 19
Figure 19. An example of the low sun angle taken at Nuiqsut on October 2nd, 2019 at 9:45 AM. 20
Figure 20. An example of an image that was adjusted in Adobe Lightroom during post-processing. 21
Figure 21. An image showing how the camera adjustments created a properly exposed photograph on October 3rd, 2019. 22
Figure 22. RGB imagery acquired by the integrated camera system on May 13th, 2019 of three caribou. The box shown shows the footprint of the FLIR image in Figure 2. 23
Figure 23. FLIR imagery acquired by the integrated camera system on May 13th, 2019 of one caribou. 24
Figure 24. A visual depiction of the 75% downrange overlap. 25
Figure 25. An example of the CINS program identifying and automatically counting the caribou on June 19th, 2019. 27

1 2019 OBJECTIVES

This year's objective was to have three nadir imaging flights conducted in spring, summer, and fall seasons. This number was extended to six individual flights that captured the spring, summer, and fall imagery of caribou for analysis. The image acquisition flights were performed in conjunction with ABR's manual caribou count flights, two flights were contracted by TerraSond to obtain imagery as well. The primary goal was to push the process of caribou count automation forward with fewer impacts on the environment; counts made from higher altitudes with less caribou herd disturbance and increased crew safety for all parties. The automatic caribou counting approach creates accurate visual data of caribou that can be reviewed later. The method also creates a historical record of imagery to increase redundancy and study repeatability.

By performing acquisition during three distinct parts of the year, automated caribou counting using aerial imagery was analyzed for seasonal viability. The development of seasonal model analytics allowed for a deeper understanding of the capabilities when utilizing this unique approach. The photographic acquisition during the contrasting conditions of spring, summer and fall benefits the automation processes by accounting for changing environmental conditions. The importance of acquiring meaningful data was to capture the seasonal changes that a script modeling regime can analyze. The application of an automated Python script that can analyze (distinguish) and quantify the caribou was developed and evaluated.

2 AERIAL IMAGING ACQUISITION

Pre-flight mobilization and testing of camera and acquisition systems became much more efficient, over the 2019 season. The aim was to minimize the amount of time it took to prepare for an operational flight and avoid indirect scheduling conflicts with the manual-count crew. Reducing the time of mobilization allowed adequate time to conduct the projects required survey transects ensuring maximized efficiency. A pre-season test flight at 1450 feet above ground level (AGL), at 5cm ground sample distance (GSD), and a ground speed of 80-90 knots was conducted. This survey season proved the capability of the integrated camera system to acquire clear, high-resolution imagery for analysis. The objective of each mission was to acquire imagery at the end of ABR's manual caribou counting flight transects, utilizing the above-mentioned operational parameters. The 2019 surveys also provided an opportunity to test the feasibility of forward-looking infrared (FLIR) in detecting caribou at 1450 feet AGL.

2.1 SPRING 2019

2.1.1 May 13 – 14, 2019 Spring Aerial Mission 01

A mission was flown, during the spring season, to acquire RGB and FLIR caribou imagery at approximately 1450 feet on May 13th, 2019 during clear sky conditions with high scattered clouds (see Figure 1 below). Heavy snow cover was still present with small rock and tundra formations beginning to show due to melting. The mission was started at the north end of the

Bear Tooth South flight-lines and continued to the Bear Tooth North flight lines beginning at the western half. Four people were present in the aircraft including two visual-count people from ABR, the 70N pilot, and one representative from Terrasond.

Figure 1. A photo taken of the conditions present during the May 13th, 2019 flight.

At the end of each flight line, two opportunities arose to capture caribou imagery. During these higher altitude passes, excellent, cloud-free, high-resolution RGB photography containing caribou was obtained. Thousands of images were collected which included the two sets of imagery that contained caribou (Figure 2).

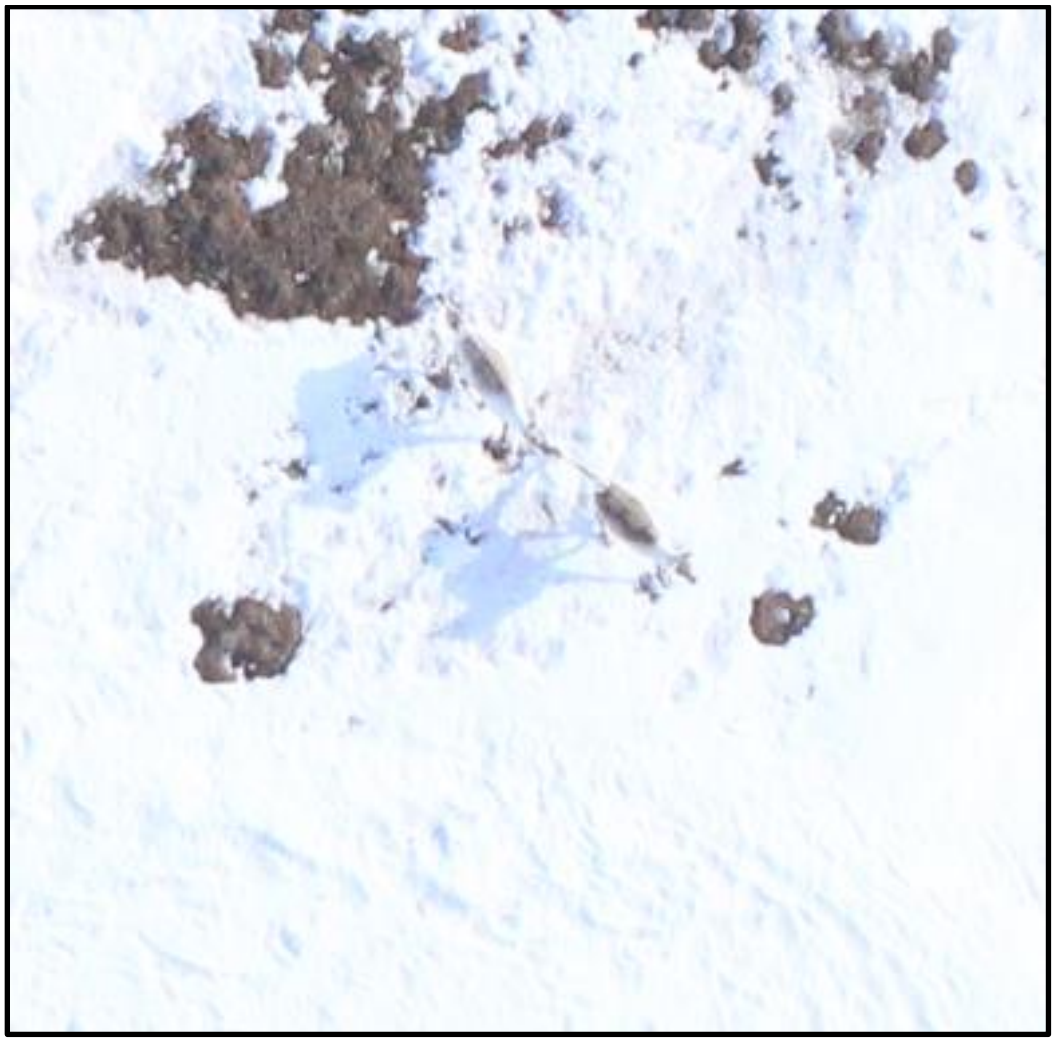

Figure 2. An image showing a close-up of two running caribou during Spring aerial mission one.

Furthermore, FLIR imagery of caribou was acquired during these passes in tandem with the RGB imagery. The RGB imagery was collected at 5cm GSD with FLIR imagery obtained at ~40 cm GSD of caribou. The RGB and FLIR pictures were shown to be a good representation of caribou that were mostly white on a white snow-filled background. TerraSond also learned that our integrated RGB camera system provides clear photos of caribou at higher altitudes with decent relative positioning.

It was anticipated that the next survey flight analysis would rely heavily on RGB imagery. Since the RGB acquisition showed good results at 1450 feet, the survey was able to refine the operational use of the integrated camera system. The survey validated the system's ability to take good clear photos at a given altitude. This experience solidified the procedural methods at the beginning of the season.

2.1.2 June 18 - 19, 2019 Summer Aerial Mission 02

On the June 18th – 19th, 2019 flight, the conditions were mostly sunny. The imagery showed light snow patches, with most of the images having no snow in them. There was a thin layer of ice on the lakes that appeared to be breaking up during this time period. A substantial number of images were collected on the flight that included caribou in white coats; the caribou appeared to be in the process of shedding their winter coats before the tundra had shown any considerable plant growth. The photos were acquired in the southwest corner of the Bear Tooth North transects. A total of 1574 images were collected, 69 of which included Caribou (Figure 3).

Figure 3. RGB imagery acquired by the integrated camera system on June 18th, 2019 of 22 caribou.

2.2 SUMMER 2019

2.2.1 July 22, 2019 Survey Summer Aerial Mission 01

The first Summer Acquisition mission was conducted on July 22, 2019. The objective was to find caribou that were recently known to be west and northwest of Nuiqsut. The weather conditions were overcast with a low cloud ceiling. The pilots had previously seen caribou in the area, and two separate missions were conducted, producing 214 images. However, the planes airspeed exceeded the maximum threshold, creating motion blur in the image set. This motion blur in

combination with the overcast skies created dark and blurry photos. These images were systematically adjusted in Adobe Lightroom to make them viable for analysis (Lightroom software is discussed in more detail within Section 4.3, Figure 4).

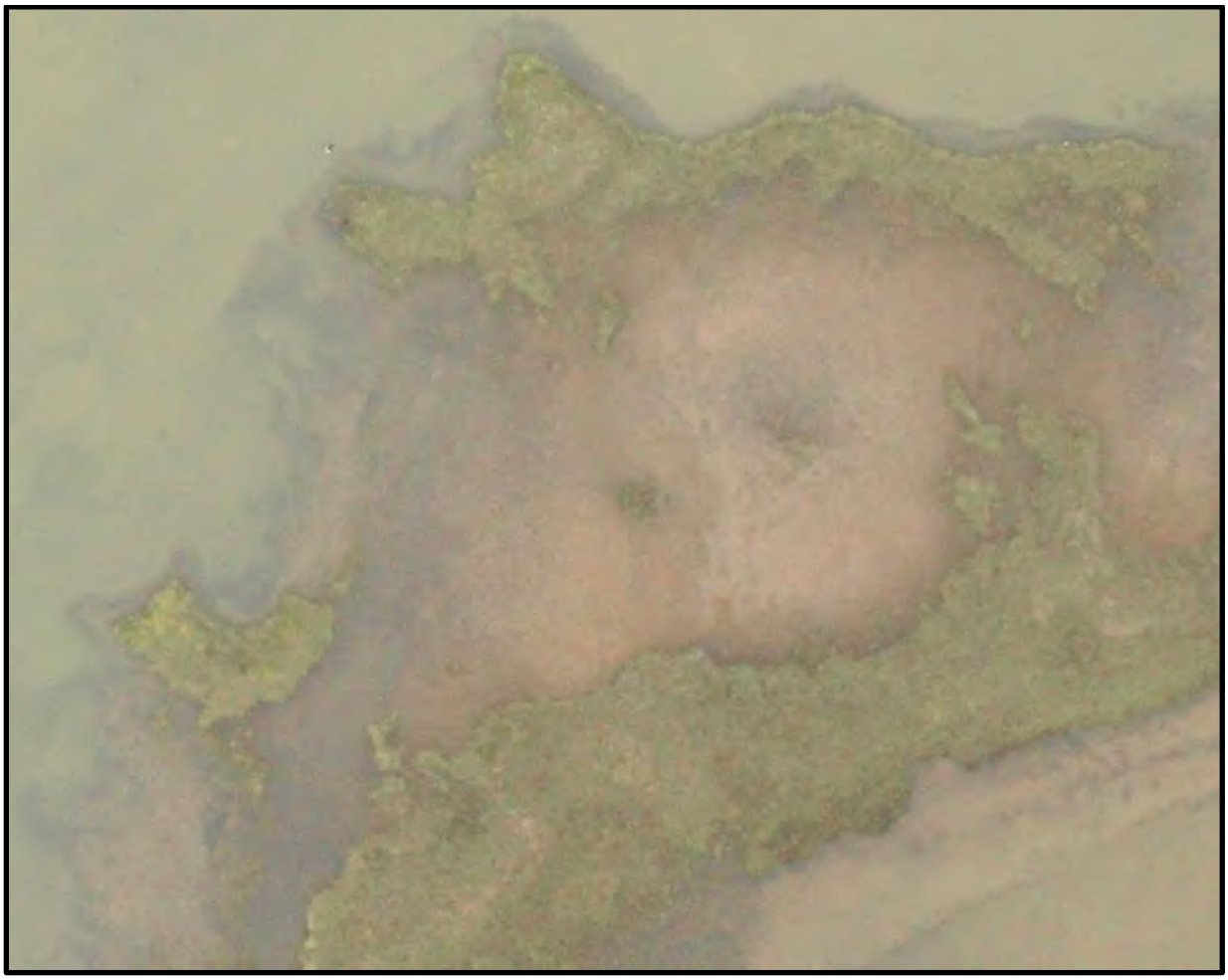

Figure 4. An image that was acquired on July 22, 2019 that was adjusted in Adobe Lightroom which consisted of a slight amount of motion blur.

2.2.2 July 31, 2019 Survey Summer Aerial Mission 02

The next date of acquisition was on July 31, 2019, during cloudy conditions. 778 images were collected in the southern bounds of the Bear Tooth North transects near a river at approximately 70°0'54.1''N, 152°22'58.0''W where one caribou or moose was photographed in the riparian area (see Figure 5 below). The imagery provided a unique opportunity to analyze a Caribou in mid-summer (brown) color-phase on a brown tundra background. Due to extensive cloud cover during this mission, the sensor let in a limited amount of light through the aperture resulting in lower gamma exposure and creating dim photos. This image set was systematically adjusted using Adobe Lightroom to increase the image quality and increase the gamma.

Figure 5. An image captured on July 31, 2019 of a moose or caribou in the riparian area.

2.2.3 August 16, 2019 Survey Summer Aerial Mission 03

A mission was flown on August 16, 2019, to try an obtain photography for caribou south of Teshekpuk Lake. Radio collar data was provided to try to find where larger populations of caribou may be. However, clouds covered the area quickly as the plane was in transit to the area of interest (AOI). The low cloud ceiling again reduced the gamma exposure of the photos creating dim photos also had to be adjusted. The pilot indicated that he didn't see any caribou in the sector south of Teshekpuk Lake. The pilot seeing no caribou could have been attributed to low visibility due to diminished lighting. These adverse conditions potentially contributed to some of the imagery having motion blur due to the plane exceeding its maximum speed threshold to collect clear imagery. Three images only had one caribou in them out of the 5953 photos that were collected during this mission (Figure 6).

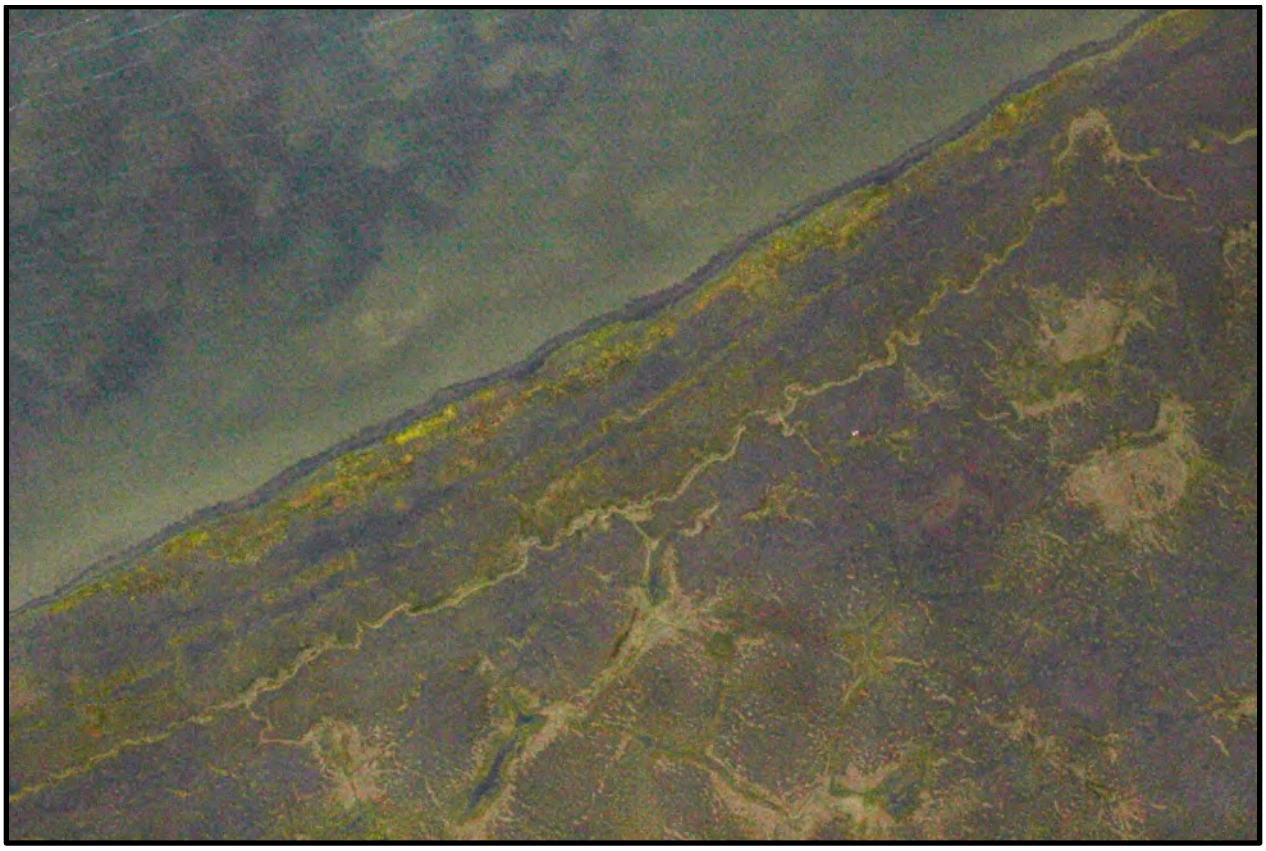

Figure 6. An image that was taken on August 16, 2019 and adjusted in Adobe Lightroom of one caribou south of Teshekpuk Lake.

2.2.4 August 28, 2019 Survey Summer Aerial Mission 04

On August 28, 2019, a survey data set was produced in conjunction with ABR around 11:00 AM. 816 images were acquired, 17 of which showed caribou (see Figure 7 below). The conditions were partly cloudy but clear, and detailed imagery was produced. The caribou showed brown fur coats on a brown background. The caribou's tail and hindquarters were still white, allowing for a good contrast between their tails and the environment.

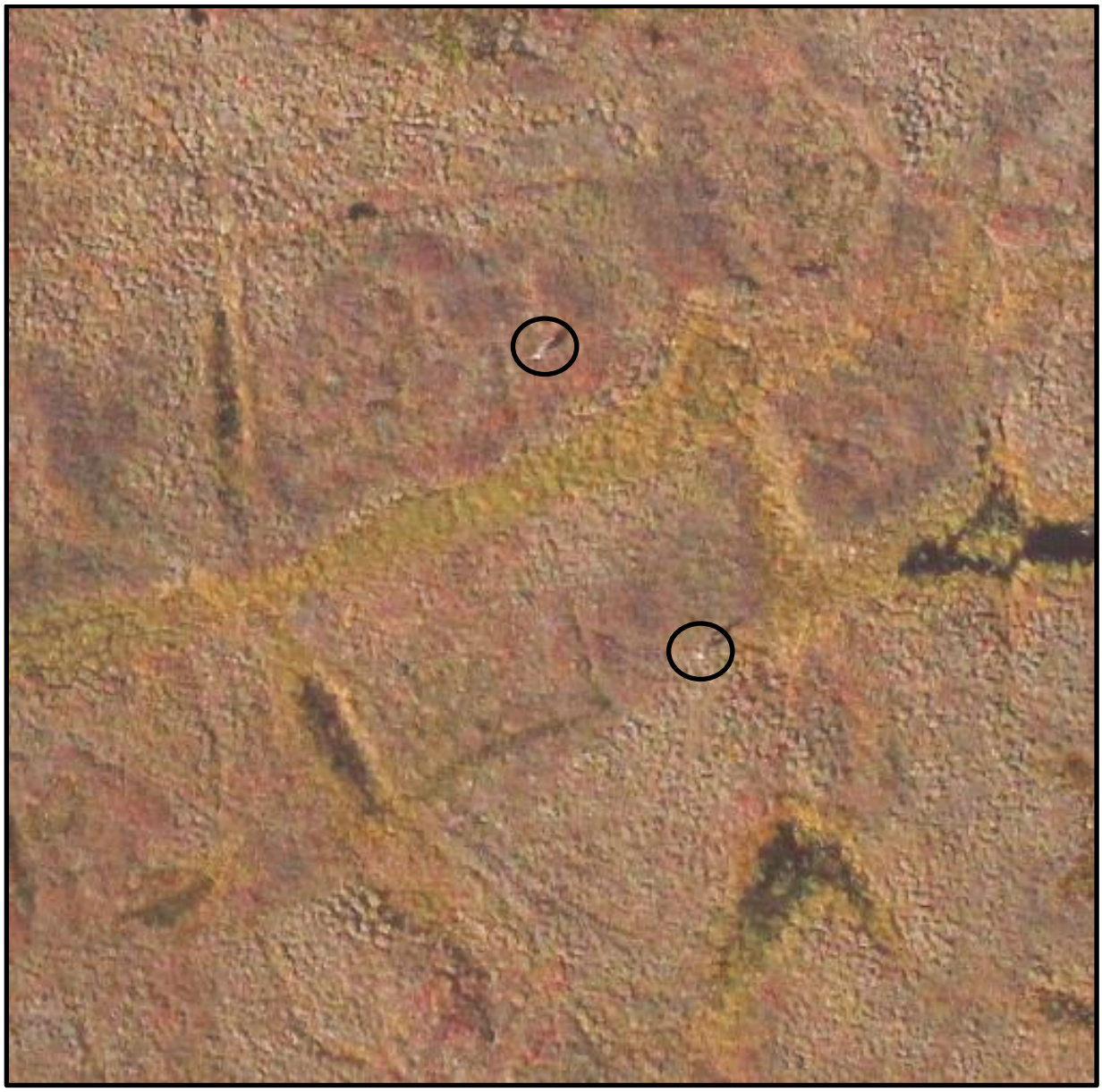

Figure 7. A zoomed in photo of two caribou in the black circles taken on August 28th, 2019.

2.3 FALL 2019

2.3.1 October 3, 2019 Survey Fall Aerial Mission

The last survey was conducted on October 3rd, 2019. 76 images of caribou were obtained from the 576 images that were collected. Additionally, this survey allowed for testing camera specification adjustments. The adjustments were intended to test new camera setting during low light conditions (discussed in sections 4.2 and 4.3). It appeared that the caribou were half white and half brown and in the process of changing to their winter camouflage (white) (Figure 8).

Figure 8. An image acquired on October 3, 2019 during the fall aerial survey of four caribou showing a high color discrepancy.

3 ANALYSIS

Automated scripting has made it possible to identify and tag caribou within the acquired imagery, automatically. The customized script is called the Caribou Identification North Slope (CINS) script. The CINS script is an object detection and contouring script that is based on color differentiation. CINS has been created to identify, tag, and quantify caribou in aerial imagery automatically for this project.

3.1 Threshold Analysis (*ImageJ*)

ImageJ is an open source image processing program designed for scientific multidimensional images. The automated approach needs some preliminary analysis with *ImageJ*. This analysis feeds threshold values into the script that are representative of each time period (spring, summer, and fall).

CINS processing does not convert the images natural look-up table pixel numbers (LUT numbers) to other values, instead; it utilizes the original color bands, image size, and dimensions keeping its original integrity with approximately 18 million pixels (18 megapixels). This approach splits the red, green, and blue bands into separate grayscale 8-bit files to do the analysis, where the grayscale pixel values range from 0 to 255.

The Python CINS script then applies the set threshold created with *ImageJ* that is usually standardized over the images to create a mask. *ImageJ* allows for the visualization of the threshold that is then applied over a period of imagery (Figure 9). It is noted that this approach was utilized at the University of Idaho for research purposes on a National Science Foundation (NSF) grant. This analysis was done to apply coefficients to sensor readings where dense vegetation (sagebrush, etc.) was in the optical view (Greth, Allen, 2013).

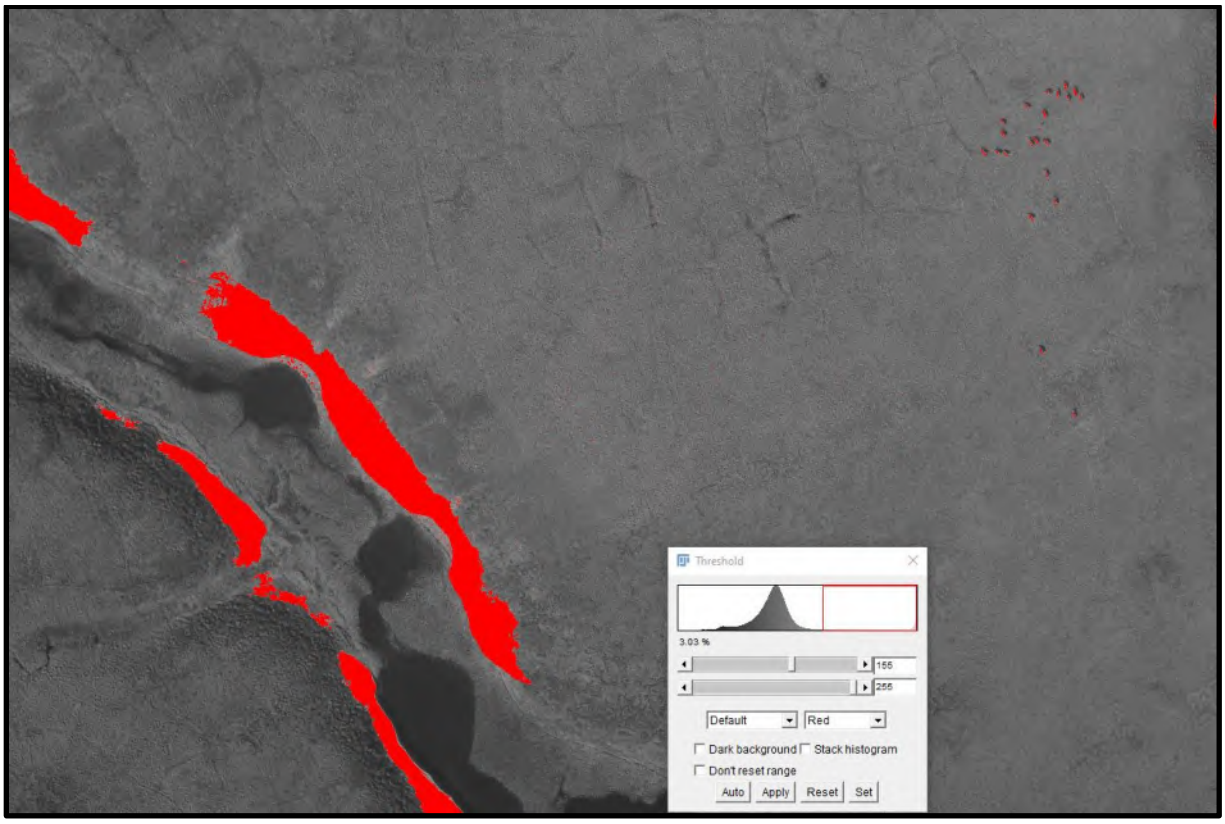

Figure 9. An example of threshold evaluation on an individual band with ImageJ.

The preliminary visualization, finding the threshold values for each RGB band, is used to calibrate the statistical script modeling regime. As the ecosystem and the colors within the imagery change, the preliminary threshold analysis is critical in encapsulating these deviations by adjusting the calibration during each distinctive phase of caribou color to background tundra color. There is potential through "machine learning" that the script could learn to dynamically change the threshold automatically as the ecosystem changes. These adjustments can also be made using a LUT table within the script, which will require further development. The red, green and blue color bands are calibrated individually with *ImageJ* and integrated into the script to set bounds for the statistics.

3.2 Script Overview

It has been shown that the combination of all band threshold analysis is a robust approach for caribou identification. The script creates an object detection map providing a generalized sense of all the objects within the image, and it also creates contours (Figure 10). The contours are then counted and calculated to absolve the larger ones that the script considers to be snow patches. CINS then computes the size of the object and differentiates between a large and small object. This information is used to classify the objects into two size groups. The script considers the first group of larger contours as being too large to be a caribou. The second group, within the correct size tolerance, is quantified as potentially being a Caribou.

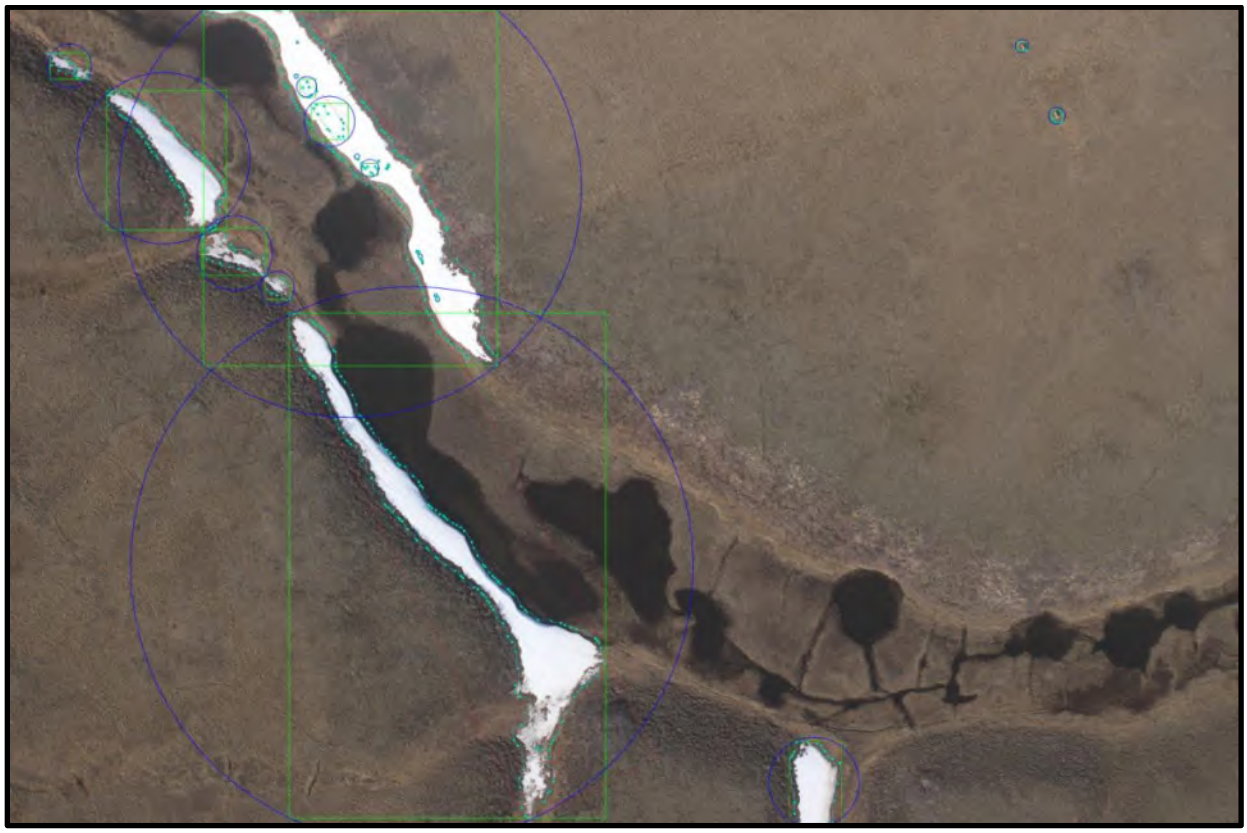

Figure 10. RGB imagery acquired by the integrated camera system on June 24th, 2019 of 2 caribou. The contours were used for sizing analysis.

CINS analyzes the remaining objects that were created from color discrepancies. The script then verifies that each object has been detected within each color band before it quantifies them. The quantity of caribou is tabulated into a running total that is equated over an entire folder. These folder structures can be broken down into the various transect sections of the survey area to aggregate their counts individually. CINS also creates a separate image folder that a technician can review to verify all the caribou were counted accurately. This approach allows the reviewer to only look at a subset of the vast amounts of imagery. The reference list can also be used in "machine learning" scripts to improve the current model by giving it more applied structure. Increasing shape detection capabilities with feature extraction could potentially increase the

accuracy of the model when color discrimination is less viable (i.e.: spring with minimum color contrasts). A workflow diagram of this process is shown in Figure 11 below.

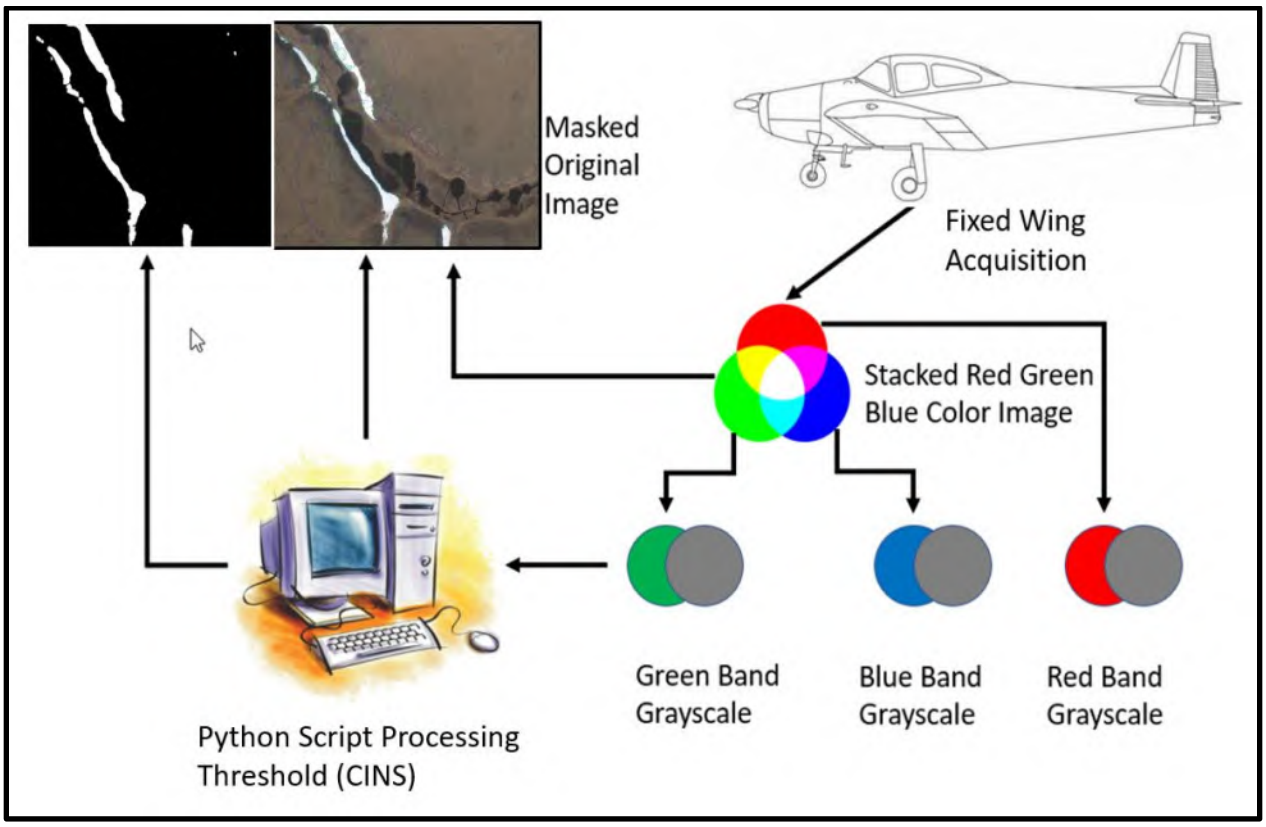

Figure 11. A workflow diagram of the CINS processing methodology.

Investigating these approaches using the existing CINS script could prove highly beneficial to increase the accuracy from a general 80-90% to consistently over 90%, substantially growing in significance. Consistent accuracies over 90%, limited to no manual review would be necessary depending on currently perceived error using current methodologies. The new CINS approach provides an actual estimation of caribou numbers without a coefficient adjustment. During certain parts of the year, the CINS Python script is already achieving high accuracy values that are very significant and consistently over 90% (Figure 12).

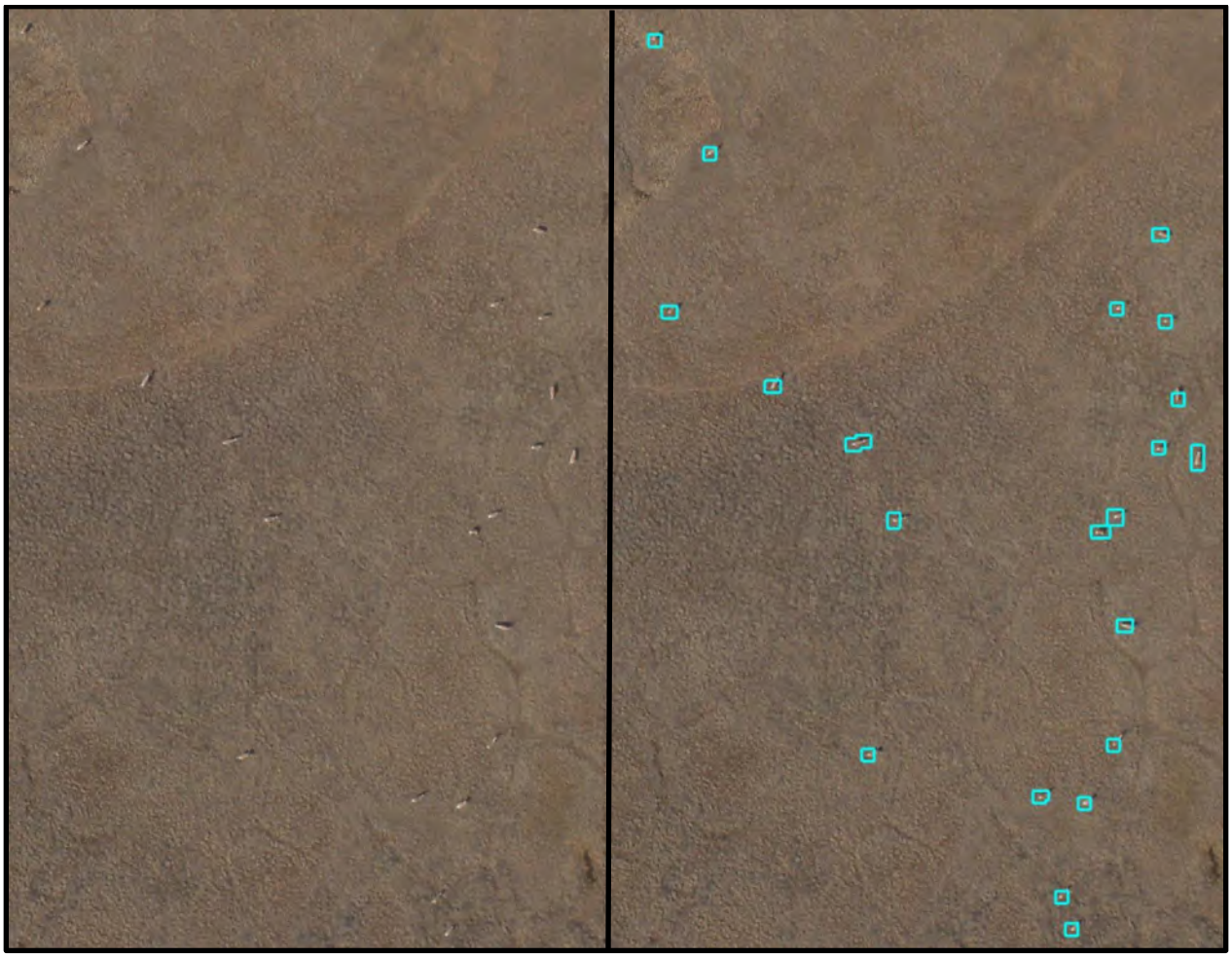

Figure 12. The CINS automated caribou script accurately identifying and tagging caribou in an image taken on June 19th, 2019.

3.3 Ecosystem Change / Biological Change

Changing the automated modeling script to account for the ecosystem and biological changes proved to be difficult during specific seasons. The early summer and fall periods showed significant color contrast that the programming exploits that created highly accurate outputs, with less accurate results during the early spring season. As mentioned previously, shape feature extraction could supplement the times of the season when color discrepancies are less significant. A modified script was created to be applied to the periods of time that were problematic by utilizing one band instead of all three. Features such as the caribou's shadows within a 16-bit black and white image can be used to identify and count them. It is understood that intricate ecosystems are generally harder to model. Due to this fact, multiple approaches were adopted for different times of the year.

3.3.1 Spring

During spring break up imagery showing caribou standing on snow and rock was acquired. Modeling during this period was difficult due to the white coats of the caribou on a

predominantly white background. It was increasingly more difficult due to the exposed rock outcrops, extensive snow cover, and shadowing. These exposed rock outcrops generally matched the caribou shadows creating diminished color contrast across the image (Figure 13).

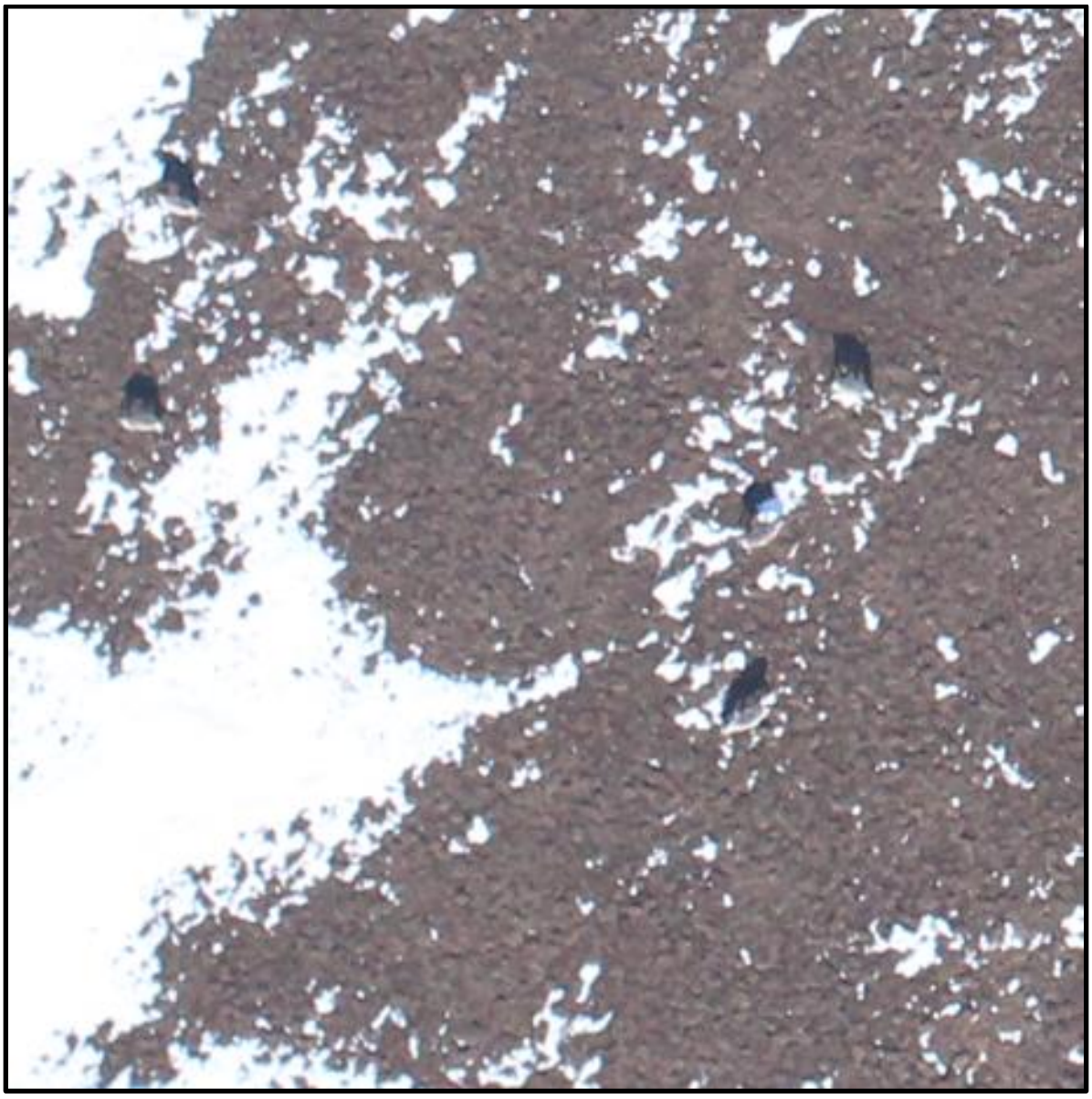

Figure 13. A photo showing caribou during the spring period and how well they blend in during this time of the year on May 14th, 2019.

Due to the issues, mentioned previously, a new approach was undertaken to automatically count caribou during the heavy snow-covered conditions. Turning the image into a 16-bit black and white image created a more substantial contrast between the image and the caribou's shadow (Figure 14). After obtaining a more significant distinction of the shadow, *ImageJ* was then applied to set the threshold and do the analysis. The accuracy will continue to be improved to model this more challenging time of the year.

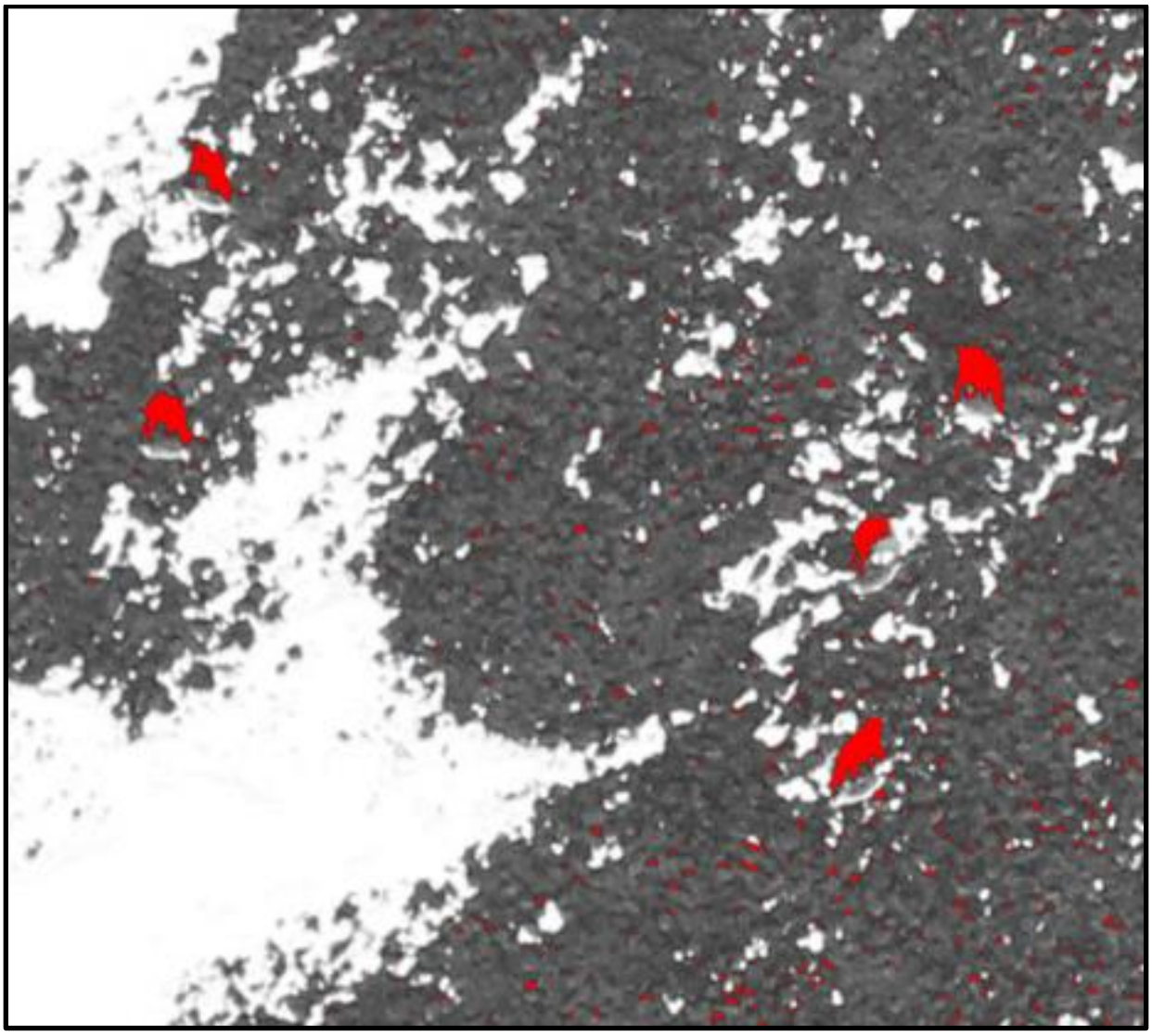

Figure 14. An image taken on May 14th, 2019 that was turned into a 16-bit black and white image with threshold analysis from ImageJ.

3.3.2 Summer

The summer and fall seasons showed the most significant progress with automation. When the ecosystem had low levels of vegetation with small patches of snow, a significant color difference was shown. Most of the season was modeled with relative ease, with high accuracy, as the snow melted, and vegetation started to grow (Figure 15).

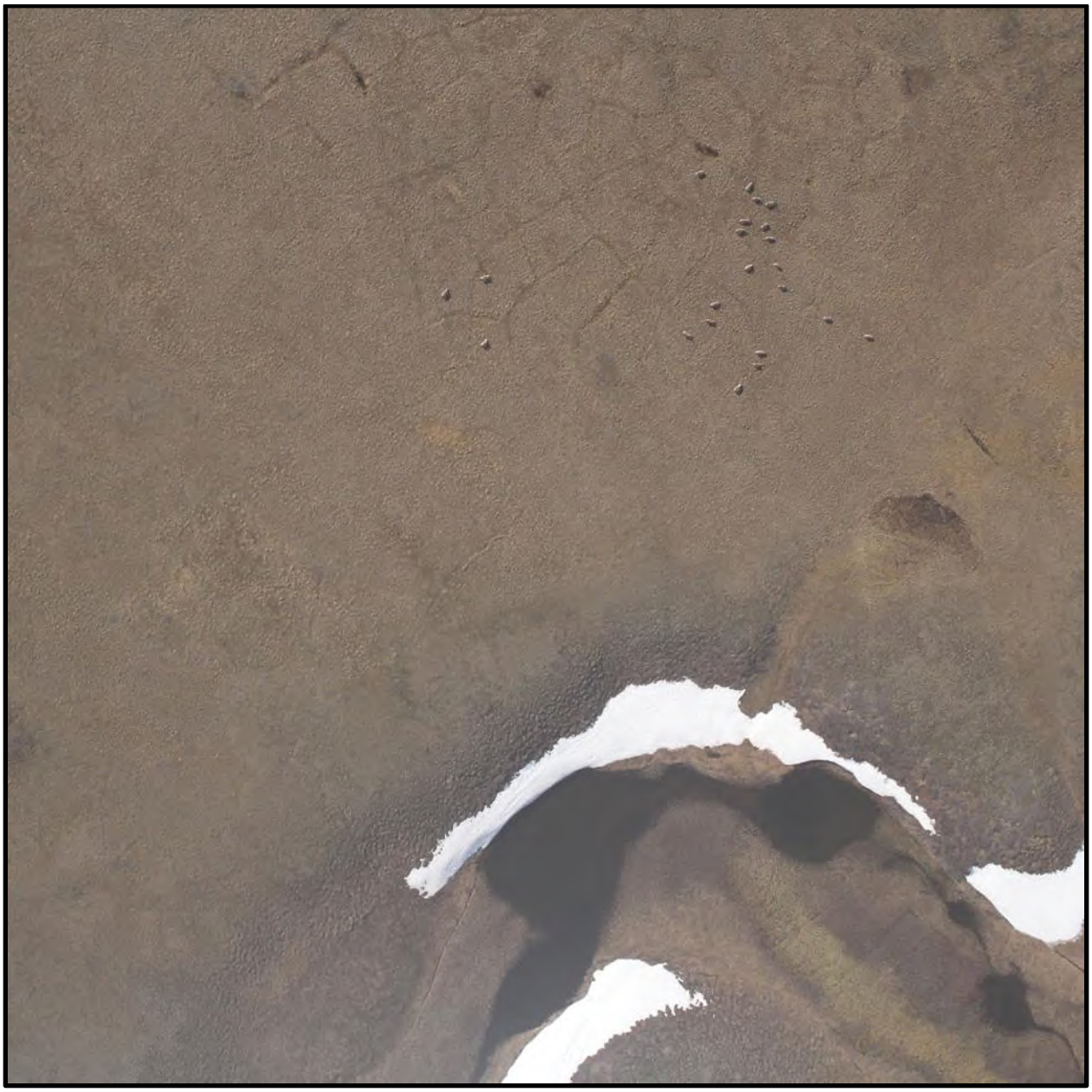

Figure 15. An example of the typical conditions in early summer with a herd of caribou.

Plant senescence is the process of aging in plants. Caribou detection became slightly more trying to model until most of the plant senescence was completed, which is relatively a quick cycle on the North Slope of Alaska.

Furthermore, it appears that the caribou's hindquarters stay white throughout the year, allowing for this unique characteristic to be modeled through the vegetative growth period. However, some areas have high concentrations of white birds and piles of white survey stakes that became problematic when modeling. One potential solution could be to utilize shape detection in these areas.

3.3.3 Fall

Fall had very similar characteristics to the early summer dynamics. Even though the caribou were completely brown by this point, their hindquarters remained white allowing for accurate color discrepancy modeling. Some factors, such as sun angle, begin to change in the fall which needs to be accounted for. As the sun angle begins to decrease, the camera settings may need to be adjusted to account for this. These ecosystem changes need to be adjusted for as they arise, to account for the environmental changes. Accounting for these changes produces imagery that needs no postprocessing (Figure 16).

Figure 16. An example of a fall image that is analogous to the early spring image after plant senescence.

4 LIMITATIONS / INSIGHT

Identifying and understanding the limitations within the methodologies used to count caribou automatically is beneficial. The insights improve the approach so the project can become operationally viable as soon as possible. Insights also allow for a better understanding of how to avoid and mitigate operational and environmental issues. Simple adjustments that are temporally dynamic ensures each mission is a success.

4.1 Motion Blur

The camera shutter speed settings limit the maximum flight speed. A commonly applied shutter speed is 1/4000sec, which means that it takes 0.00025 seconds for the camera to expose the imaging sensor. Moving over 90 knots creates motion blur because the camera system moves too far (over 50% of the pixel size), as the image is being taken. The image then shows drastically diminished clarity (Figure 17).

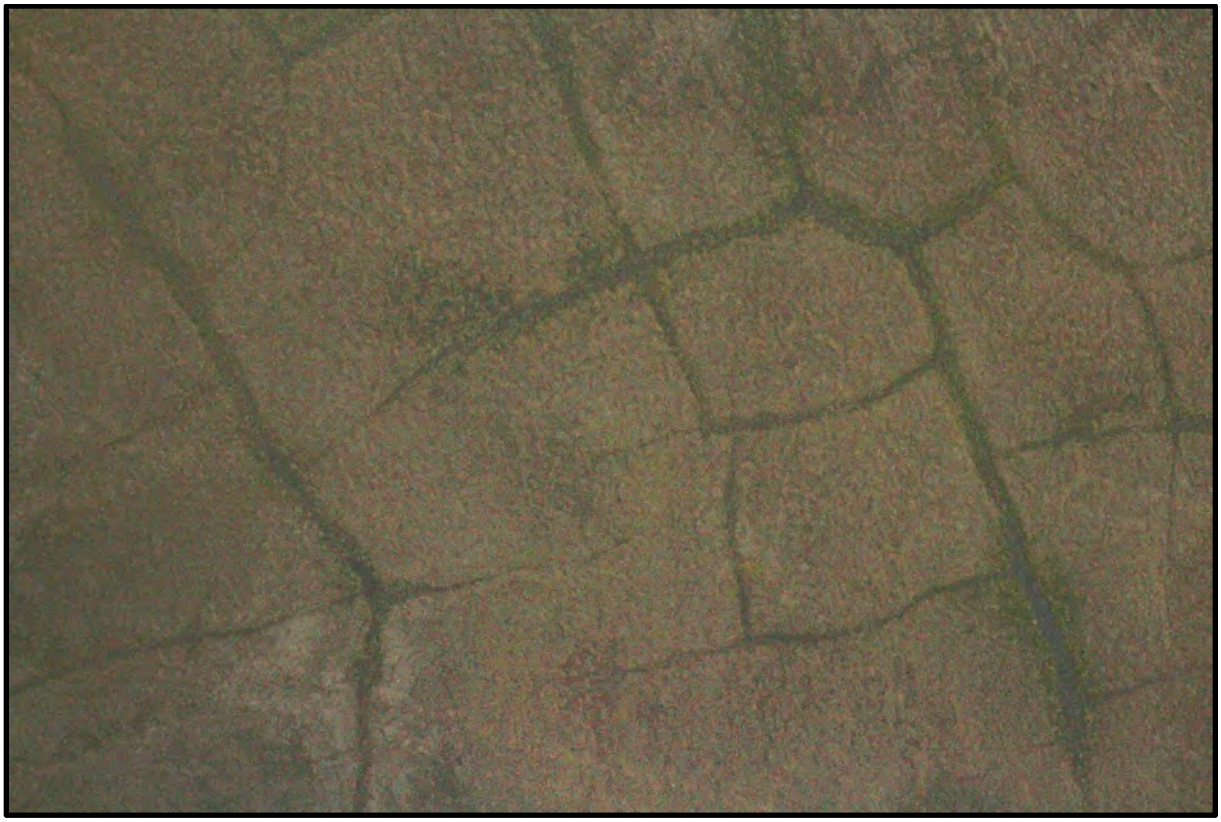

Figure 17. An example of motion blur that was captured on July 22nd, 2019.

Motion blur cannot be fixed in post-processing. To mitigate this issue, TerraSond is providing direct feedback to each pilot after each respective mission to educate them on cause and effect. However, this potential issue is easily fixed by maintaining an 80 to 90-knot airspeeds during image acquisition. The pilots need to learn through experience how to fly within those limits to create proper imagery. A spec shoot is necessary for a new pilot's training before the season begins. Reviewing the imagery and giving the pilots good feedback alleviates this potential issue before the "production" missions start.

4.2 Sun Angle

The sun angle and cloud cover play a significant role in the illumination of the imagery. During early spring and fall, the sun angle is extremely low, creating a challenge when acquiring photography. During these time frames, the solar elevation is between 10 and 20 degrees above the horizon (Figure 18). When the solar elevation is so low (<30°) the photons from the sun must travel much further through the atmosphere compounding the problem of low, exposure levels

in combination with cloud cover. These issues can be alleviated with relative ease as discussed in section 4.1.

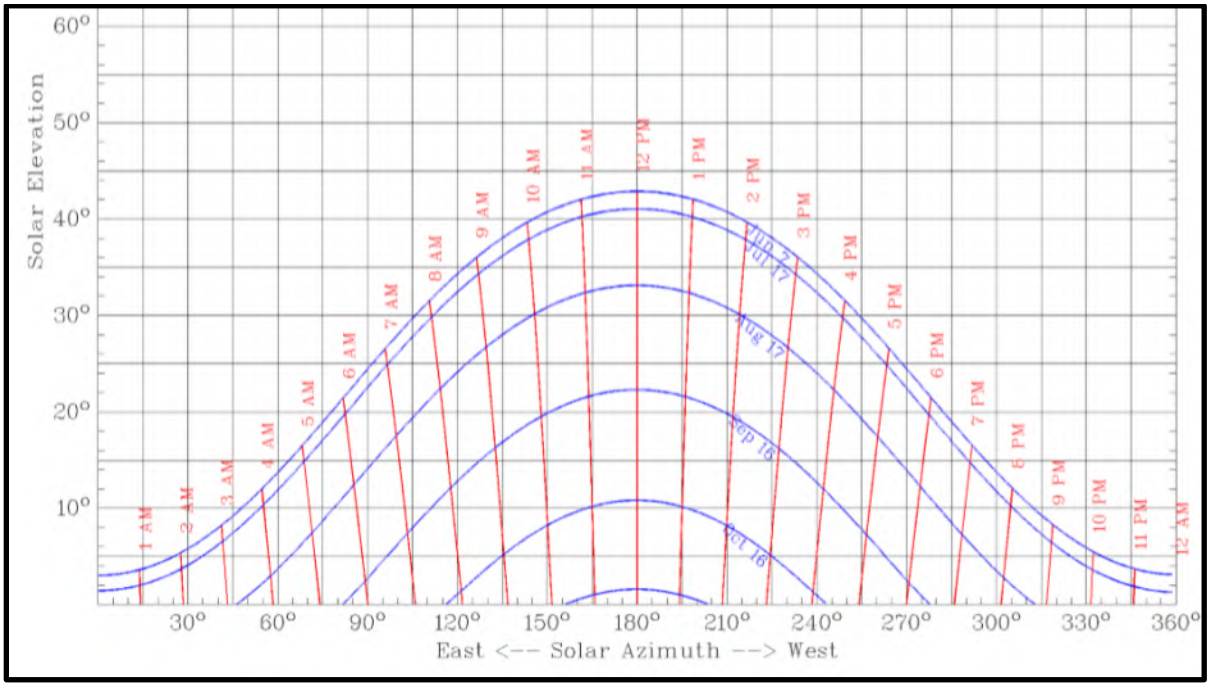

Figure 18. The solar elevation on the North Slope of Alaska throughout the season.

The low sun angle can also provide opportunity with the increased size and intensity of the shadows it creates (Figure 19). As discussed previously, the dark shadows that the caribou cast across uniform landscapes can be modeled to help in the automation processes.

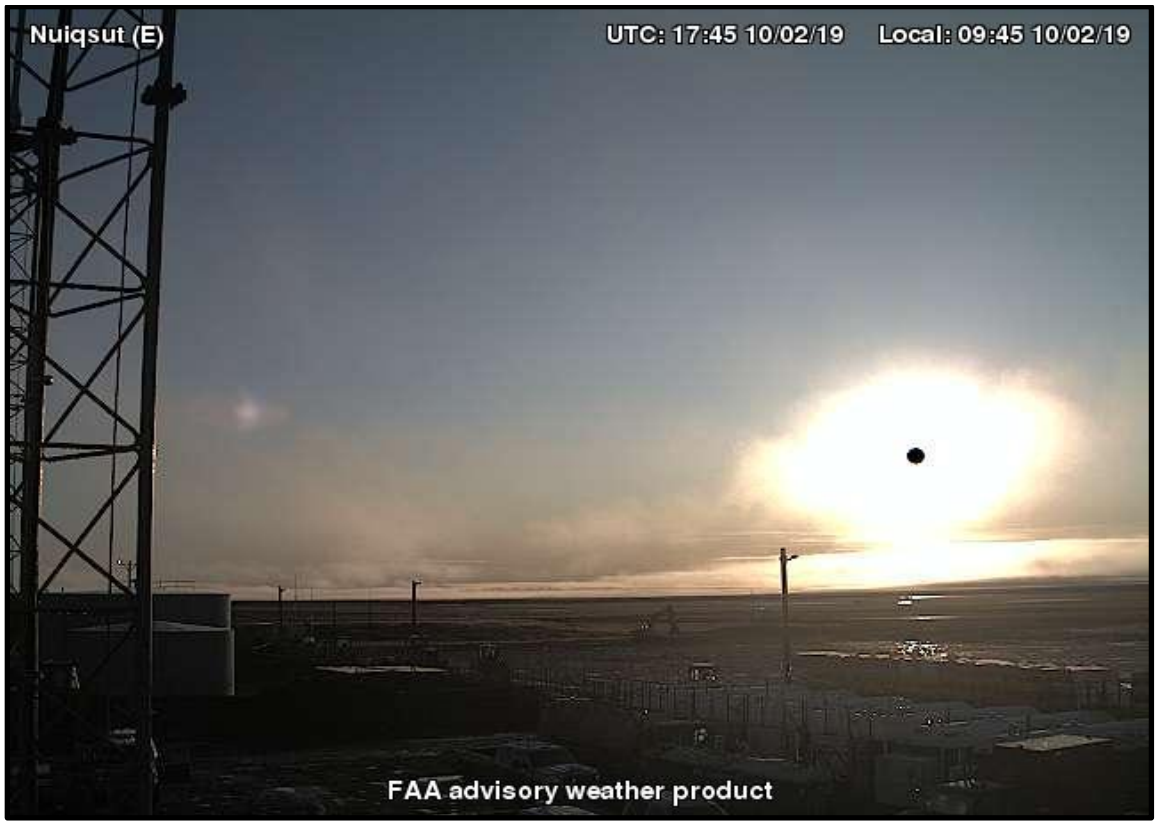

Figure 19. An example of the low sun angle taken at Nuiqsut on October 2nd, 2019 at 9:45 AM.

4.3 Adobe Lightroom, Aperture Adjustments, Shutter Speed, and Dim Photos

Some missions produced dim photos due to cloud cover and sun angle as described above. These images were post-processed in Adobe Lightroom. Generally, all the images were adjusted in such a way that no effect was seen from the low light levels after processing.

The photos do not lose any detail or sharpness by adjusting them. The imagery usually has a gamma adjustment coupled with a dehazing application. Mitigation of the issue in post-processing and with batch processing cuts down the time it takes to obtain a well-adjusted image (Figure 20).

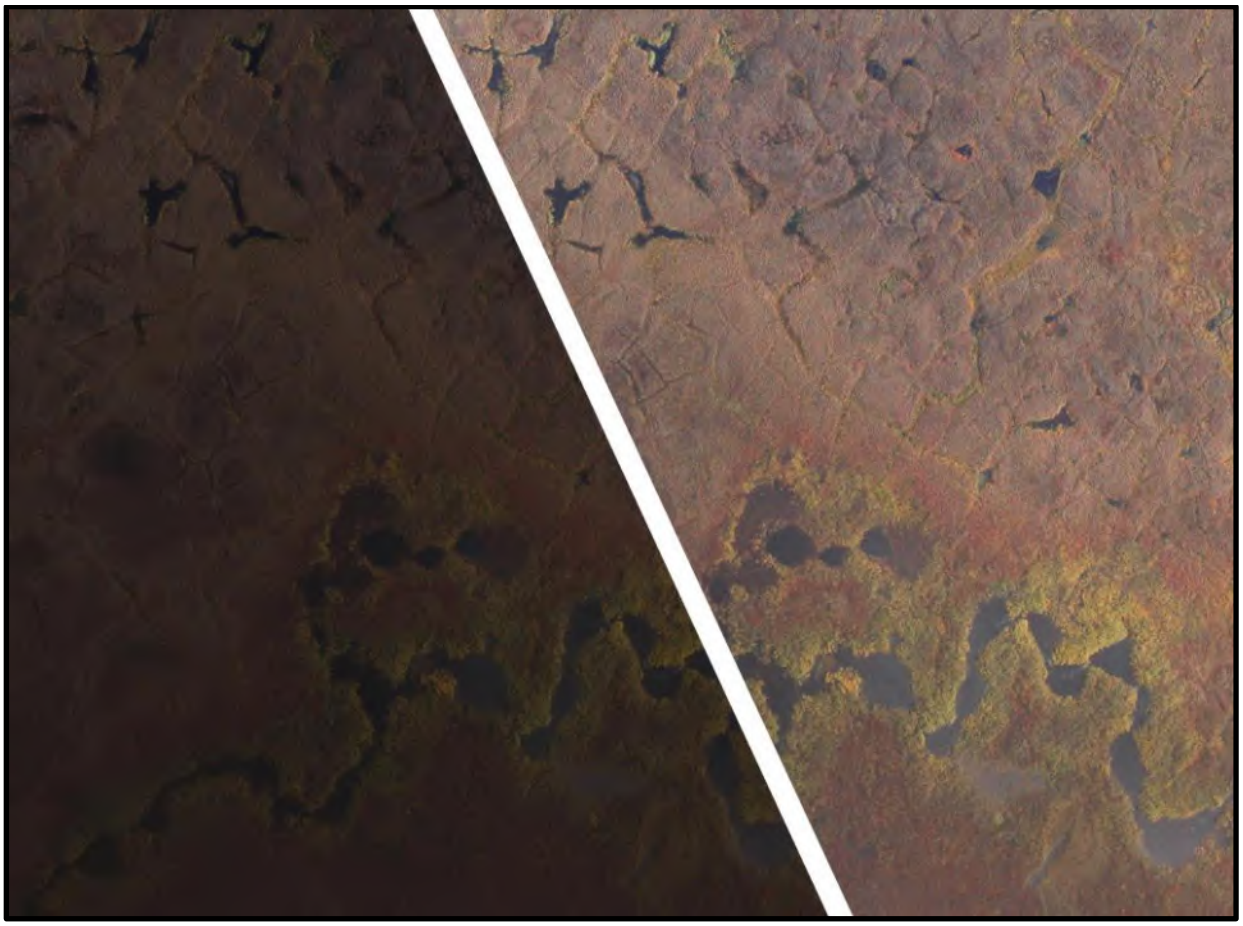

Figure 20. An example of an image that was adjusted in Adobe Lightroom during post-processing.

On the October 2nd, 2019 flight, due to low sun angle and a high probability of cloud cover, a camera aperture adjustment was tested. The ratio of the camera lens focal length to the diameter of the lens opening is known as the f/stop. Adjusting this camera feature allows more (lower f/stop value), or less (higher f/stop value), light let in when the photo is taken. Adjusting the f/stop does affect the depth of view. However, since the topography is relatively flat, and the plane is so high, the changes in the depth of view was not an issue. This aperture adjustment was tested to help alleviate the impacts of having low light levels when the imagery is being acquired due to the unique environmental conditions. The aperture (f/stop) was decreased from 5.6 to 4.0, allowing for more light to enter the sensor.

Furthermore, the time it takes to expose the image sensors was also adjusted. This value was adjusted (decreased 1 stop) from 1/4000 seconds to 1/2000 seconds. It was changed to also let more light in by keeping the shutter open longer as the photo is being taken, effectively doubling the time of the exposure. The changes that were made created imagery which showed good detail, clarity, and the correct light intensity, with no loss or gain to the overall exposure (Figure 21).

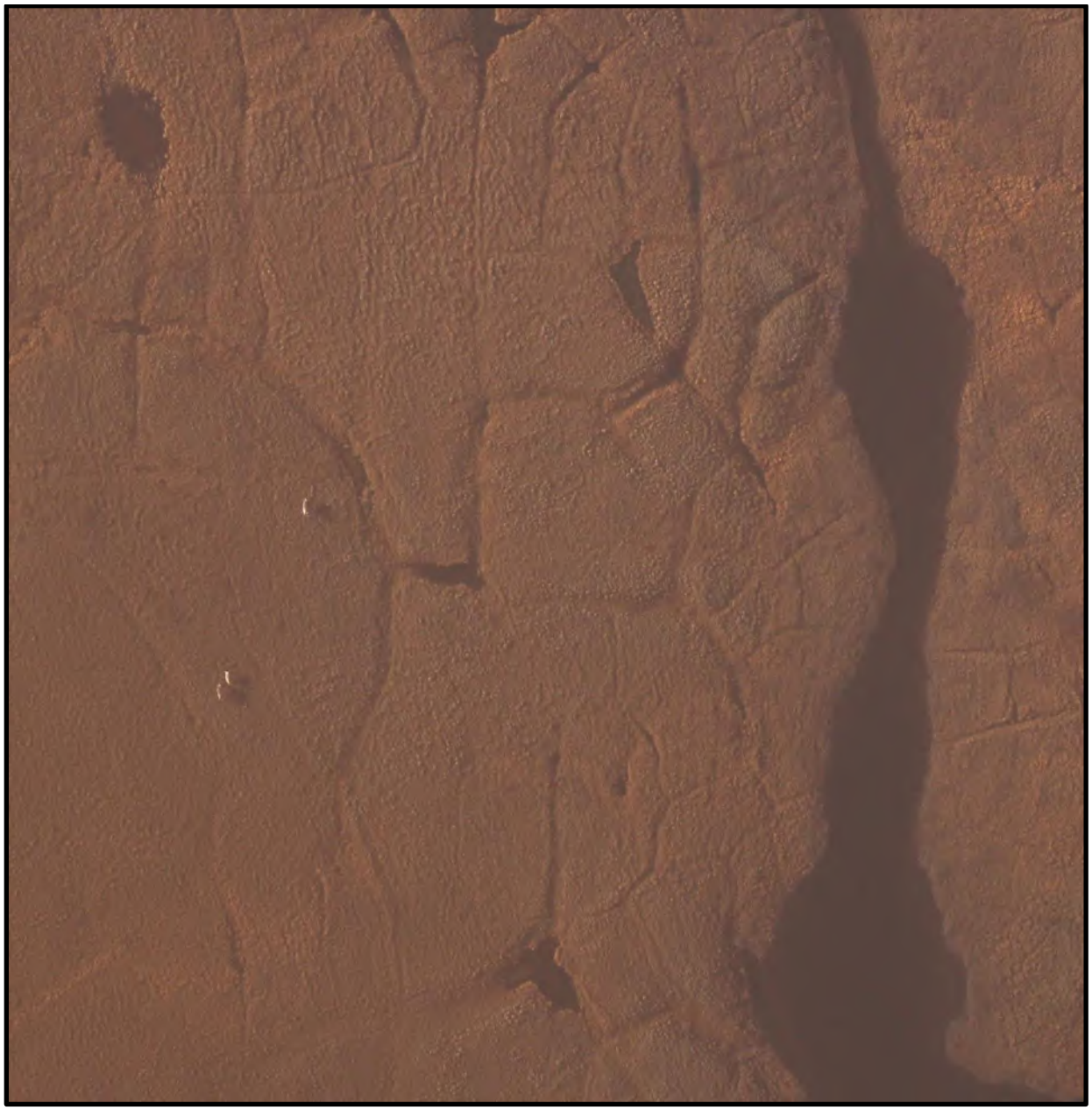

Figure 21. An image showing how the camera adjustments created a properly exposed photograph on October 3rd, 2019.

4.4 Forward Looking Infrared (FLIR)

The success of the FLIR imagery, picking up warm-bodied caribou on a colder snow-covered background, showed the viability of identifying them during these conditions. However, capturing FLIR images during the early morning at a lower sun angle may prove beneficial due to higher temperature differences between the caribou and the background during this timeframe. It was concluded that FLIR imagery at high altitude is useful in supporting the automation of caribou counting even though it was limited by a few factors as discussed below.

It was anticipated, that the summer and fall flight(s) analysis would rely heavily on RGB imagery, not the FLIR photography. This statement was proven during the review of the spring, summer, and fall photography. The conclusion was that the FLIR signal of the caribou was too analogous to the ground cover during this period of the year effectively washing out the image in most cases.

However, when caribou are standing next to a riverbank, they are noticeable in both the FLIR and the RGB imagery. The snow-covered background with warm caribou created a more significant difference in the FLIR signature, unlike warm bodied caribou on a generally warm uniform landscape (Figure 22 & 23).

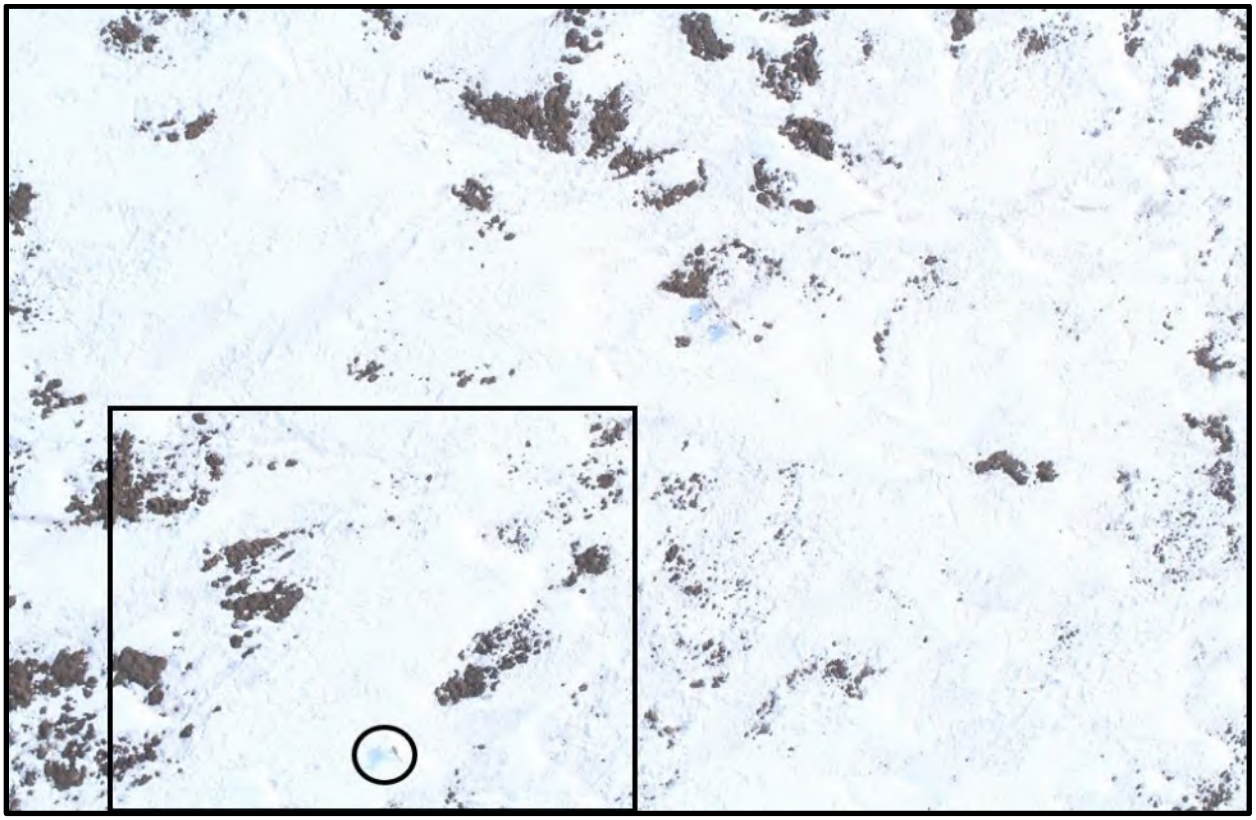

Figure 22. RGB imagery acquired by the integrated camera system on May 13th, 2019 of three caribou. The box shown shows the footprint of the FLIR image in Figure 2.

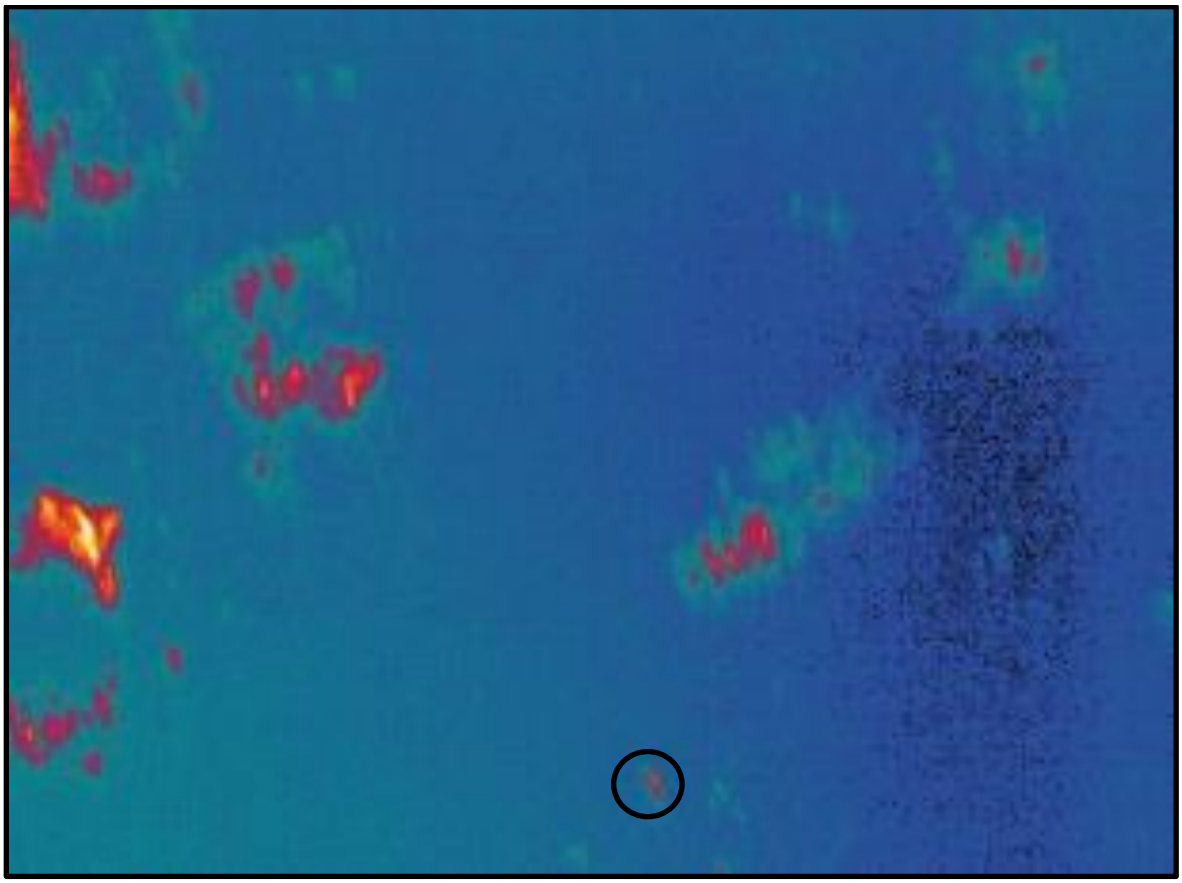

Figure 23. FLIR imagery acquired by the integrated camera system on May 13th, 2019 of one caribou.

The current FLIR camera system has a resolution of ~40cm GSD at 1450 feet AGL. Higher resolution would be needed to make it more viable. Double or triple the resolution would be ideal at <~20cm GSD. It would also be useful to move away from a standard thermal camera to a radiometric camera for game management. A radiometric camera produces an image with actual temperature values instead of a temperature profile. A more advanced and refined radiometric camera with a higher resolution would allow for more reliable analysis through increased capability.

4.5 Overlap

The overlap was set at 65% cross-range overlap and 75% downrange overlap during the 2019 season. This insured substantial photographic redundancy when caribou were visible in the camera systems footprint, providing more data for analysis (see Figure 24 below). Generally, with more image-to-image overlap (faster trigger time) any given caribou would be photographed three times as the camera system passed overhead.

However, when standard imaging overlap settings are moved into caribou herd imaging operations, the settings will need to be adjusted. The overlap changes would ensure that a caribou is only photographed once and counted once. Front and side overlap need to be

considered when setting the overlap values since every side of the image has overlap increasing the chance for redundancy significantly.

It is suggested that the front and side overlap be changed to 1-2 percent. At 1% front and side overlap, only 4% of the image would be recreated in other images reducing the chance of double counting significantly. This also has a large time saving in processing as well because less imagery would be acquired for analysis.

Figure 24. A visual depiction of the 75% downrange overlap.

5 CONCLUSION

In conclusion, successful and progressive imagery was acquired of caribou during the spring, summer, and fall months, strengthening the achievement of the project goals overall. The additional image collection has strengthened the modeling that has already been created by

increasing the sample size. More challenges in image acquisition and processing has led the way to further integration and development of problem-solving tools. CINS will continue to be trained and improved upon; increasing its adaptability and precision.

During the 2019 summer and fall seasons the CINS modeling script automated caribou accounting extremely well with increasingly higher accuracy rates. The spring period proved to be much more difficult to model due primarily to the unique environmental conditions containing extensive snow cover, rock outcrops, and increased shadowing. The FLIR did prove to be beneficial during this period and with increased capabilities FLIR could become even more beneficial for the project. Additionally, different approaches were developed to model the spring dynamics and are continuing to be refined. Shape detection will also help to make counting caribou more viable during the spring period.

Insight into the limitations helped to mitigate their impacts on the project. Some of the limitations included plane speed restrictions, camera adjustments, accounting for solar elevation, and image overlap adjustments. All these limitations and issues were addressed so the new approach can become operational as soon as possible.

The automation of caribou counting has advanced significantly during the 2019 season. The approach has been refined so that it can be implemented as soon as possible. Additional development is needed to better quantify caribou during the spring period. From the early summer to the fall, color discrepancy modeling has proven to produce highly accurate caribou counts (Figure 25).

TerraSond plans to continue the development of automated caribou counts through aerial imaging and processing techniques in partnership with ABR. Providing a safe and viable solution in answer to the primary concerns of current visual and labor-intensive methodologies and their inherent expenses is TerraSond's highest priority. TerraSond looks forward to providing ABR with continued support in the development of these processes in 2020.

Figure 25. An example of the CINS program identifying and automatically counting the caribou on June 19th, 2019.

References:

Greth, J., Allen, R., 2013. EPSCoR Evapotranspiration and Energy Balance Flux Site in Southern Idaho supports Hydroclimate Modeling., Master's thesis, University of Idaho, Moscow, Idaho.

Page intentionally left blank.

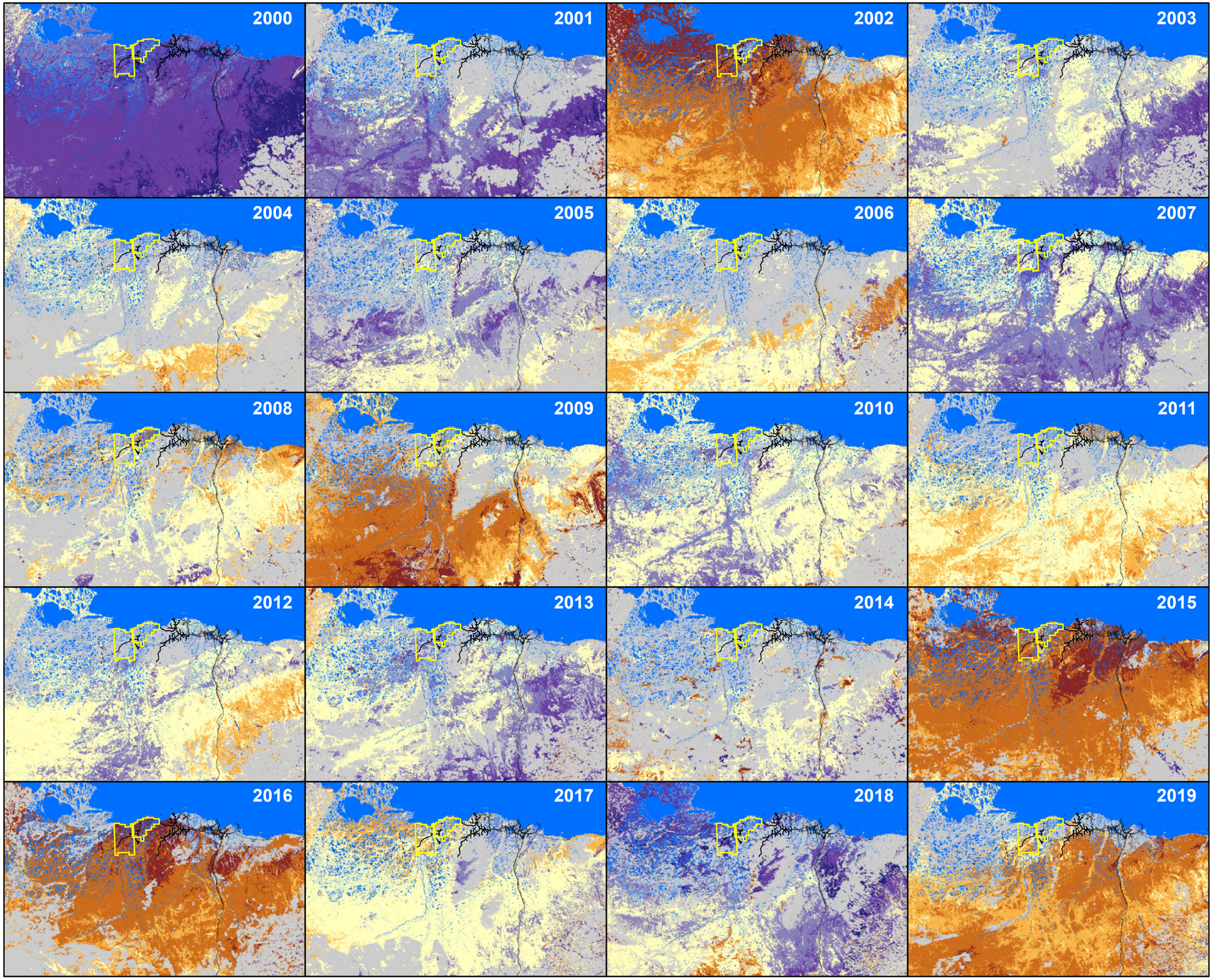

Timing of Snow Melt

Compared to Median (2000–2019)

- Date not known within one week
- > 14 days earlier than median
- 8–14 days earlier than median
- 4–7 days earlier than median
- Within 3 days of median
- 4–7 days later than median
- 8–14 days later than median
- > 14 days later than median
- >= 50% Water Cover

Aerial Survey Area

N
W E
S

0 20 40 60 80 100 Miles

0 50 100 150 Kilometers

Appendix D.
Timing of annual snowmelt (<50% snow cover), compared with median date of snowmelt, on the central North Slope of Alaska during 2000–2019, as estimated from MODIS satellite imagery.

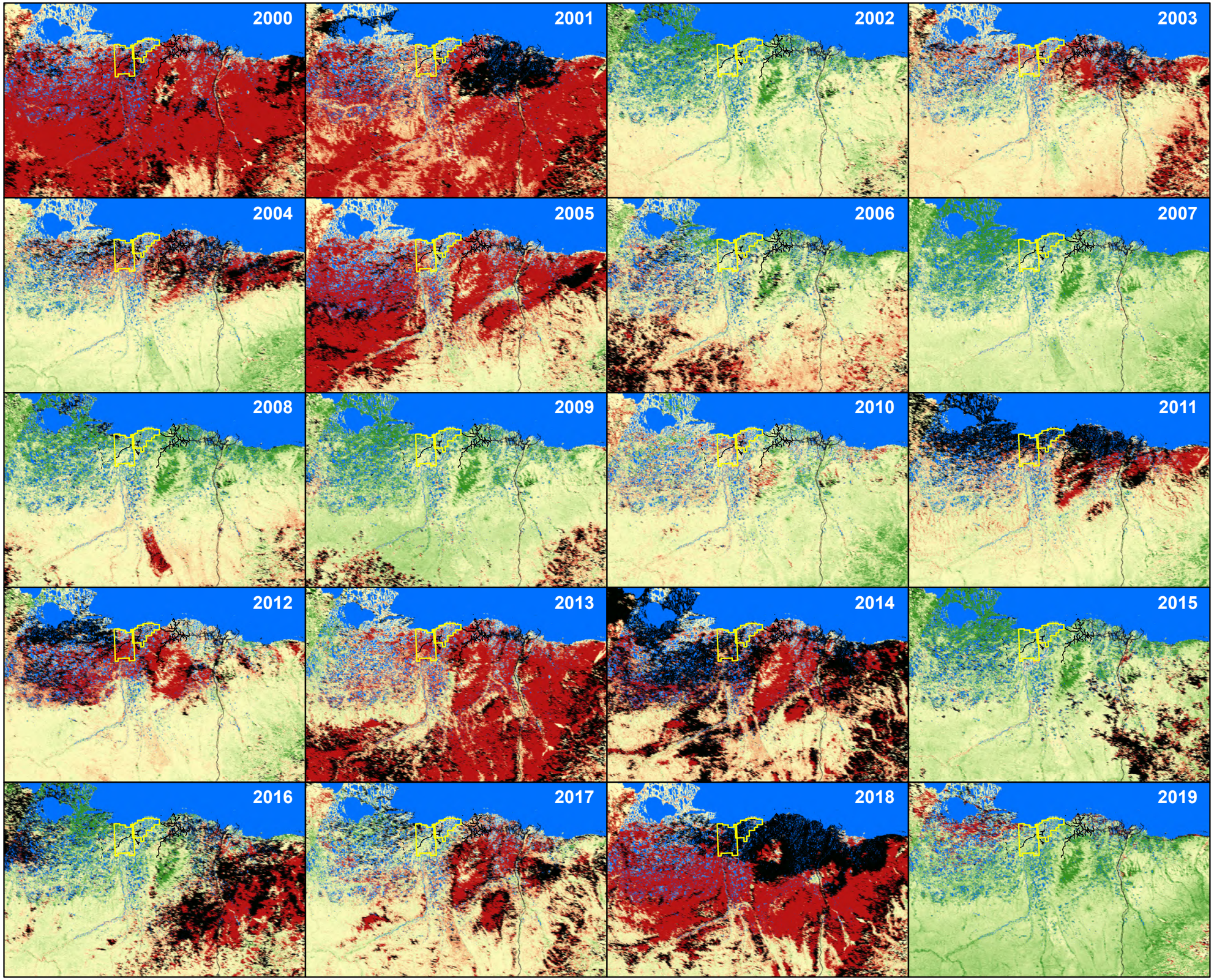

Appendix E.
Differences between annual relative vegetative biomass values and the 2000–2019 median during the caribou calving season (1–10 June) on the central North Slope of Alaska, as estimated from NDVI calculated from MODIS satellite imagery.

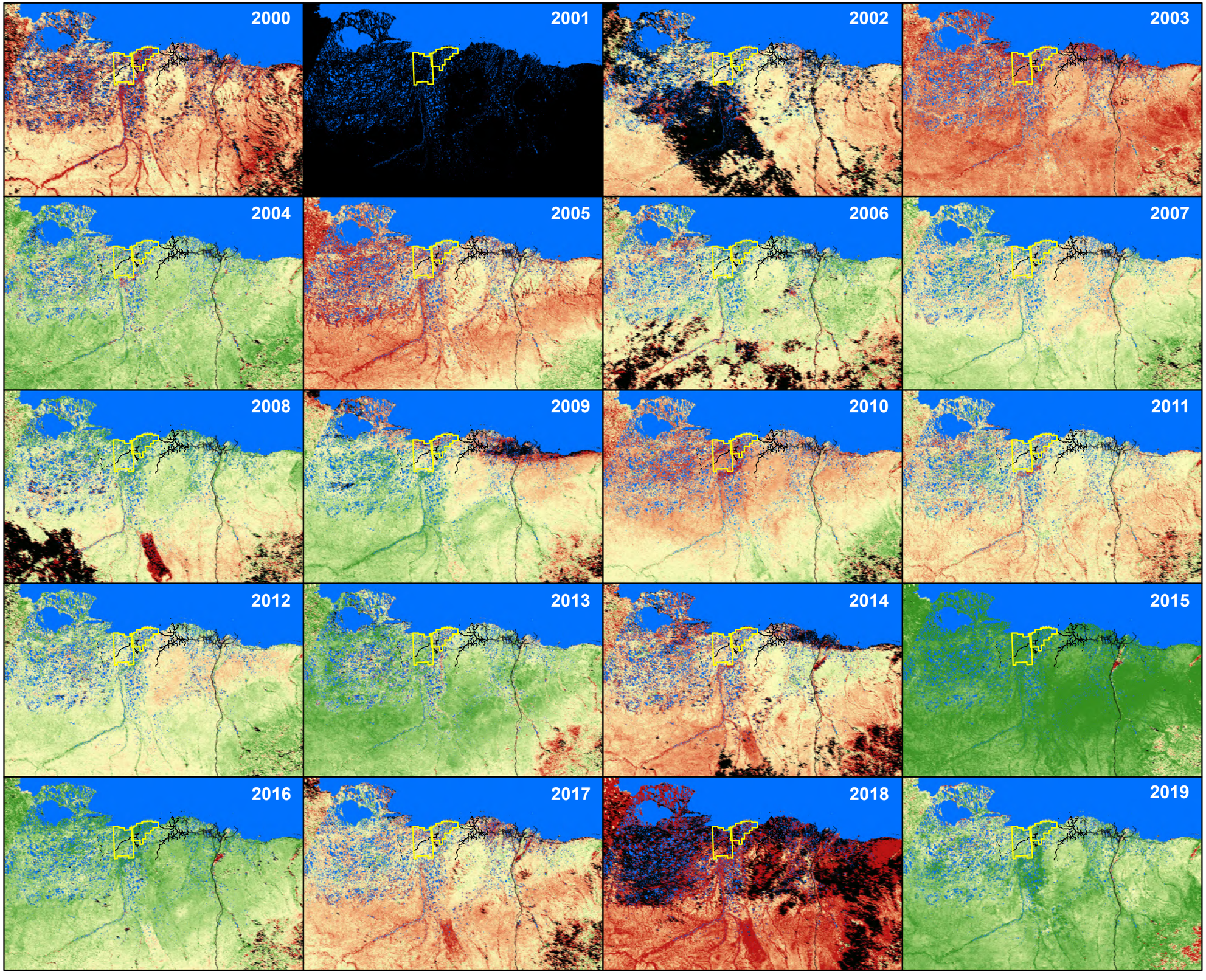

Appendix F.
Differences between annual relative vegetative biomass values and the 2000–2019 median at estimated peak lactation for caribou (21 June) on the central North Slope of Alaska, as estimated from NDVI calculated from MODIS satellite imagery.

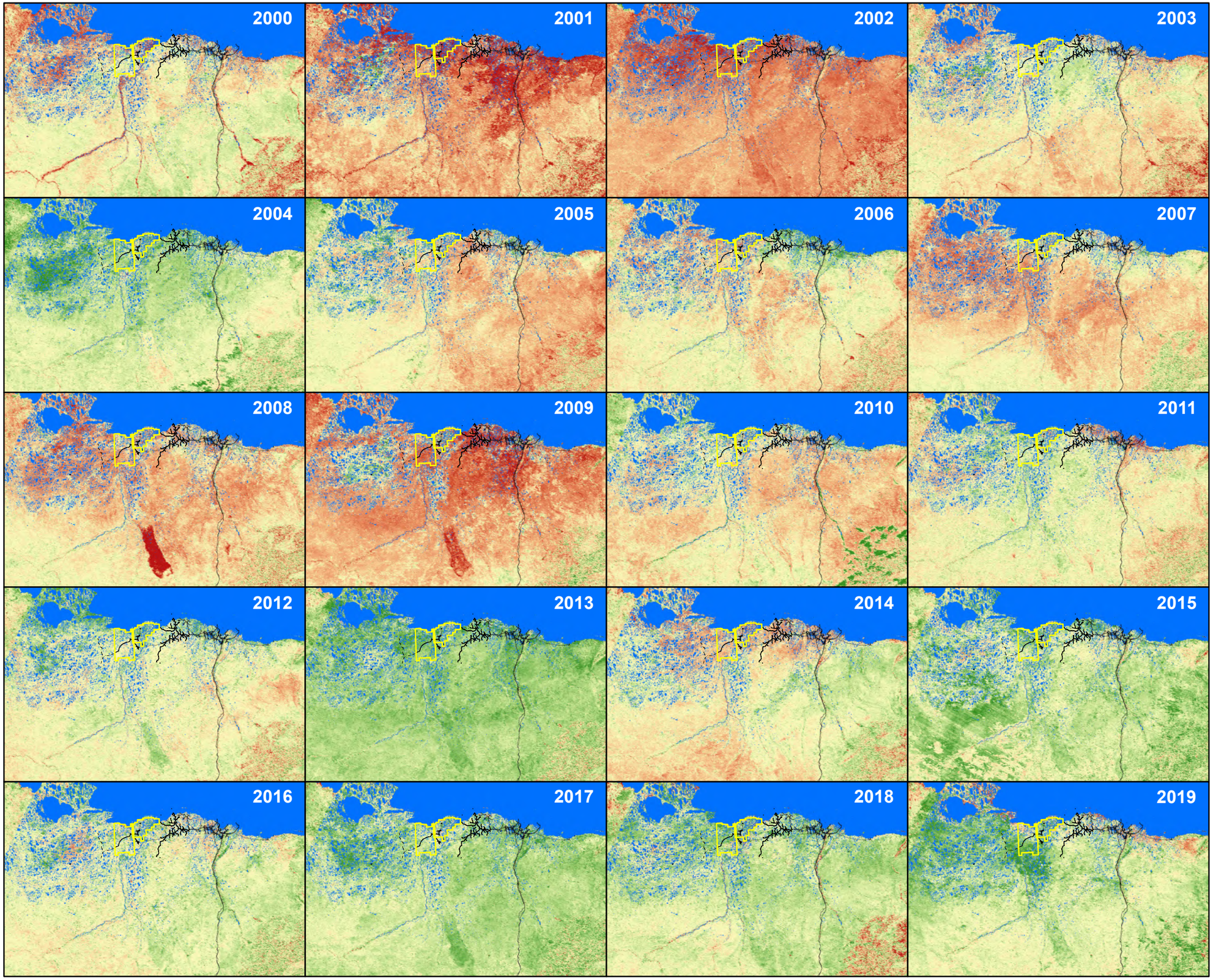

Appendix G.
Differences between annual relative vegetative biomass values and the 2000–2019 median for estimated peak biomass on the central North Slope of Alaska, as estimated from NDVI calculated from MODIS satellite imagery.